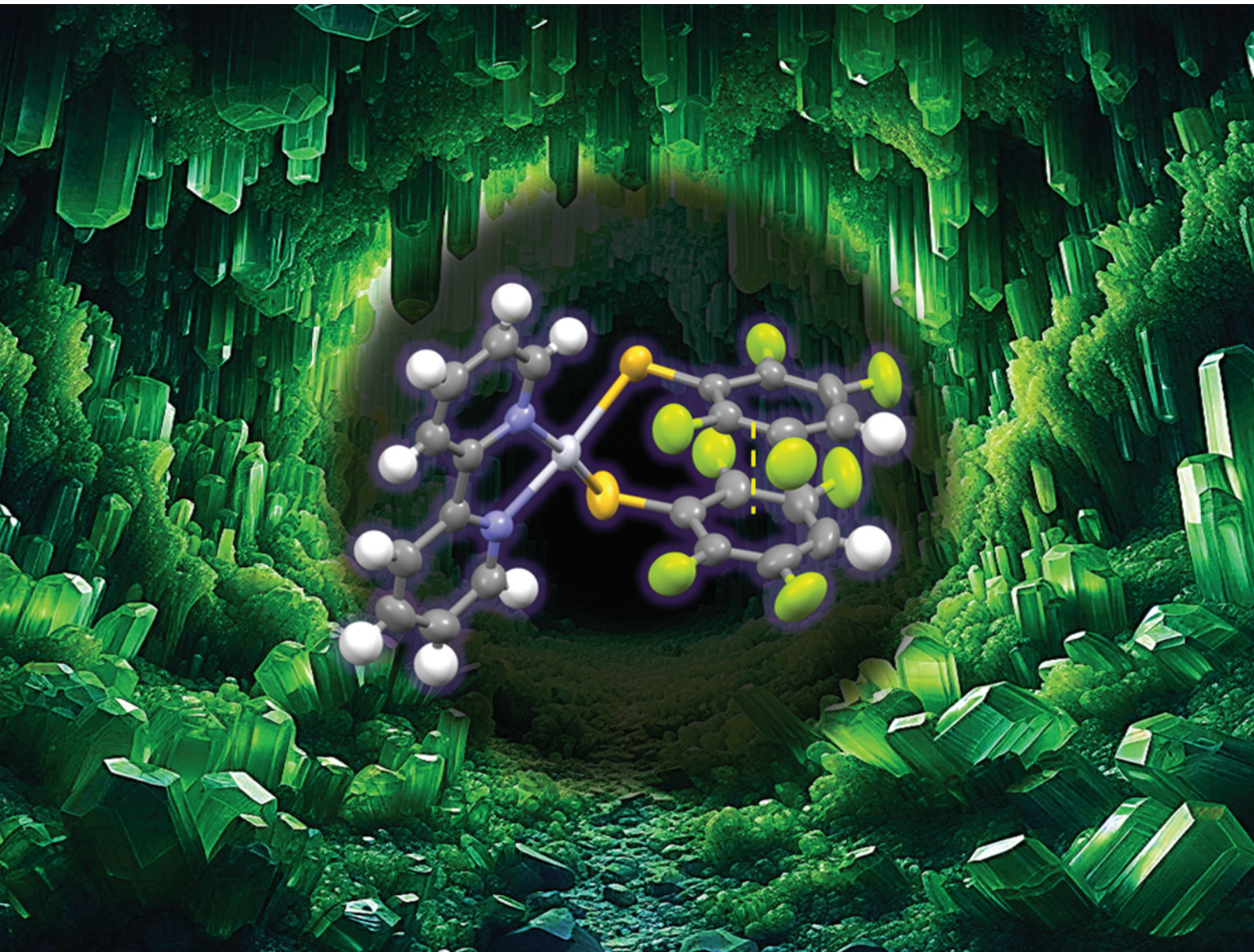


# Dalton Transactions

An international journal of inorganic chemistry

[rsc.li/dalton](http://rsc.li/dalton)



ISSN 1477-9226

## PERSPECTIVE

Juan Manuel Germán-Acacio, David Morales-Morales *et al.*  
Exploring the persistence of the fluorinated thiolate  
2,3,5,6-S(C<sub>6</sub>F<sub>4</sub>H-4) motif to establish  $\pi_F$ - $\pi_F$  stacking in metal  
complexes: a crystal engineering perspective

## PERSPECTIVE

[View Article Online](#)  
[View Journal](#) | [View Issue](#)



Cite this: *Dalton Trans.*, 2024, **53**, 16090

## Exploring the persistence of the fluorinated thiolate 2,3,5,6-S(C<sub>6</sub>F<sub>4</sub>H-4) motif to establish $\pi_F-\pi_F$ stacking in metal complexes: a crystal engineering perspective<sup>†</sup>

Everardo Jaime-Adán, <sup>a</sup> Juan Manuel Germán-Acacio, <sup>\*b</sup> José Carlos Páez-Franco, <sup>b</sup> Víctor H. Lara, <sup>c</sup> Viviana Reyes-Marquez <sup>d</sup> and David Morales-Morales <sup>\*a</sup>

$\pi-\pi$  stacking interactions are versatile because they are involved in many processes, such as protein folding, DNA stacking, and drug recognition. However, from the point of view of crystal engineering, there is an incipient knowledge of its exploitation. A comparison of these interactions with hydrogen bonds shows a huge difference in their employment as a reliable non-covalent interaction. And different reasons can be listed to explain why hydrogen bonding can be considered a more robust interaction than  $\pi-\pi$  stacking. For instance, hydrogen bonds encompass a wide energy range (25–40 kJ mol<sup>-1</sup>). From this, these interactions can be classified as strong, moderate, and weak. Hence, the first two can be considered highly to moderately directional to be exploited in crystal engineering. This aspect is relevant for them to be used in a relatively reliable way in this area of supramolecular chemistry. On the other hand, in the case of  $\pi-\pi$  stacking, the energy range is 0–10 kJ mol<sup>-1</sup>, thus implying that hydrogen bonds or any other energetically more robust contact would predominate in the competition for establishing packing interactions in a given arrangement. In this sense, if stacking is pretended to be exploited from the point of view of crystal engineering, one of the points that must be ensured is that this interaction will be the one energetically predominant. However, although there are other factors to consider, it seems that energetics is the dominant one. In this line, our research group has obtained and studied many single-crystalline structures of coordination and organometallic compounds containing fluorinated thiolates. This being particularly true in the case of the thiolate 2,3,5,6-S(C<sub>6</sub>F<sub>4</sub>H-4) bound to different metals, where it has been observed that they preferentially tend to establish  $\pi_F-\pi_F$  stacking interactions, results that have been reported in several papers. Thus, from this perspective, we have explored, using ConQuest (CCDC) a number of structures to observe how feasible is to find stacking in coordination and organometallic compounds containing the thiolate 2,3,5,6-S(C<sub>6</sub>F<sub>4</sub>H-4).

Received 9th July 2024,  
Accepted 14th August 2024

DOI: 10.1039/d4dt01978d

rsc.li/dalton

<sup>a</sup>Instituto de Química, Universidad Nacional Autónoma de México, Circuito Exterior, Ciudad Universitaria, Ciudad de México, C. P. 04510, Mexico.

E-mail: [damor@unam.mx](mailto:damor@unam.mx)

<sup>b</sup>Red de Apoyo a la Investigación, Universidad Nacional Autónoma de México-CIC, Instituto Nacional de Ciencias Médicas y Nutrición SZ, C. P.14000 Ciudad de México, Mexico. E-mail: [jmga@cic.unam.mx](mailto:jmga@cic.unam.mx)

<sup>c</sup>Universidad Autónoma Metropolitana, Iztapalapa, Av. San Rafael Atlixco No. 186, Col. Vicentina, 09340 Ciudad de México, Mexico

<sup>d</sup>Departamento de Ciencias Químico-Biológicas, Universidad de Sonora, Luis Encinas y Rosales s/n, Hermosillo C.P. 83000, Sonora, Mexico

<sup>†</sup>Electronic supplementary information (ESI) available. See DOI: <https://doi.org/10.1039/d4dt01978d>

## 1. Introduction

Crystal engineering is a branch of supramolecular chemistry that focuses on obtaining crystalline materials exhibiting extended arrangements (molecular networks) using tectons (building blocks) with recognition sites capable of forming covalent or non-covalent interactions to attain the desired molecular array.<sup>1</sup>

Thus, the appropriate use of bonding interactions is essential for assembling these molecular aggregates. For which there is a wide variety of interactions; many being isotropic or anisotropic and exhibiting a broad difference in the range of energies.<sup>2</sup>

For instance, organic crystal engineering (OCE) is interested in assembling molecular crystals with organic tectons exploit-



ing non-covalent bonds, mainly van der Waals forces and hydrogen bonds (neutral and charge-assisted).<sup>3,4</sup> And covalent organic frameworks (COF) assemblies uses building blocks linked by covalent bonds that can be exploited in OCE.<sup>5</sup> These supramolecular entities have high molecular ordering and well-defined porosities. Conversely, inorganic crystal engineering (ICE) employs transition metals and main group atoms since metal ions give more varied geometries uncommon in organic chemistry.<sup>6</sup> It also introduces the metal's inherent properties, such as catalytic, photophysical, or magnetic attributes.<sup>7</sup> From the ICE point of view, there are two approaches for forming supramolecular structures: one exploiting convergent ligands (coordination compounds) and divergent ligands (coordination networks), Fig. 1.<sup>8,9</sup> In the latter case, it allows the formation of periodic coordination complexes (1D, 2D, 3D, cages, metallocycles).<sup>10–14</sup> Also within this category we have metal–organic frameworks (MOFs).<sup>6,15,16</sup>

Another approach (using coordination compounds) is to use tectons with a metallic center coordinated to a ligand containing functional groups that may form hydrogen bonds. The geometry adopted by the coordination compound will help to

orient the ligand to another functional group, forming hydrogen bonds to give place to a network. This being referred as organic–inorganic hybrid materials, Fig. 2.<sup>17</sup>

This approach has several advantages over coordination networks that involve the incorporation of strong bonds (coordination) and the flexibility conferred by the hydrogen bonds (weaker interaction).<sup>18–20</sup> A useful tool/resource that within the variety of non-covalent interactions used in supramolecular chemistry stands out as it is very directional and highly specific.<sup>6,21</sup>

The formation of compounds with strong bonds (covalent or coordinative) generally involves irreversible processes during self-assembly since forming these bonds is governed by  $\Delta H$ . In hydrogen bonds, the  $\Delta H$  and  $\Delta S$  contributions are almost the same. Therefore, there should be a great deal of pre-organization in the system so that interactions can occur.<sup>22,23</sup> The hydrogen bond is kinetically labile; that is, it can be cleaved or reformed depending on the system's requirements in the self-assembly processes.<sup>24</sup> Molecularly ordered crystalline materials can be obtained through this interaction under mild self-assembly conditions (room temperature); forming coordination networks requires more drastic conditions (hydro- or solvothermal reactions). In this sense, reliable hydrogen bonds must be used to ensure the construction of the extended crystalline arrangement.<sup>25,26</sup>

Dance proposed (later modified by Brammer) a model of the regions or domains of these hybrid organic–inorganic materials, where hydrogen bonding can be exploited depending on the region of these complexes.<sup>21</sup> Brammer refined this model, resolving some ambiguities in the Dance model, Fig. 3. The modified Brammer model is delimited into four regions: the metal domain (blue), the ligand domain (green), the periphery domain (red), and the environment domain (light blue). In the metal domain, the metal is part of the M–H…A hydrogen bond, where the donor is the M–H fragment (M = metal), and A is an acceptor. The formation of this bond is imminently dependent on the electronic properties of the metal. In the case of the ligand domain, the metal exerts an

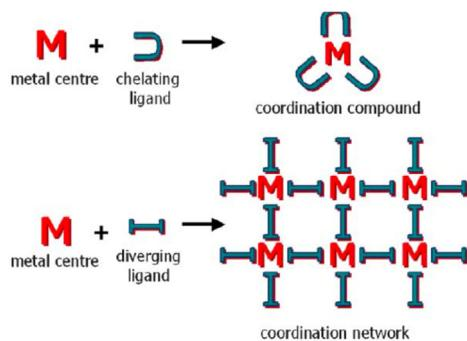


Fig. 1 Schematic representation of the relationship between molecular (top) and periodical (bottom) coordination chemistry. Reproduced with permission of the Royal Society of Chemistry from ref. 9.

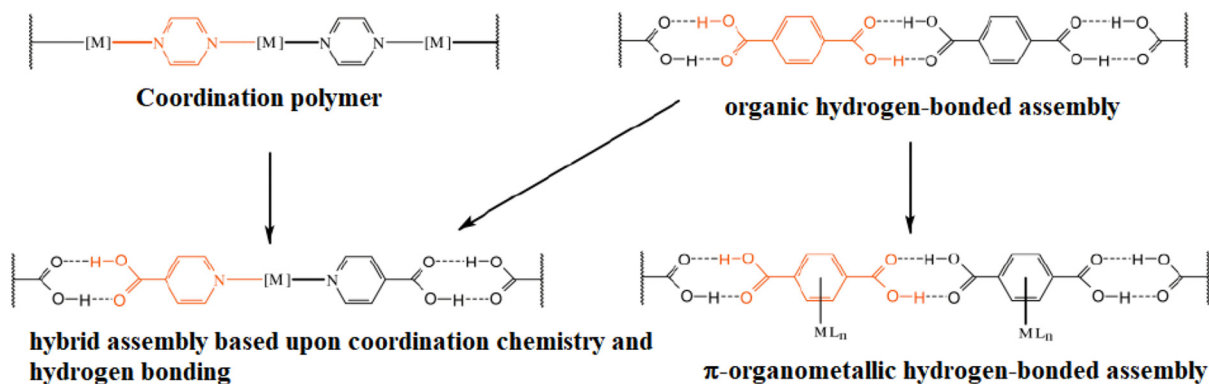


Fig. 2 Schematic representation of the incorporation of metals into 1D hydrogen bonded assemblies *via* coordination chemistry, or  $\pi$ -organometallic chemistry, and their relationship to the parent organic hydrogen-bonded assemblies and coordination polymers. Reproduced with permission of the Royal Society of Chemistry from ref. 17.

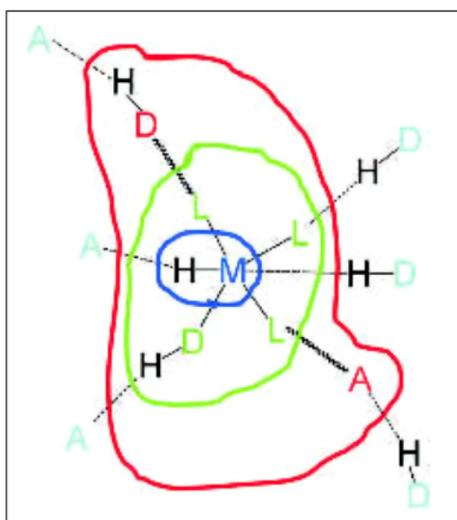


Fig. 3 Domain model for hydrogen bonding involving metal complexes. Metal domain (blue); ligand domain (green); periphery domain (red); environment (cyan). Reproduced with permission of the Wiley from ref. 21.

electronic influence on the formation of the hydrogen bond, where there are two possibilities: the metal can work as a donor  $M-D-H\cdots A$  or the metal may act as an acceptor  $D\cdots H-A-M$ . In both cases, the electronic properties can be modulated, the acidity in the first type or the basicity in the second. In the periphery domain, the electronic dependence of the metal is lower, and the outer part of the metal/coordination compound can interact with the environment domain. In this region (environment domain), the electronic influence of the metal fragment is almost null. Brammer has explained how these domains have been exploited to form interesting molecular arrangements linked by hydrogen bonds.<sup>6,21</sup>

Thus, in this perspective, we look to perform an analysis using the data found in the Cambridge Structural Database (CSD, using Conquest)<sup>27</sup> to explore the possibility of exploiting the formation of  $\pi-\pi$  stacking interactions. In this sense, it is necessary to remember what Aakeröy pointed out about a “supramolecular synthon” defined as a connector that binds molecules through non-covalent interactions.<sup>28</sup> In this way, the “supramolecular synthons” describe molecular recognition events between the participating components that, during the self-assembly processes, will produce the desired crystalline arrangement. With this in mind, this analysis pretends to explore how reliable and robust these interactions are to be exploited in supramolecular chemistry.

## 2. Fundamentals and theoretical aspects of the $\pi$ interactions

$\pi$  interactions (mainly  $\pi-\pi$  stacking) have received less attention in their exploitation in crystal engineering than hydrogen bonding, especially because their nature still needs to be

better understood. Nevertheless,  $\pi-\pi$  stacking interactions are involved in several important biological processes, like protein folding,<sup>29</sup> DNA stacking,<sup>30</sup> and drug recognition.<sup>31,32</sup> Recently, it has been reported an Scopus analysis revealing an exponential increase in the number of titles, keywords, or abstracts including  $\pi-\pi$  interactions.<sup>33</sup> The little interest shown by the crystal engineering community towards using this interaction is probably because their formation is so difficult to predict, as parameters such as force, geometric preferences, and substituent electronic influence need to be better understood. Energetically, a hydrogen bond is slightly stronger than a  $\pi-\pi$  interaction ( $25-40 \text{ kJ mol}^{-1}$  vs.  $10 \text{ kJ mol}^{-1}$ ).<sup>1,34</sup> Therefore, studying  $\pi-\pi$  stackings can be a difficult task from an experimental point of view since these results depend on interpretation when secondary interactions and solvation effects can perturb the formation of this interaction.<sup>35</sup> For these reasons, efforts to understand the fundamentals that define  $\pi-\pi$  interactions have been addressed using theoretical models.<sup>35,36</sup>

For instance, Sanders and Hunter have proposed a model based on the competition of electrostatic forces and van der Waals contacts in a benzene-benzene dimeric system to explain the variety of geometries observed in the interactions and qualitatively predict the energies associated with each interaction.<sup>36</sup> From these calculations, they found the preferred geometries in the interactions between benzene rings from an electrostatic interaction map in the function of their relative orientations. Electrostatic effects greatly dictate the geometrical preferences adopted in benzene dimers, and other forces such as induction, dispersion, and exchange-repulsion are irrelevant. However, Sherrill *et al.* have disputed this, mentioning that electrostatics effects are not dominant.<sup>35</sup> But, since they are all significant, Sherrill suggested that electrostatic, dispersion, induction, and exchange-repulsion components must be considered.<sup>37</sup>

The geometric preferences of the  $\pi-\pi$  interactions in benzene dimers can be classified into three different configurations: sandwich (S) configuration when both benzenes sit on top of each other, T-shaped (T) when one benzene points to the center of the other, and parallel displaced (PD) that is reached from the sandwich configuration by parallel displacement of one ring away from the other, Fig. 4.<sup>10</sup> There can be eclipsed and staggered arrangements within the S confor-

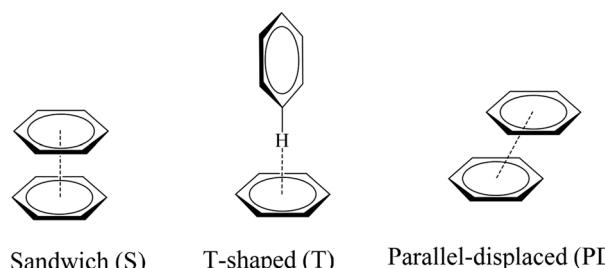


Fig. 4 Most common orientations of  $\pi-\pi$  interactions.



mation, although the energetic differences between one and the other are insignificant.<sup>10</sup>

These three arrangements can be found in the crystalline state, thus raising a fundamental question seen from the discernment of crystal engineering: what defines any of these geometric conformations? The answer is probably related to energy. The balance of fundamental forces such as electrostatics, induction, dispersion, and exchange-repulsion can be responsible for the adopted geometric preference.<sup>35</sup> In this sense, subtle modifications in the contribution of these forces can completely change the geometric conformation adopted; thus, the possibility of considering  $\pi$ – $\pi$  interactions as a reliable and predictable working tool in crystal engineering can be difficult to handle. However, the substituent effect has been proposed as an efficient way to handle this situation. A suitable tuning in the ring's withdrawing/donating electronic properties has given excellent results.<sup>38,39</sup> Electron-withdrawing substituents or heteroatoms within the ring make the aromatic system an electron-deficient center, favoring the *S* configuration because repulsive effects are reduced. Meanwhile, electron-donating substituents promote electron-rich aromatic rings, which disfavors the *S* configuration because repulsion effects are enhanced. The order of stability of the configuration *S* can be  $\pi_{\text{poor}}\text{--}\pi_{\text{poor}} > \pi_{\text{poor}}\text{--}\pi_{\text{rich}} > \pi_{\text{rich}}\text{--}\pi_{\text{rich}}$ .<sup>38</sup> Janiak explains that the *S* configuration is rare, and the PD arrangement is more frequent.<sup>38</sup> Janiak has also established the geometric parameters to consider a stacking in systems containing pyridine rings attached to a metal center, Fig. 5.<sup>38</sup> As can be observed, these parameters define both edges to consider an *S* or a PD configuration: centroid–centroid distance (ccd); plane–plane distance (ppd); angle between the ring normal and the centroid vector (ancv) (in our description, instead of using the ancv angle we use the plane–plane angle (ppa), since both are representative of the rotation between the rings involved); and slippage, Fig. 5. In this sense, within the search made in the CSD, we will stick to the limits of these parameters to consider that a genuine  $\pi$ – $\pi$  stacking interaction has been established. Throughout the perspective, we will display the values of the parameters as follows: [operation symmetry; ccd Å; ppd Å; slippage Å; and ppa°]. These crystallographic parameters will be determined using the Olex 2, and Platon programs.<sup>40,41</sup>

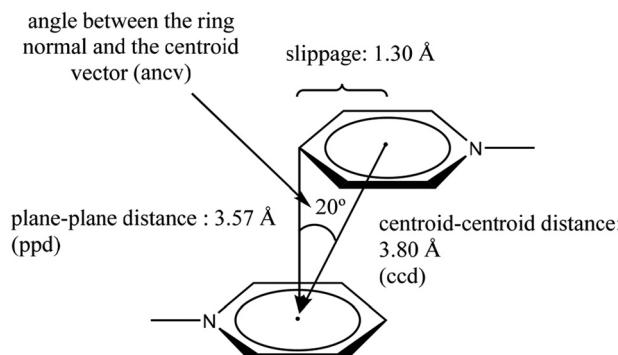


Fig. 5 Geometric parameters to consider a  $\pi$ – $\pi$  stacking.

### 3. Fluorination of ligands

The fluorination of molecules has been an excellent strategy for producing important physicochemical and biological improvements in different compounds. For instance, we have recently published the advantages of preparing fluorinated metallodrugs.<sup>42</sup> In the case of metallodrugs, hurdles such as aqueous-solubility issues, low bioavailability, and short circulation time, can be circumvented by employing two strategies: design of novel metallodrug-delivering vehicles and the structural optimization of the ligand(s). In the latter case, substituting H atoms with F within the ligand can produce important modifications at the molecular and supramolecular level<sup>43,44</sup> since F atoms participate in various non-covalent interactions, contributing greatly to crystal stabilization. Among these can be mentioned C–H…F–C, C–F…F–C, C–F… $\pi$ , C–F… $\pi_F$ , C–F…M<sup>+</sup>, C–F…X (N, O, S, halogen),  $\pi$ – $\pi_F$ , and  $\pi_F$ – $\pi_F$ .<sup>44–46</sup>

Thus, introducing fluorine atoms in aromatic rings has proven to be an efficient way to have electron-deficient aromatic components that establish F…F contacts and  $\pi_F$ – $\pi_F$  stacking.<sup>44,46,47</sup> Much has been said about showing  $\pi$ – $\pi_F$  and  $\pi_F$ – $\pi_F$  interactions when they compete with hydrogen bonds since this interaction may be dominant in the packing array, relegating the stacking motif.<sup>48</sup> If one wishes to exploit the  $\pi$ – $\pi$  stacking as a “supramolecular synthon”, one must avoid stronger competitive interactions prevailing in the system.<sup>49</sup>

### 4. Previous contributions made by our research group

For over 20 years, our group has synthesized coordination and organometallic compounds with different metals containing fluorinated benzenethiolates (mono, di, tri, tetra, and pentafluorinated). In this sense, innumerable single-crystal structures have been obtained. The versatility shown by fluorinated benzenethiolates has already been mentioned since these ligands can stabilize unusual geometries and high and low oxidation states.<sup>50</sup> Moreover, their steric and electronic properties can be finely modulated by manipulating the content of fluorine atoms within the aromatic ring.<sup>50</sup>

Our results show that the tetrafluorinated ligand 2,3,4,6-S (C<sub>6</sub>F<sub>4</sub>H-4) preferentially establishes  $\pi_F$ – $\pi_F$  interactions. However, this has been observed less frequently in the pentafluorinated thiolate S(C<sub>6</sub>F<sub>5</sub>). In this regard, we have published some papers referring to this.

Initially, we observed that depending on the degree of fluorination in the thiolate ring, the compounds [Pt(II)(2,2'-bipy)(SR<sub>F</sub>)<sub>2</sub>] (bipy = bipyridine, R = (2,3,4,6-C<sub>6</sub>F<sub>4</sub>-H) or (C<sub>6</sub>F<sub>5</sub>); REF CODE: MIXFAB and MIXDUT), could establish  $\pi_F$ – $\pi_F$  stacking interactions or not, Fig. 6.<sup>51</sup> Complex MIXFAB presents an intra  $\pi_F$ – $\pi_F$  stacking between rings C13–C18…C19–C24 with values of [+X, +Y, +Z, 3.478 Å; 3.397 Å; 0.749 Å; and 7.085°], and an inter  $\pi_F$ – $\pi_F$  interaction between C13–C18…C19–C22 [–X, 1 – Y, 1 – Z, 3.899 Å; –3.667 Å; 1.323 Å; and 0.0°].

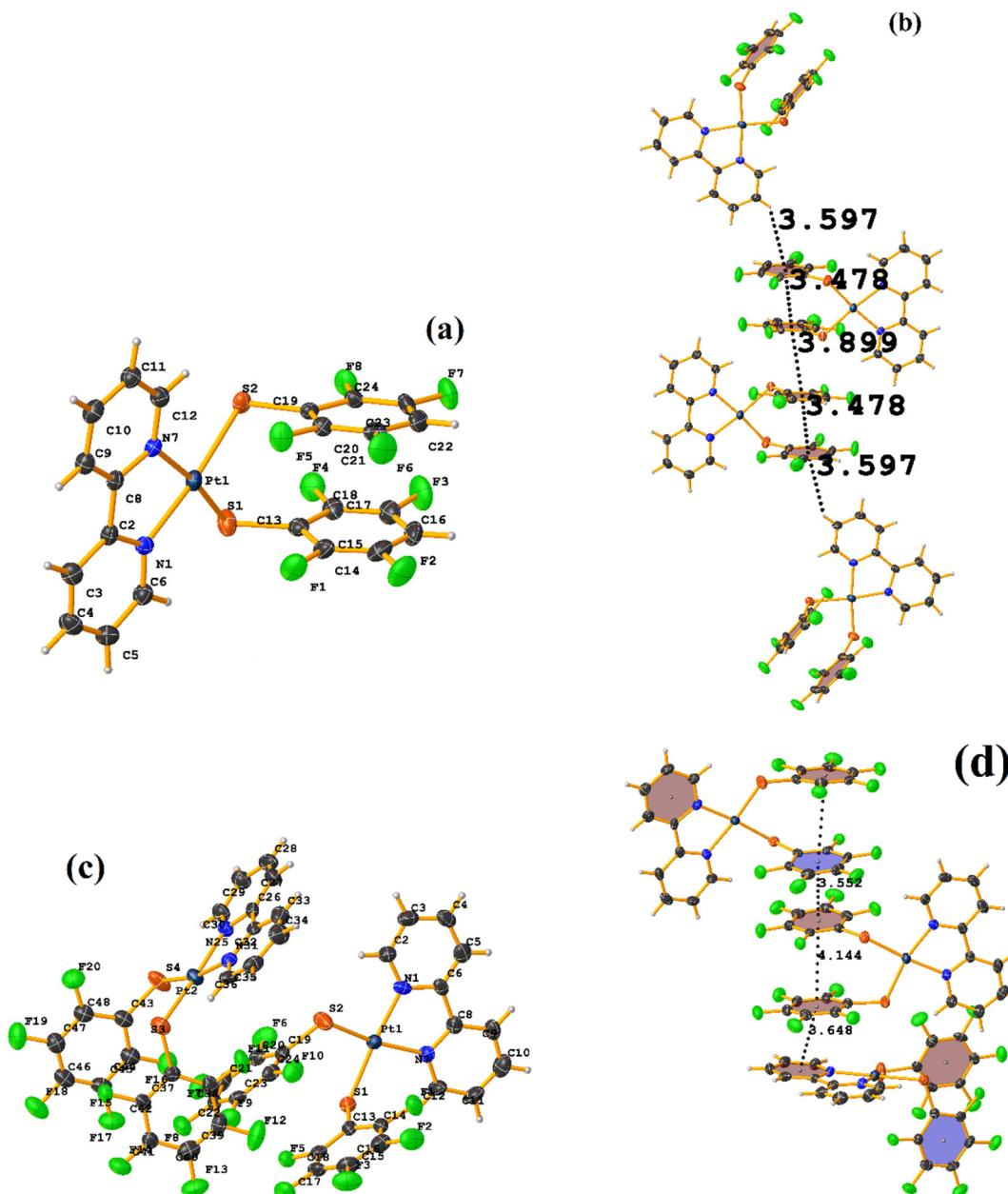


**Fig. 6** (a) Molecular structure of MIXFAB. (b) Stacking interactions of MIXFAB. (c) Molecular structure of MIXDUT. (d) Stacking interactions of MIXDUT.

In general, in these complexes, having an extra F atom (pentafluorinated MIXDUT) limited the establishment of the interaction compared with the tetrafluorinated. In the case of the pentafluorinated complex an inter  $\pi_F-\pi_F$  interaction was observed between C13–C18…C37–C42 [ $-1/2 + X, 3/2 - Y, 1/2 + Z, 3.552 \text{ \AA}; 3.390 \text{ \AA}; 1.092 \text{ \AA}; \text{ and } 0.581^\circ$ ] and no intra  $\pi_F-\pi_F$  stacking was noted. Similarly, a  $\pi_F-\pi$  interaction was found between a pentafluorinated ring and the aryl of the 2,2'-bipy ligand *i.e.* C43–C48…N1/C2–C6 [ $+X, 1 + Y, +Z, 3.648 \text{ \AA}; 3.402 \text{ \AA}; 1.526 \text{ \AA}; \text{ and } 6.672^\circ$ ]. It is proposed that this happens because when the 2,3,4,6-S( $C_6F_4$ -H-4) fragments are stacked, the S atoms point in the opposite directions, allowing a positive

dipole of one molecule to interact with the negative dipole of the other, fact that does not occur in S( $C_6F_5$ ).<sup>51</sup>

Specifically, in these tectons  $[\text{Pt}(\text{II})(2,2'\text{-bipy})(\text{SR}_F)_2]$ , it was observed that  $\pi_F-\pi_F$  stacking interactions were preferentially established when tetrafluorinated thiolates were used instead of the pentafluorinated ones.

From this, we sought to test the robustness of these tectons to form  $\pi_F-\pi_F$  interaction, which now varies in certain aspects. In this way, complexes of the type  $[\text{Pt}(\text{II})(1,10\text{-phen})(\text{SR}_F)_2]$  (phen = phenanthroline,  $\text{SR}_F = \text{SC}_6\text{H}_3\text{-}3,4\text{-F}_2, 2,3,4,6\text{-SC}_6\text{F}_4\text{-}4\text{-H}$ , and  $\text{SC}_6\text{F}_5$ ; REF CODE: LUQMIW, LUQMOC, and LUQMUI) were published,<sup>52</sup> where although the crystalline packing was

not described in deep detail, it was observed that stacking interactions were formed. It should be noted that there was a change in the chelating ligand (1,10-phen to 2,2'-bipy) to a ligand with a larger  $\pi$  surface area that can preferentially form  $\pi$ - $\pi$  stacks.<sup>53,54</sup> This is mentioned because, as indicated, the formation of the desired synthon depends on other competing interactions. In the case of LUQMIW (difluorinated), this tecton did not show the establishment of  $\pi_F$ - $\pi_F$  stacking interactions.

On the other hand, the pentafluorinated thiolate compound (LUQMOC) has an intra  $\pi_F$ - $\pi_F$  stacking between C17-C22...C11-C16 [+X, +Y, +Z, 3.600 Å; 1.337 Å; and adpp 4.249°], Fig. 7. There was also an inter  $\pi_F$ - $\pi_F$  interaction between C17-C22...C11-C16 [1-X, 2-Y, 1-Z, 3.990 Å; 1.813 Å; and 0.0°]. Contrary to the tetrafluorinated one (LUQMUI), where it was

found a  $\pi_F$ - $\pi_F$  intramolecular stacking C51-C56...C45-C50 [+X, +Y, +Z, 3.530 Å; 1.480 Å; and 2.221°], Fig. 7. It must be emphasized that the LUQMUI structure presents two crystallographically independent molecules. The other crystallographically independent molecule exhibits intermolecular  $\pi_F$ - $\pi_F$  interactions C45-C50...C15-C20 [+X, 1+Y, +Z, 3.546 Å; 1.290 Å; and 4.610°]. Interactions intra  $\pi_F$ - $\pi$  were also found between the tetrafluorinated ring and a phen fragment C45-C50...N10/C9-C14 [1-X, 1-Y, 1-Z, 3.509 Å; 0.965 Å; and 6.214°]. Thus,  $\pi_F$ - $\pi_F$  interactions prevailed despite the phen ligands favoring stacking due to their larger  $\pi$  surface area.<sup>53,54</sup> Thus indicating that these interactions may persist even in competing interactions.

Based on these results, we wanted to continue exploiting this tecton but varying the metal to observe if the formation

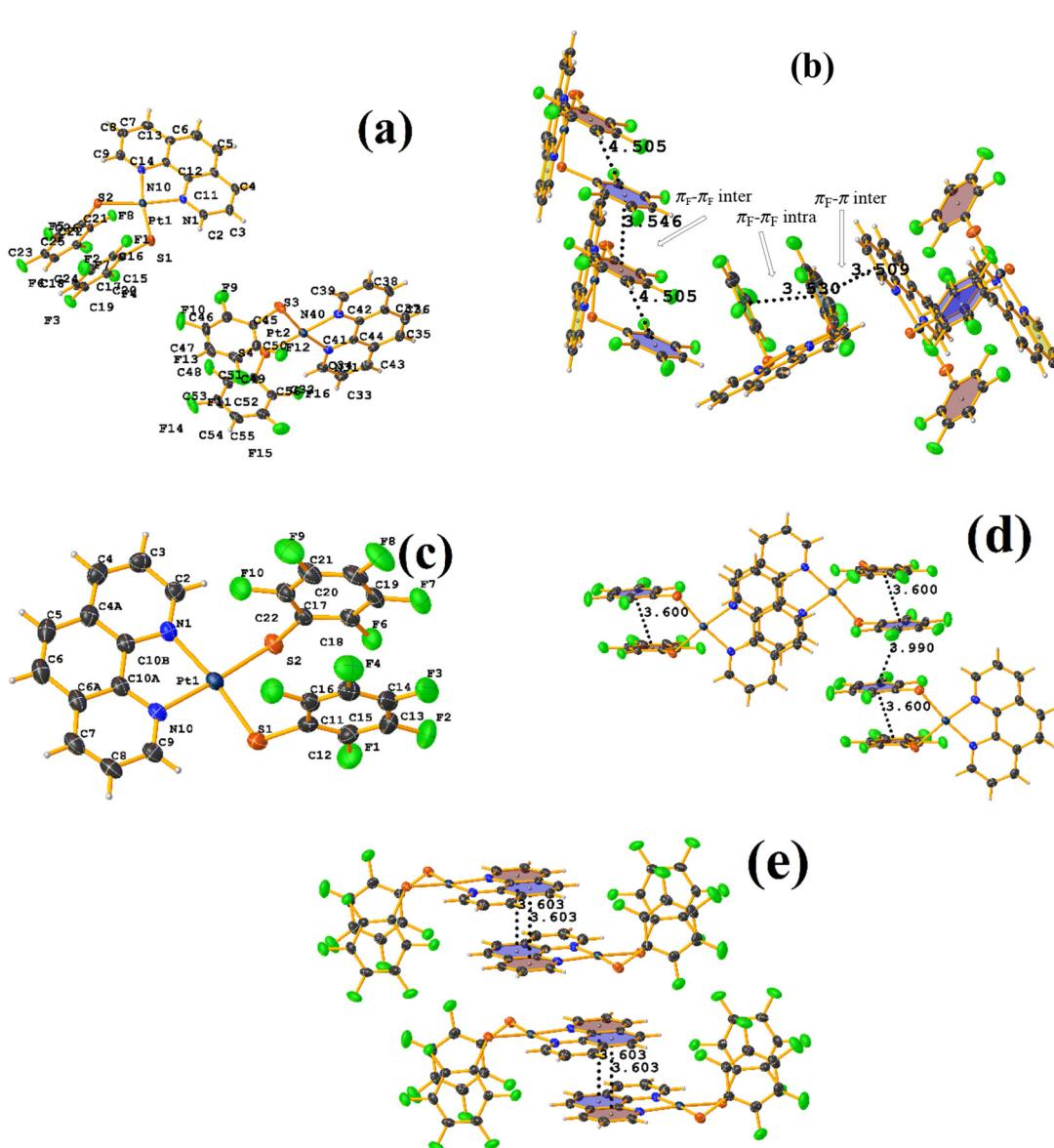


Fig. 7 (a) Molecular structure of LUQMUI. (b) Stacking interactions of LUQMUI. (c) Molecular structure of LUQMOC. (d and e) Stacking interactions of MIXDUT.



of the stacking persisted thus we synthesized complex  $[\text{Pd}(\text{II})(1,10\text{-phen})(\text{SR}_\text{F})_2]$ . Most recently we reported the preparation of solvatomorphs of the type  $[(\text{Pd}(\text{II})(1,10\text{-phen})(2,3,4,6\text{-SC}_6\text{F}_4\text{-4-H})_2)\cdot\text{S}]$ ,  $\text{S} = \text{C}_6\text{H}_6$ ,  $\text{C}_6\text{H}_6\text{Cl}$ , and  $\text{C}_6\text{H}_6\text{Br}$ ; REF CODE: DEQLUK, DEQMIZ, DEQMEV), solvate  $[(\text{Pd}(\text{II})(1,10\text{-phen})(\text{SC}_6\text{F}_5)_2)\cdot\text{C}_6\text{H}_6\text{Br}$ , REF CODE: DEQLOE), and non-solvated  $[(\text{Pd}(\text{II})(1,10\text{-phen})(2,3,4,6\text{-SC}_6\text{F}_4\text{-4-H})_2)]$  REF CODE: HHREX01).<sup>49</sup> Unexpectedly, in this series of tectons, various solvatomorphs and solvates were preferentially crystallized, and the hypothesis of establishing stacked  $\pi_\text{F}-\pi_\text{F}$  interactions did not materialize compared with the same tecton but with  $\text{Pt}(\text{II})$ , where  $\pi_\text{F}-\pi_\text{F}$  interactions were established.

According to these three papers, it was observed that even when using a tecton with slightly modified characteristics to evaluate the persistence of  $\pi_\text{F}-\pi_\text{F}$  interactions, they were only detected in two of the three cases, being preferably established with thiolate  $2,3,4,6\text{-SC}_6\text{F}_4\text{-H-4}$ . In this way, the question arises: is this a sufficiently robust and reliable ligand to establish  $\pi_\text{F}-\pi_\text{F}$  interactions regardless of the nature of the tecton's in a metal complex? Then, using the Cambridge Structural Database (CSD),<sup>27</sup> the deposited structures were explored, looking for metal complexes including the thiolate  $2,3,5,6\text{-SC}_6\text{F}_4\text{-H-4}$  coordinated at least once. From this, each of the structures was analyzed, as shown next.

## 5. Results from CSD

Using Conquest (Version 2022.3.0) from the CSD (Version 5.43), we searched for tetrafluorinated thiolate  $2,3,5,6\text{-SC}_6\text{F}_4\text{-H-4}$  metal complexes using the label 4M. We found 87 crystal structures from which we obtained the  $\pi-\pi$  parameters using the PLATON software. As referenced above, we are interested in the  $\pi_\text{F}-\pi_\text{F}$  parameters centroid–centroid distance (ccd), plane–plane distance (ppd), slippage, and plane–plane angle (ppa).

Of these parameters, we filter the results using  $\text{ccd} < 4 \text{ \AA}$  and  $\text{ppa} < 20^\circ$ . Ending up with 51 crystal structures. Analysis of this group of structures will be discussed depending on the metal involved. As mentioned in section 2, the study to determine the stacking  $\pi-\pi$  interactions will use the crystallographic parameters [operation symmetry,  $\text{ccd} \text{ \AA}$ ;  $\text{ppd} \text{ \AA}$ ; slippage  $\text{\AA}$ ; and  $\text{ppa}^\circ$ ]. These will be obtained through the Olex 2, and Platon programs.<sup>40,41</sup> The study of each structure will be made and discussed according to the metal atom involved, arranged alphabetically. Worth to mention that there will not be an exhaustive study of the secondary interactions, or any other contact involved in the analysis, even though they are important in molecular packing. Still, only the geometric parameters will be described. The results obtained from ConQuest from the CSD are shown in the ESI.<sup>†</sup> A discussion will be made at the end of all the structures corresponding to structures containing a particular metal atom. This will be done based on the results obtained through ConQuest. Additionally, the geometric parameters of the  $\pi_\text{F}-\pi_\text{F}$  interactions were corroborated using the Platon program.<sup>41</sup> Each CIF will be analyzed individually to detect the desired interactions.

## 6. $\pi_\text{F}-\pi_\text{F}$ stacking analysis

### Au metal complexes

**AROSUV and AROSV01.** Watase *et al.* published the formation of complex  $[\text{Au}(\text{i})(2,3,5,6\text{-SC}_6\text{F}_4\text{-H-4})(\text{PPh}_3)]$  (AROSUV).<sup>55</sup> Moreno-Alcántar *et al.* have also reported the same structure deposited as AROSV01.<sup>56</sup> In this case, the AROSV structure will be used for the analysis, where two types of stacking interactions were found ( $\pi_\text{F}-\pi_\text{F}$  and  $\pi_\text{F}-\pi$ ). Here the inter  $\pi_\text{F}-\pi_\text{F}$  interaction was established between  $\text{C1-C6}\cdots\text{C1-C6}$  [ $1 - X, -Y, 1 - Z, 3.652(5) \text{ \AA}$ ;  $3.454(3) \text{ \AA}; 1.187 \text{ \AA}$ ; and  $0.0(4)^\circ$ ], while the intermolecular  $\pi_\text{F}-\pi$  stacking established between the fluorinated thiolate ring and a

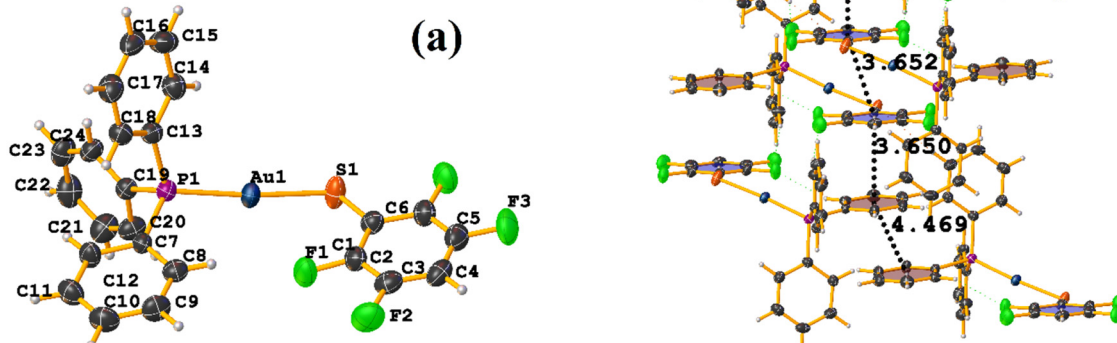


Fig. 8 (a) Molecular structure of AROSV. (b) Stacking interactions of AROSV.

triphenylphosphine ring C1–C6…C7–C12 [ $1 - X, -Y, 1 - Z$ , 3.650 (5) Å; 3.376(3) Å; 1.143 Å; and 4.3(4)°]. According to the authors, a dual quadrupole effect between both rings favors this intermolecular  $\pi_F$ – $\pi$  interaction. The authors did not describe the intermolecular  $\pi_F$ – $\pi_F$  stacking (Fig. 8).

**BUSROZ.** Romo-Islas *et al.* reported the structure  $[\text{Au}(\text{i})(2,3,5,6-\text{SC}_6\text{F}_4\text{-H-4})_2(\mu\text{-vdpp})]$  (vdpp: vinylidene-bis(diphenylphosphine)) BUSROZ, Fig. 9.<sup>57</sup>

In this instance, two stacking  $\pi_F$ – $\pi_F$  and  $\pi$ – $\pi$  interactions were found. An intra  $\pi_F$ – $\pi_F$  interaction, with the parameters found to be  $[+X, +Y, +Z$ , 3.707 Å; 3.400(4) Å; 1.378 Å; and 4.277°] between the rings C1–C6…C7–C12 and a  $\pi$ – $\pi$  inter stacking between two

rings of the  $\mu$ -vdpp ligand, that was established between C19–C24…C19–C24 presenting the geometric parameters  $[1 - X, 1 - Y, -Z, 3.916(5)$  Å; 3.685(4) Å; 1.326 Å; and 0.0(4)°].

**IMAKOZ.** In addition, Moreno-Alcántar *et al.* reported the coordination complex  $[\text{Au}(\text{i})(2,3,5,6-\text{SC}_6\text{F}_4\text{-H-4})(\text{Xphos})]$  (Xphos = 2-dicyclohexylphosphino-2',4',6'-triisopropylbiphenyl) IMAKOZ, Fig. 10.<sup>58</sup> This structure exhibits an inter  $\pi_F$ – $\pi_F$  stacking between the fluorinated rings of the thiolates C1–C6…C1–C6 [ $2 - X, 1 - Y, 1 - Z, 3.4903(16)$  Å; 3.3463(12) Å; 0.992 Å; and 0.03(14)°].

**LOKWEO and LOKVUD.** Besides, Bachman *et al.* published two Au(i) and Au(III)-containing structures of the ditopic and tetratopic type  $[\text{Et}_4\text{N}][\text{Au}(\text{i})(2,3,5,6-\text{SC}_6\text{F}_4\text{-H-4})_2]$  and  $[\text{Et}_4\text{N}][\text{Au}(\text{III})(2,3,5,6-\text{SC}_6\text{F}_4\text{-H-4})_4]$

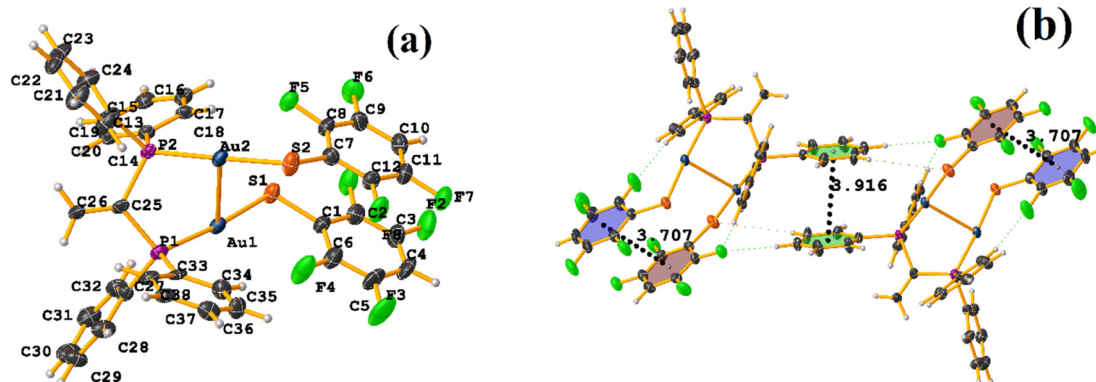


Fig. 9 (a) Molecular structure of BUSROZ. (b) Stacking interactions of BUSROZ.

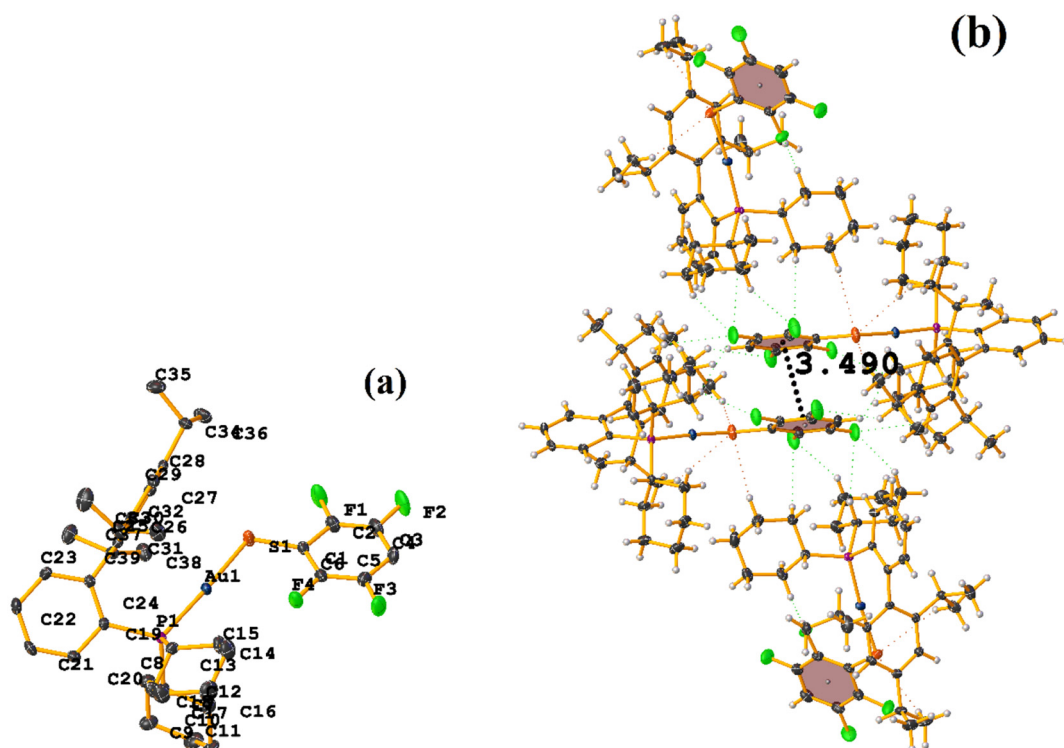


Fig. 10 (a) Molecular structures of IMAKOZ. Hydrogen atoms are omitted for more clarity. (b) Stacking interactions of IMAKOZ.



( $\text{III}(2,3,5,6-\text{SC}_6\text{F}_4\text{-H-4})_4\text{-EtOH}$  (LOKWEO and LOKVUD), Fig. 11. It should be mentioned that the results obtained by ConQuest with the determined restrictions only returned LOKWEO and not LOKVUD. However, reviewing the article, we find that this structure meets the constraints.

Both the ditopic (LOKWEO) and tetratopic (LOKVUD) molecules exhibit wind blade shapes that facilitate the formation of 1D and 2D networks. From the supramolecular point of view, propagation occurs predominantly through  $\pi_{\text{F}}-\pi_{\text{F}}$  interactions. Noteworthy the fact that even the presence of  $\text{Et}_4\text{N}$  or  $\text{EtOH}$  perturbs the establishment of this interaction. LOKWEO structure exhibits  $\pi_{\text{F}}-\pi_{\text{F}}$  interstacking between the fluorinated rings of  $\text{C}_1\text{-C}_6\cdots\text{C}_1\text{-C}_6$  thiols [ $1-X, -Y, -Z, 3.504 \text{ \AA}; 3.318(2) \text{ \AA}; 1.127 \text{ \AA}; \text{ and } 0.00^\circ$ ]. In the case of LOKVUD, the following parameters were determined:  $\text{C}_1\text{-C}_6\cdots\text{C}_1\text{-C}_6$  thiolates [ $-X$ ,

$-Y, -Z, 3.636 \text{ \AA}; 1.426 \text{ \AA}; 3.346(3) \text{ \AA}; \text{ and } 0.00^\circ$  and  $\text{C}_1\text{-C}_6\cdots\text{C}_1\text{B-C}_6\text{B}$  thiolates [ $1-X, -Y, 1-Z, 3.645 \text{ \AA}; 3.412(3) \text{ \AA}; 1.282 \text{ \AA}; \text{ and } 0.00^\circ$ ].

**Discussion  $\pi_{\text{F}}-\pi_{\text{F}}$  interactions of Au complexes.** In general, it can be observed that the  $\pi_{\text{F}}-\pi_{\text{F}}$  interactions in LOKWEO and LOKVUD fully predominate when there are no non-covalent interactions that compete with them. It is also important to remember that, for the propagation of molecules to be favored, they must have high symmetry (ditopic and tetratopic arrangement). This is mentioned because, in the case of the other structures (BUSROZ and IMAKOZ), their lower symmetry group disfavors the establishment of 1D, 2D, or 3D networks. Concerning AROSV and AROSV01, a 1D network is formed, but  $\pi_{\text{F}}-\pi_{\text{F}}$  does not predominantly establish the interaction, and this is product of  $\pi_{\text{F}}-\pi_{\text{F}}$  and  $\pi_{\text{F}}-\pi$  contacts. Therefore, an

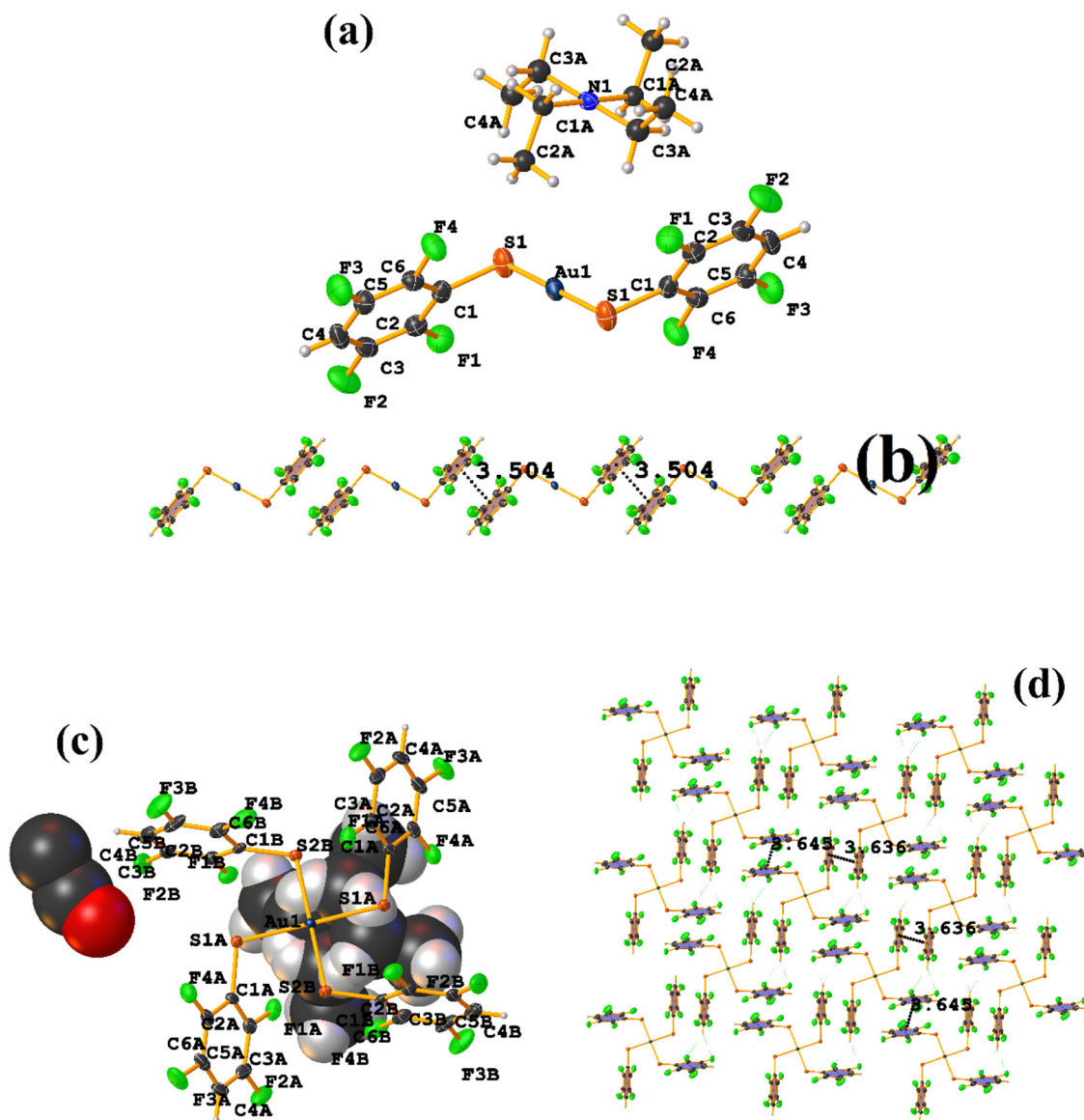


**Fig. 11** (a and c) Molecular structures of LOKWEO and LOKVUD. In the case of LOKVUD,  $\text{Et}_4\text{N}$  and  $\text{EtOH}$  are displayed in spacefill mode. (b and d) Stacking interactions LOKWEO and LOKVUD. In the case of both supramolecular structures, the molecules  $\text{Et}_4\text{N}$  or  $\text{EtOH}$  were omitted for clarity.



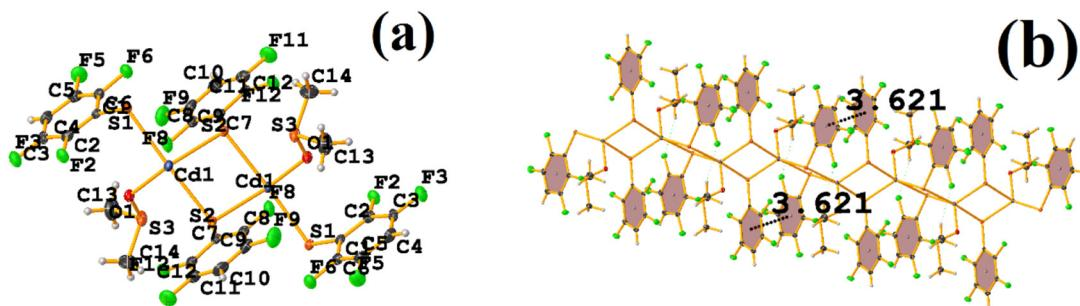


Fig. 12 (a) Molecular structure of CANVUL. (b) Stacking interactions of CANVUL.

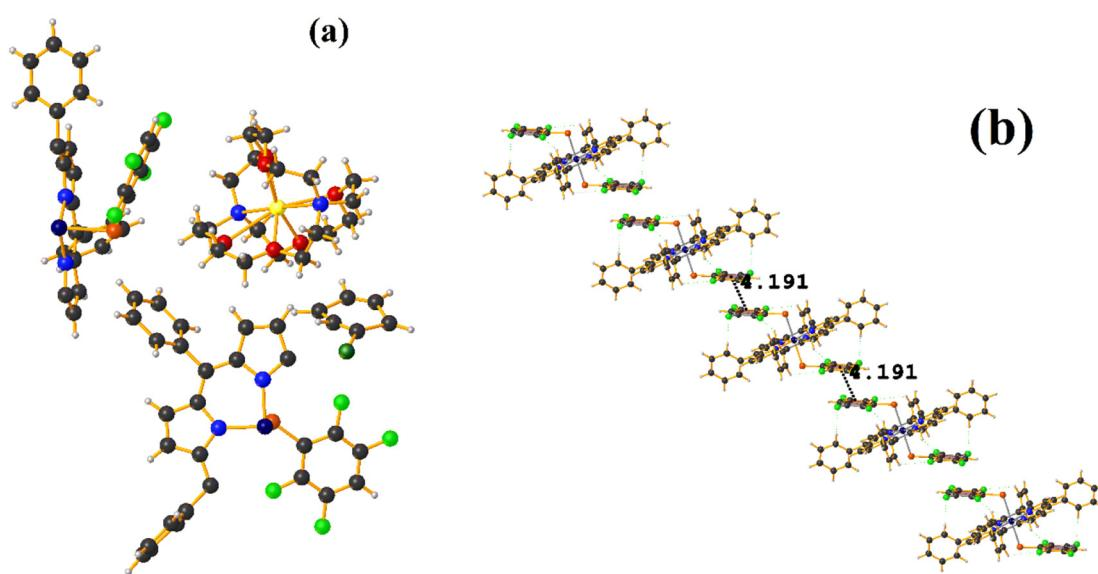


Fig. 13 (a) Molecular structure of COSJOJ. For clarity, the numbering of the atoms is not shown. (b) Stacking interactions of COSJOJ. For greater clarity, the molecules [Nac222] and  $C_6H_5Cl$  are not shown.

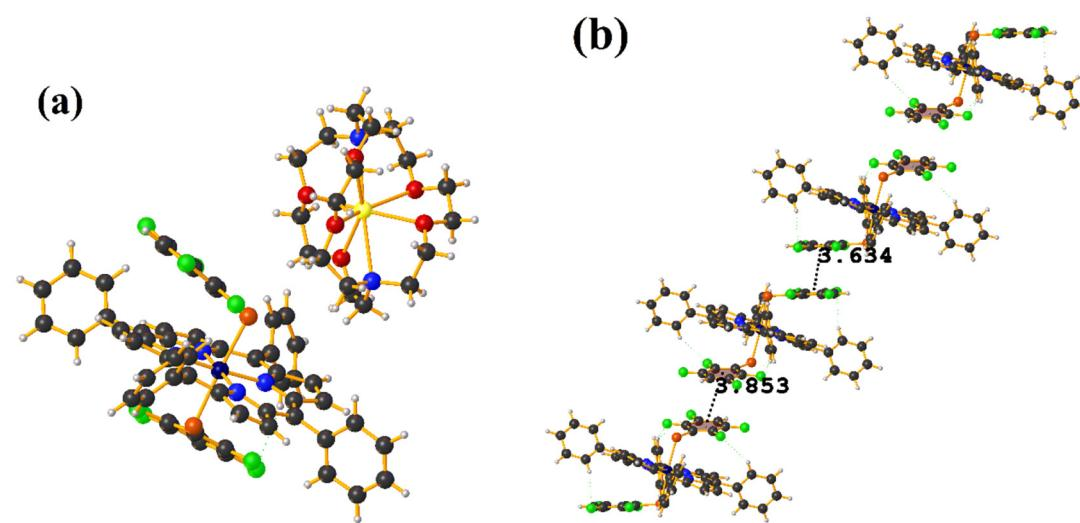


Fig. 14 (a) Molecular structure of COSJUP. For clarity, the numbering of the atoms is not shown. (b) Stacking interactions of COSJUP. For greater clarity, the molecule [Nac222] is not shown.



adequate balance between the appropriate symmetry group and no interaction impeding the  $\pi_F-\pi_F$  stacking can favor supramolecular networks.

### Cd metal complexes

**CANVUL.** Burwood *et al.*, through a private communication, deposited the structure *catena-[Cd(II)-bis(μ-2,3,5,6-SC<sub>6</sub>F<sub>4</sub>-H-4)₂(DMSO)]* (<https://doi.org/10.5517/ccdc.csd.cc1385q8>) (Fig. 12).

It can be observed in the supramolecular structure that a 1D network is formed, which is directed by the Cd-S coordination bond, forming a chain. In this way, an intra  $\pi_F-\pi_F$  stacking is established, determined by the chain imposed by the coordination bond Cd-S. The geometrical parameters were found: C1-C6…C7-C12 [1 + X, +Y, +Z, 3.621(3) Å; 3.4218(19) Å; 1.186 Å; and 4.0(2)°].

**Discussion  $\pi_F-\pi_F$  interactions of Cd complexes.** The CCDC search found that CANVUL was the only structure meeting the geometric parameters to be recognized as  $\pi_F-\pi_F$  stacking interaction. Given this, it is difficult to discuss, but it can be mentioned that establishing the 1D network, imposed by the Cd-S coordinative bond, forces the  $\pi_F-\pi_F$  stacking to occur. As mentioned in the introduction, the geometry adopted by the coordination compound will help to orient the ligand to another functional group, forming hydrogen bonds propagating the network. In this particular case, this imposed stacking.

### Co metal complexes

**COSJOJ.** Doppelt *et al.* have reported the synthesis of Co complexes of the type bis(thiolate)cobalt(III) *meso*-tetraphenyl

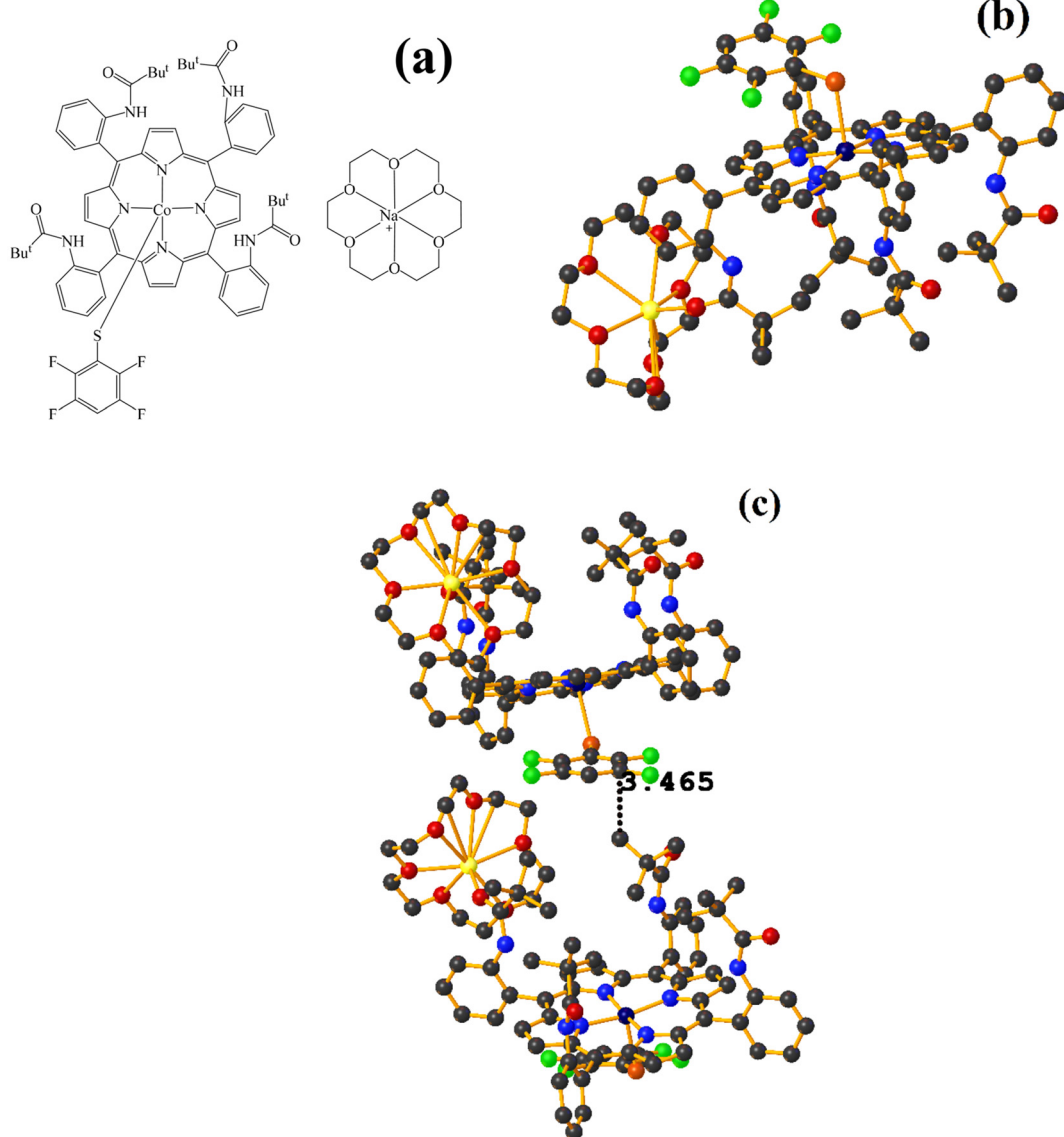


**Fig. 15** (a) Schematization of the molecular structure FOLWIM. (b) Molecular structure of FOLWIM. For clarity, the numbering of the atoms is not shown. (c) Supramolecular array of FOLWIM.



porphyrin.<sup>59</sup> The asymmetric unit of COSJOJ contains half of two crystallographically independent anions  $[\text{Co}(\text{III})(2,3,5,6-\text{SC}_6\text{F}_4\text{-H-4})_2(\text{TPP})]^-$  together with the cation  $[\text{NaC}222]$  and a  $\text{C}_6\text{H}_5\text{Cl}$  solvent molecule (where: TPP: *meso*-tetraphenyl porphyrin); and NaC222: 222 cryptand ( $4,7,13,16,21,24$ -hexaoxa-1,10-diazabicyclo[8.8.8]hexacosane), Fig. 13. COSJOJ forms 1D arrays through  $\pi_{\text{F}}-\pi_{\text{F}}$  interactions. It is highlighted that the geometric parameters indicate that they were found to be out of the cut-off to consider it a genuine stacking interaction C51-C56…C51-C56  $[-X, 1 - Y, 2 - Z, 4.192(5) \text{ \AA}; 3.346(3) \text{ \AA}; 2.525 \text{ \AA}; \text{ and } 0.0(4)^\circ]$ . At least in what concern to the ccd parameter, because considering ppa and slippage, it does comply.

**COSJUP.** COSJUP was also reported by Doppelt *et al.*<sup>60</sup> However, this structure did not present occluded  $\text{C}_6\text{H}_5\text{Cl}$ ,  $[\text{Co}(\text{III})(2,3,5,6-\text{SC}_6\text{F}_4\text{-H-4})_2(\text{TPP})][\text{NaC}222]$  compared with COSJOJ.<sup>59</sup> Different crystallization methods were used to obtain COSJOJ and COSJUP. In the case of the supramolecular arrangement of COSJUP, it is observed that a 1D arrangement exists through  $\pi_{\text{F}}-\pi_{\text{F}}$  interactions. In comparison with COSJOJ,

both established the same supramolecular arrangement. However, in the case of COSJUP, the parameters are within the cut-off to consider both to be true  $\pi_{\text{F}}-\pi_{\text{F}}$  interactions C45-C50…C45-C50  $[1 - X, -Y, -Z, 3.633(4) \text{ \AA}; 1.497 \text{ \AA}; \text{ and } 0.0(3)^\circ]$  and C51-C56…C51-C56  $[-X, 1 - Y, -Z, 3.853(4) \text{ \AA}; 3.218(3) \text{ \AA}; 2.119 \text{ \AA}; \text{ and } 0.0(3)^\circ]$  (Fig. 14).

**FOLWIM.** Doppelt *et al.* have published the preparation of complexes similar to those previously described  $[\text{Co}(\text{II})(2,3,5,6-\text{SC}_6\text{F}_4\text{-H-4})_2(\text{TPP})][\text{NaC}18\text{C}_6]$  (FOLWIN and FOLWOS), which compared with COSJOJ and COSJUP, the porphyrin is decorated with amide functional groups.<sup>60</sup> This probably influences the establishment of the  $\pi_{\text{F}}-\pi_{\text{F}}$  stacking since they were not formed. FOLWIM presents one cation of the crown ether  $[\text{NaC}18\text{C}_6]^+$  (18-crown-6) (Fig. 15).

**FOLWOS.** Like FOLWIN, this structure is similar, but with the difference that a dioxygen molecule is coordinated to the metallic center.<sup>60</sup> Also, this structure has no  $\pi_{\text{F}}-\pi_{\text{F}}$  interactions. Once again, the presence of amide functional groups prevents stacking from being established (Fig. 16).

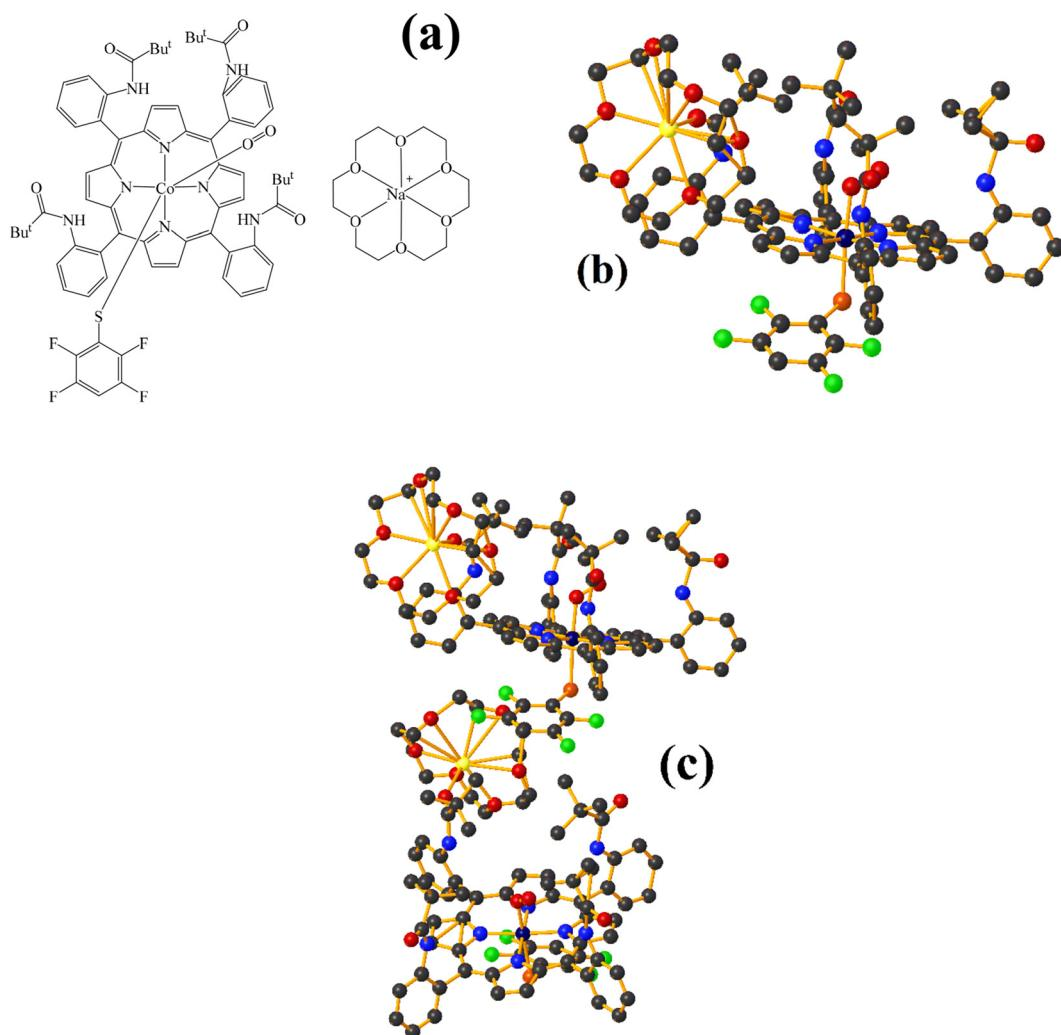


**Fig. 16** (a) Schematization of the molecular structure FOLWOS. (b) Molecular structure of FOLWOS. For clarity, the numbering of the atoms is not shown. (c) Supramolecular array of FOLWOS.



**Discussion  $\pi_F\cdots\pi_F$  interactions of Co complexes.** COSJOJ and COSJUP both structures establish stacking interactions. Even though the value of the ccd parameter for COSJOJ is above the limit, the other parameters are within the restrictions established to be considered genuine stacking. Both structures formed 1D packing structures through  $\pi_F\cdots\pi_F$  interactions. For both FOLWIN and FOLWOS, the fact that the porphyrin included amide groups prevents the stacking from forming. Again, the appearance of interactions that compete with stacking prevents their establishment.

### Fe metal complexes

**DIDCEY.** Doppelt *et al.* reported the synthesis of the low-spin complex containing a porphyrin derivative  $[\text{Fe}(\text{III})(2,3,5,6\text{-SC}_6\text{F}_4\text{-H-4})_2(\text{TPP})][\text{NaC18C}_6]\cdot\text{C}_6\text{H}_6$ , Fig. 17.<sup>61</sup> This complex presents two crystallographically independent centrosymmetric anions  $[\text{Fe}(2,3,5,6\text{-SC}_6\text{F}_4\text{-H-4})_2\text{TPP}]^-$  and two crown ether cations  $[\text{NaC18C}_6]^+$  and an occluded benzene molecule.

Supramolecularly it is observed that there is an  $\text{S1}\cdots\text{Na1}$  (red cotton balls, Fig. 17c) interaction between the S atom of the thiolate and the alkali metal of the cation  $[\text{NaC18C}_6]^+$ . This imposes the cation on both faces of the porphyrin, which prevents  $\pi_F\cdots\pi_F$  stacking interactions from forming since several  $\text{C}\cdots\text{H-C}$  interactions are established.

**GAHLIK and GAHLIK01.** Schappacher *et al.* reported obtaining the structure  $[\text{Fe}(\text{II})(2,3,5,6\text{-SC}_6\text{F}_4\text{-H-4})(\text{O}_2)(\text{TPP})][\text{KCl222}]_2\cdot(\text{C}_6\text{H}_5\text{Cl})(2,3,5,6\text{-SC}_6\text{F}_4\text{-H-4})(\text{H}_2\text{O})$ , Fig. 18.<sup>62</sup> According to the repository, the structures GAHLIK and GAHLIK01, are both cryptands and contain the  $\text{K}^+$  ion as cation. However, in the article, one structure has a  $\text{Na}^+$  ion and the other one  $\text{K}^+$ .

As seen in Fig. 18(b and c), it is observed that above the thiolate ring, there is the cryptand  $[\text{KCl222}]$  stabilized by interactions of type  $\text{C-H}\cdots\text{F-C}$ ,  $\text{S}\cdots\text{H-C}$ . This prevents stacking from being established. On the other side of the  $\text{TPP}^-$  ligand face, the amide groups stabilize the  $\text{Fe-O=O}$  fragment through  $\text{C-H}\cdots\text{O}$  contacts.

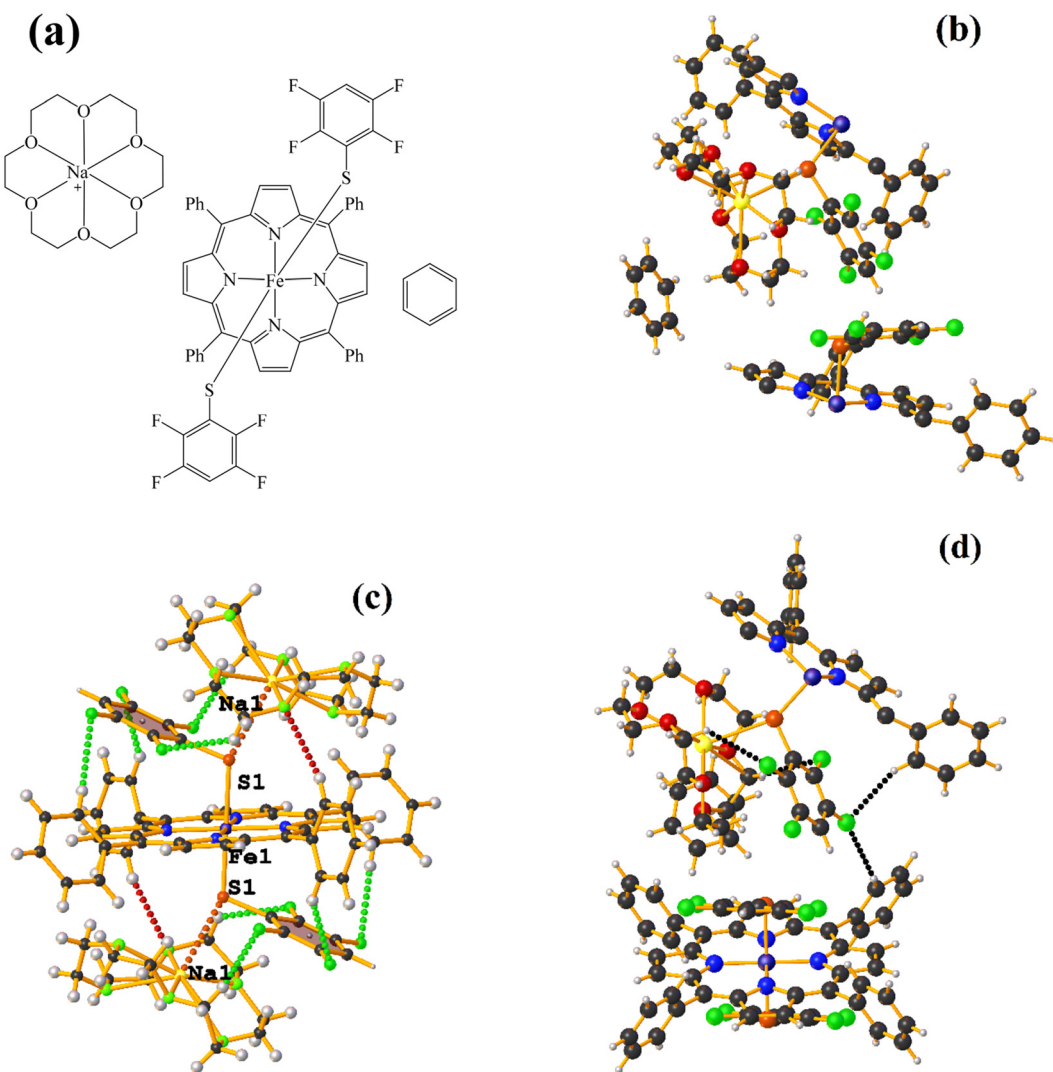


**Fig. 17** (a) Schematization of the molecular structure DIDCEY. (b) Molecular structure of DIDCEY. For clarity, the numbering of the atoms is not shown. (c and d) Supramolecular arrays of DIDCEY. For clarity, benzene is not shown.



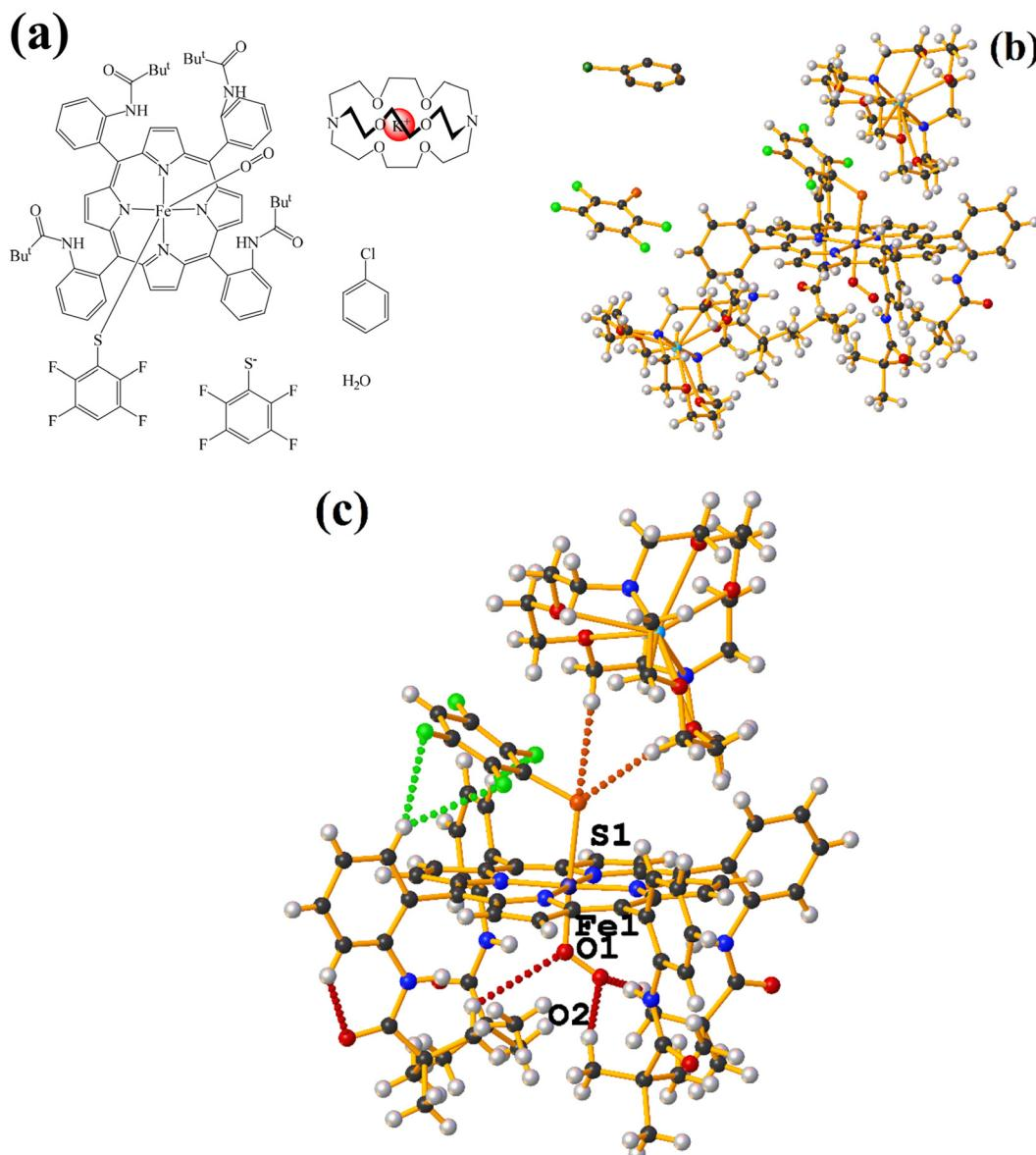


**Fig. 18** (a) Schematization of the molecular structure GAHLIK. (b) Molecular structure of GAHLIK. For clarity, the numbering of the atoms is not shown. (c) Supramolecular array of GAHLIK. For clarity, chlorobenzene and fluorinated thiolate are not shown.

**GAHLOQ.** Schappacher *et al.* also crystallized complex  $[\text{Fe}(\text{II})(2,3,5,6-\text{SC}_6\text{F}_4\text{-H-4})(\text{O}_2)\text{TPP}][\text{NaC}18\text{C}_6]$  GAHLOQ, Fig. 19.<sup>62</sup>

Again, as in GAHLIK, the amide groups help stabilize the Fe-bound dioxygen molecule. On the other hand, the fluorinated thiolate does not form stacking since it establishes interactions with the cation  $[\text{NaC}18\text{C}_6]$  of the C-H $\cdots$ F-C type.

**KULWOD.** Nasri *et al.* have reported the synthesis of the compound  $[\text{Fe}(\text{III})(2,3,5,6-\text{SC}_6\text{F}_4\text{-H-4})(\text{NO}_2)\text{TPP}][\text{KC}18\text{C}_6]\cdot(\text{C}_6\text{H}_6)$  (*n*-pentane) (KULWOD), Fig. 20.<sup>63</sup>

In this case the amide functional groups establish N-H $\cdots$ O-N interactions and on the other side of the TPP<sup>-</sup> ligand face, the thiolate exhibits C-H $\cdots$ F-C interactions, preventing stacking.

**Discussion  $\pi_{\text{F}}\cdots\pi_{\text{F}}$  interactions of Fe complexes.** The fact that the ligand TPP<sup>-</sup> contains amide groups influences stacking preventing them in all the crystalline structures analyzed in this series of Fe compounds. These functional groups usually form non-covalent interactions with the ligands attached apically to the Fe center. Therefore, the stronger competitive interactions avoid the stacking.

#### Ir metal complexes

**LULJOU.** Eslava-Gonzalez *et al.* have reported the synthesis of the Ir complex containing N-heterocyclic carbene  $[(\text{NHC})\text{Ir}(\text{I})(2,3,5,6-\text{SC}_6\text{F}_4\text{-H-4})(\text{COD})]$  (NHC: theophylline-imidazolylidene ligand; COD: 1,5-cyclooctadiene), Fig. 21.<sup>64</sup>

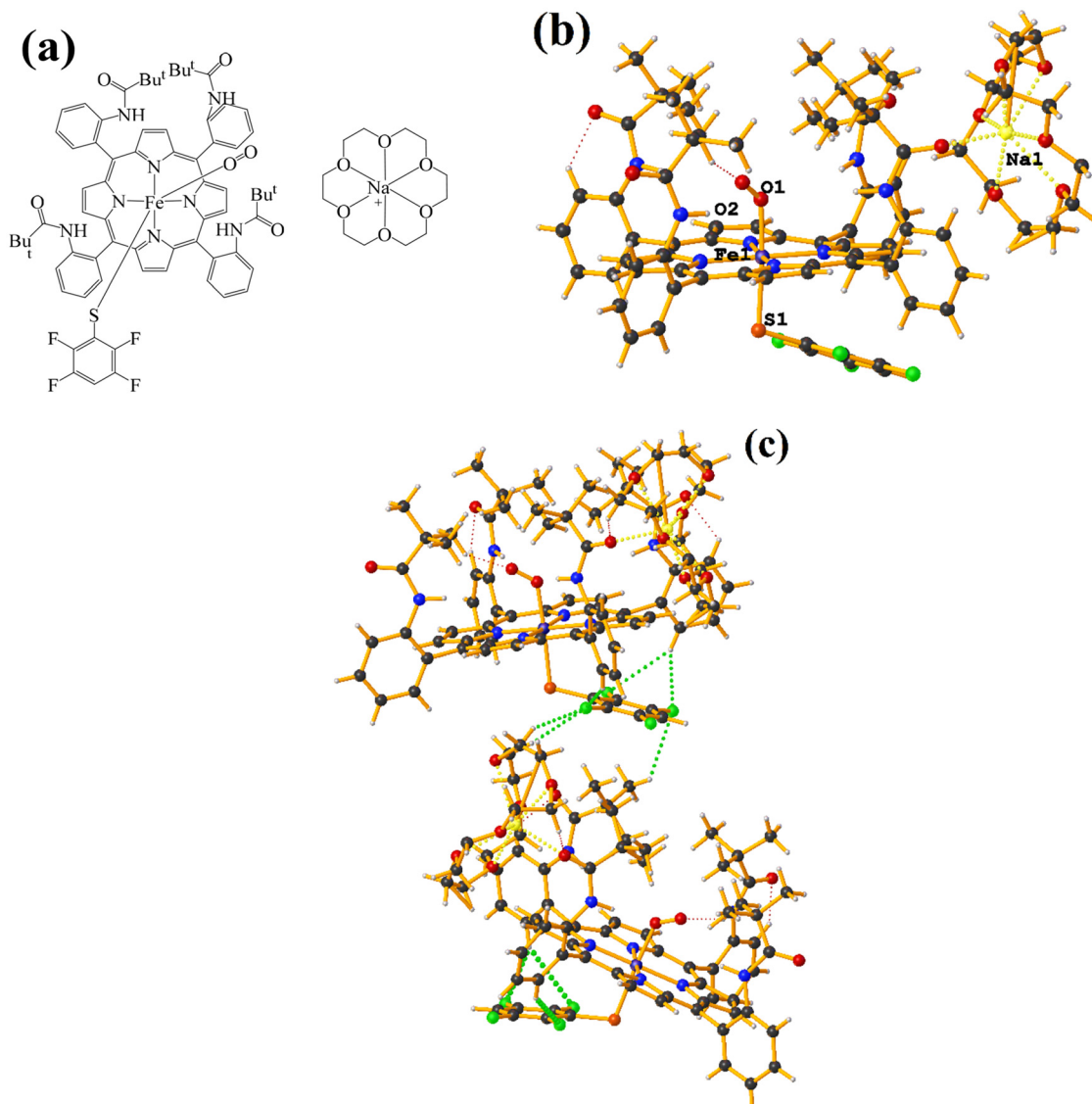


**Fig. 19** (a) Schematization of the molecular structure GAHLOQ. (b) Molecular structure of GAHLOQ. For clarity, the numbering of the atoms is not shown. (c) Supramolecular array of GAHLOQ.

The supramolecular arrangement shows a 2D array stabilized mainly by  $\pi$ - $\pi_F$  stacking and C-H...F-C and C-H...O=C hydrogen bonds. The stacking was established between the fluorinated ring of the thiolate and the six-membered ring of the theophylline C24-C29...N3/N4/C2-C5 [-1 + X, Y, Z, 3.856 (3) Å; 3.4334(17) Å; 2.096 Å; and 6.0(2)°] and C24-C29...N3/N4/C2-C5 [X, Y, Z, 3.624(3) Å; 3.3797(17) Å; 1.444 Å; and 6.0(2)°]. Stacking  $\pi$ - $\pi_F$  was favored since Janiak has mentioned that the stability order should be considered as follows:  $\pi_{\text{poor}}-\pi_{\text{poor}} > \pi_{\text{poor}}-\pi_{\text{rich}} > \pi_{\text{rich}}-\pi_{\text{rich}}$ .<sup>38</sup> In this case, hierarchical stacking occurred between the two most electronically deficient rings.

**Discussion  $\pi_F$ - $\pi_F$  interactions of Ir complexes.** Only LULJOU was returned among the results obtained through ConQuest for structures containing Ir. As mentioned above stacking was established between the two most electronically deficient rings.

### Ni metal complexes

**WUNQUR.** Usón *et al.* have reported the synthesis of WUNQUR  $[\text{Ni}(\text{n})(2,3,5,6-\text{SC}_6\text{F}_4-\text{H}-4)_2(\text{dppe})]$  (dppe: 1,2-bis (diphenylphosphine)ethane), Fig. 22.<sup>65</sup>

In the supramolecular structure there is intra  $\pi$ - $\pi_F$  stacking C9-C14...C27-C32 [X, Y, Z, 3.448(3) Å; 3.367(2) Å; 1.072 Å; and 7.1(3)°]. The 1D arrangement is not due to this interaction but to the C-F...H-C and S...S contacts.

**WUNRAY.** Usón *et al.* also reported the preparation of  $[(\text{dppe})\text{Ni}(\text{n})(\mu-2,3,5,6-\text{SC}_6\text{F}_4-\text{H}-4)_2\text{Pd}(\text{n})(\text{C}_6\text{F}_5)_2]$  WUNRAY, Fig. 23.<sup>65</sup> This dinuclear complex forms 1D supramolecular structures establishing various  $\pi$ - $\pi_F$ ,  $\pi$ - $\pi$ , and  $\pi_F$ - $\pi_F$  interactions. The  $\pi$ - $\pi_F$  interaction is established between a dppe ring and the thiolate ring C9-C14...C27-C32 [X, Y, Z, 3.4643(19) Å; 3.3071(14) Å; 0.713 Å; and 5.52(15)°]. In the case



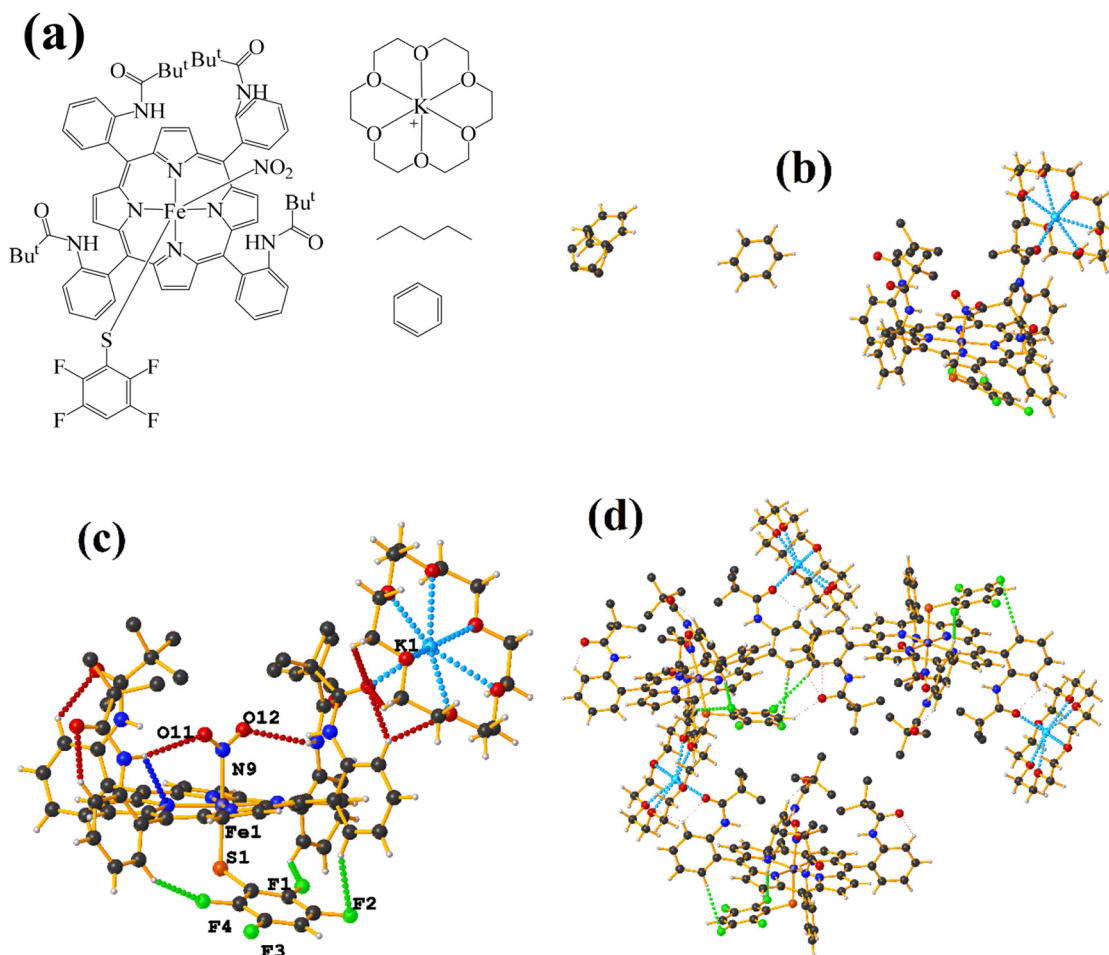


Fig. 20 (a) Schematization of the molecular structure KULWOD. (b and c) Molecular structure of KULWOD. (d) Supramolecular array of KULWOD. For clarity, benzene and *n*-pentane are not shown.

of the  $\pi$ - $\pi$ , and  $\pi_F$ - $\pi_F$  interactions, they were formed between a dppe and the thiolate ring C9-C14...C9-C14 [ $-X$ ,  $1 - Y$ ,  $-Z$ ,  $3.900$  (2) Å;  $3.3713(14)$  Å;  $1.961$  Å; and  $0.00$  (16)°], and the latter between two tetrafluorinated rings of two thiolates C27-C32...C27-C32 [ $-X$ ,  $-Y$ ,  $-Z$ ,  $3.3915(18)$  Å;  $3.1879(12)$  Å;  $1.158$  Å; and  $0.00(14)$ °].

**Discussion  $\pi_F$ - $\pi_F$  interactions of Ni complexes.** Of the two deposited structures that met the search criteria (mononuclear (WUNQUR) and dinuclear), only the bimetallic complex (WUNRAY) presented the desired interaction  $\pi_F$ - $\pi_F$ , as well as a wide variety of stacking interactions. It is difficult to explain accurately using only geometric parameters as to why the change from mononuclear to dinuclear, the incorporation of Pd, and the presence of pentafluorinated rings influence the formation of interactions  $\pi_F$ - $\pi_F$ ,  $\pi$ - $\pi$ , and  $\pi_F$ - $\pi_F$ . This indicates that in the dinuclear complex, the dppe and tetrafluorinated thiolate rings must be very similar energetically and form the interactions mentioned above. In the case of the pentafluorinated ring, it must be energetically different since it does not establish stacking with the other rings. This based on the premise:  $\pi_{\text{poor}}-\pi_{\text{poor}} > \pi_{\text{poor}}-\pi_{\text{rich}} > \pi_{\text{rich}}-\pi_{\text{rich}}$ .<sup>38</sup>

## Os metal complexes

**ECERIP and ECERIP01.** Cerón *et al.* have published the formation of the complex  $[\text{Os}(\text{iv})(2,3,5,6-\text{SC}_6\text{F}_4\text{-H-4})_2(\text{SC}_6\text{F}_3\text{-H-4}(2,3,5,6-\text{SC}_6\text{F}_4\text{-H-2})(\text{C}_6\text{H}_5)]$  product of the thermolysis of the compound  $[\text{Os}(2,3,5,6-\text{SC}_6\text{F}_4\text{-H-4})_4(\text{PPh}_3)]$  in non-dried toluene.<sup>66</sup> ECERIP and ECERIP01 appear in the CSD, referring to the same reference. In this case, we used ECERIP to carry out the analysis (Fig. 24).

This structure exhibited several types of stacking:  $\pi$ - $\pi_F$  and  $\pi_F$ - $\pi_F$ . With the expected  $\pi_F$ - $\pi_F$  interaction found on C19-C24...C19-C24 [ $1 - X$ ,  $Y$ ,  $3/2 - Z$ ,  $3.654(4)$  Å;  $3.348(3)$  Å;  $1.463$  Å; and  $2.7$  (3)°]. Stacking was also observed between a ring of one tetrafluorinated thiolate and the phenyl that is attached to Os: C19-C24...C25-C30 [ $X$ ,  $Y$ ,  $Z$ ,  $3.686(4)$  Å;  $3.418(3)$  Å; not found; and  $23.1(3)$ °]. A  $\pi$ - $\pi_F$  interaction was also found between the ring of the trifluorinated fragment that forms the metallacycle ( $\text{SC}_6\text{F}_3\text{-H-4}$ ) with the phenyl that is bonded to Os: C1-C6...C25-C30 [ $1 - X$ ,  $1 - Y$ ,  $1 - Z$ ,  $3.932(4)$  Å;  $3.702(2)$  Å;  $1.673$  Å; and  $19.0$  (3)°]. All rings participating in the observed stackings must be energetically similar.

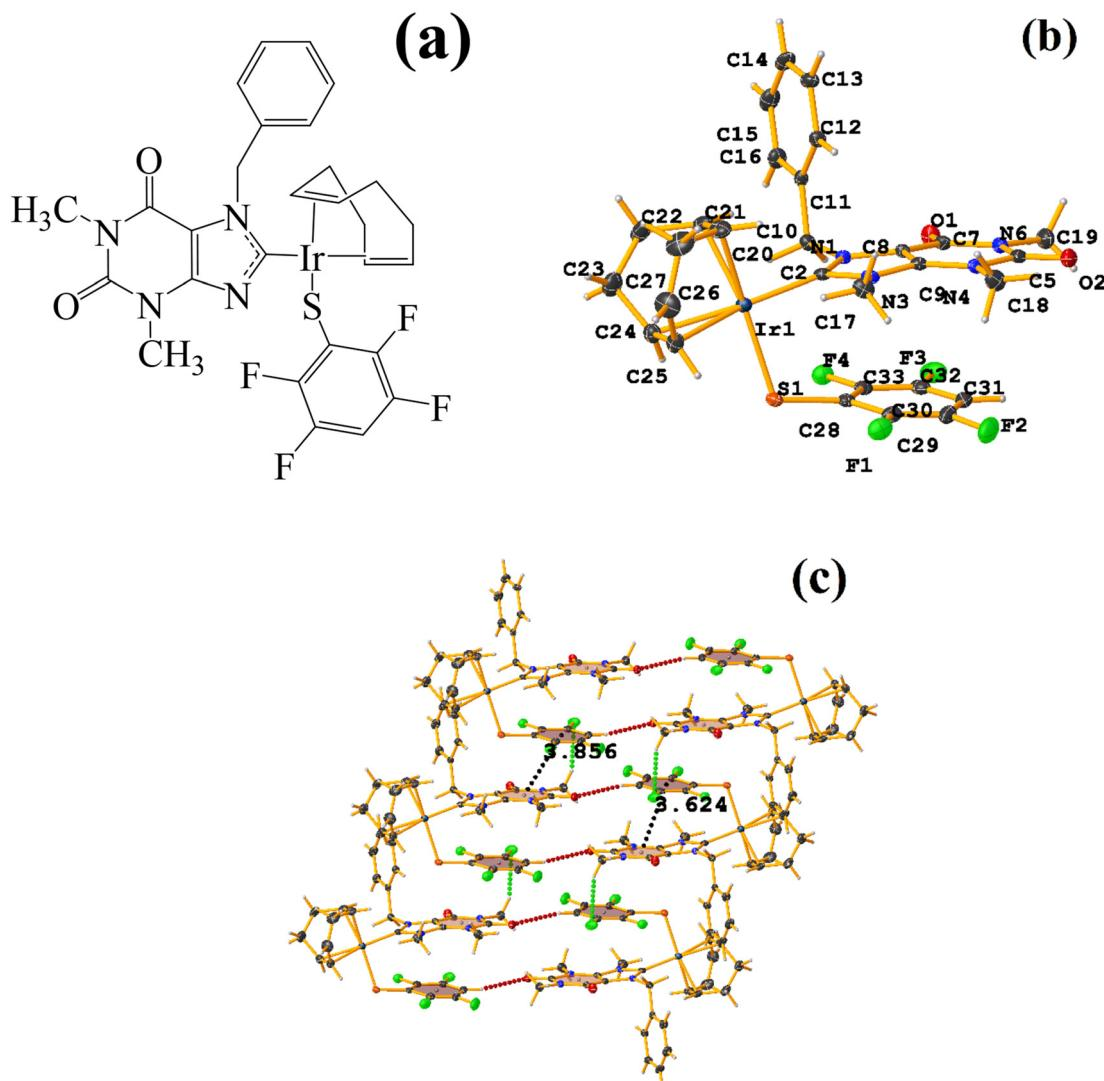


Fig. 21 (a) Schematization of the molecular structure LULJOU. (b) Molecular structure of LULJOU. (c) Supramolecular array of LULJOU.

**ERUHII.** Arroyo *et al.* have published the formation of the complex *trans*-[Os(III)(SR<sub>F</sub>)<sub>2</sub>(S<sub>2</sub>CSR)(PMe<sub>2</sub>Ph)<sub>2</sub>] (R: 2,3,5,6-SC<sub>6</sub>F<sub>4</sub>-H-4), Fig. 25.<sup>67</sup> Although the results from Conquest showed the establishment of stacking, when checking the structure we didn't find any  $\pi_F\cdots\pi_F$  interaction. Packing stabilization is mainly carried out by C-H $\cdots$ F-C and S $\cdots$ S interactions.

**GENWOM.** Cerón *et al.* have described the obtaining of the complex [Os(IV)(2,3,5,6-SC<sub>6</sub>F<sub>4</sub>-H-4)<sub>4</sub>(PPh<sub>3</sub>)<sub>0.5</sub>C<sub>6</sub>H<sub>14</sub>], Fig. 26.<sup>68</sup> The hexane solvate presents disorder in the structure.

In the packaging, the  $\pi_F\cdots\pi_F$  stacking indicated by Conquest is observed, which is intramolecular C19-C24 $\cdots$ C37-C42 [X, Y, Z, 3.464(6) Å; 3.415(4) Å; 1.318 Å; and 13.0(5)°]. And, a 1D network assisted by C-H $\cdots$ F-C and C-H $\cdots$ S interactions is observed.

**HANGEI.** Collman *et al.* report the obtaining of the Os porphyrin compound containing the tetrafluorinated thiolate [Os(IV)(TPP)(2,3,5,6-SC<sub>6</sub>F<sub>4</sub>-H-4)<sub>2</sub>]·C<sub>6</sub>H<sub>12</sub>, Fig. 27.<sup>69</sup> Searching for the stacking interactions indicated by Conquest, it was

observed that it is an interaction between the metallocycle Os1/N1/C10-C12/N2 and the tetrafluorinated thiolate ring C1-C6: [-X, -Y, -Z, 3.699(5) Å; 2.899(2) Å; not defined; and 26.3(4)°]. The other stacking was formed between the metallocycle Os1/N1A/C10A-C12A/N2A and the tetrafluorinated thiolate ring C1-C6: [X, Y, Z, 3.699(5) Å; 3.592(4) Å; not defined; and 26.3(4)°].

As seen in Fig. 27, the interaction ( $\pi_F\cdots\pi$ , 3.699 Å) indicated by Conquest is established internally. However, the tetrafluorinated thiolate rings do not exhibit any  $\pi_F\cdots\pi_F$  stacking, and instead, 1D networks are formed due to the centrosymmetric C-F $\cdots$ H-C interaction, R<sub>2</sub><sup>2</sup>(8).<sup>70,71</sup>

**HENXIH y HENXIH01.** Firstly, Arroyo *et al.* published complex HENXIH [Os(IV)(PPh<sub>3</sub>)(2,3,5,6-SC<sub>6</sub>F<sub>4</sub>-H-4)<sub>4</sub>], which crystallized in the triclinic *P*1 space group, Fig. 28.<sup>72</sup> However, years later, Zeleny *et al.* reported obtaining a polymorph of this structure, which is monoclinic *P*2<sub>1</sub>/c (HENXIH01).<sup>73</sup> From the point of view of the molecular structure, there are differ-

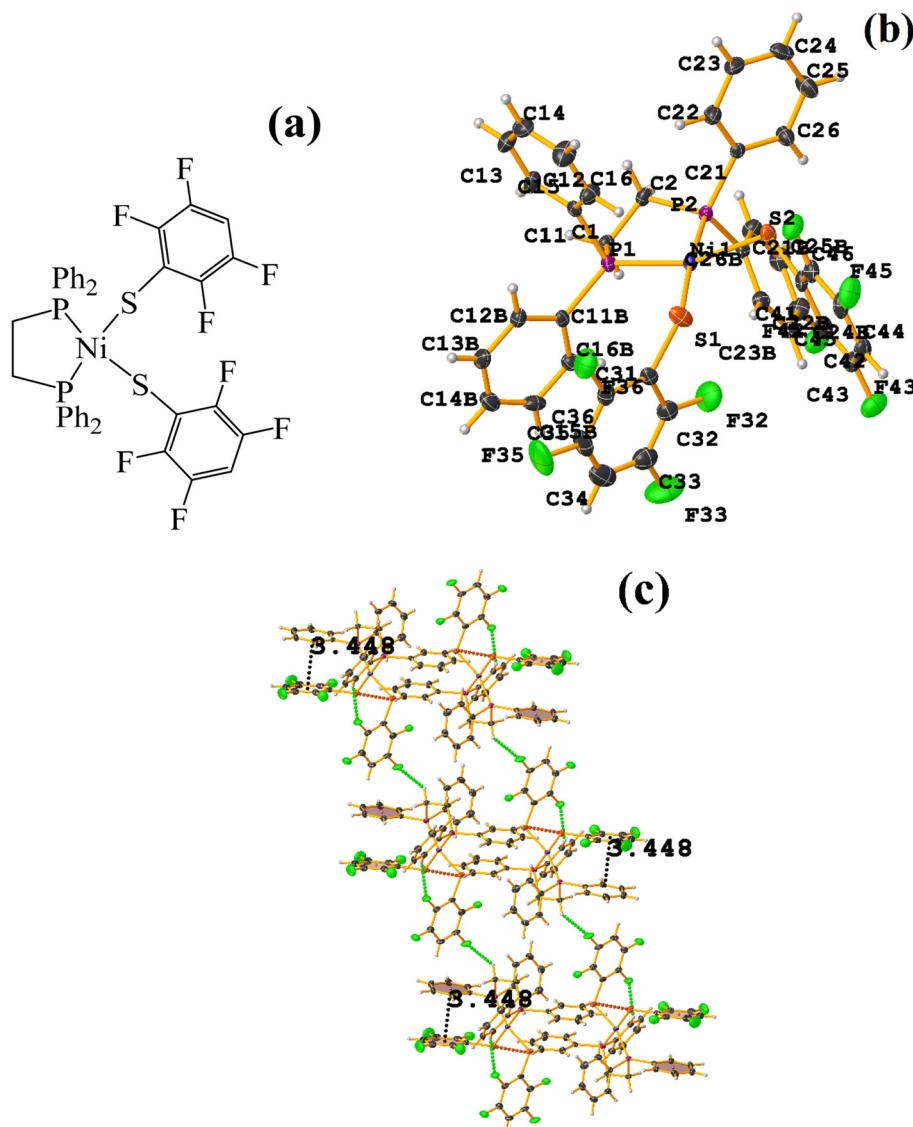


Fig. 22 (a) Schematization of the molecular structure WUNQUR. (b) Molecular structure of WUNQUR. (c) Supramolecular array of WUNQUR.

ences in the conformations adopted by the polymorphs, mainly with aromatic rings (either thiolates or phosphine) that affect the establishment of stacking, Fig. 28f.

Analyzing the supramolecular arrangement of HENXIH, it is observed that different type stackings ( $\pi_F-\pi_F$  intra and intermolecular) were formed. Regarding the intramolecular  $\pi_F-\pi_F$  interaction, the following parameters were found: C19-C24...C19-C24:  $[-X, -Y, -Z, 3.75(2) \text{ \AA}; 1.955 \text{ \AA}; \text{ and } 0^\circ]$ . On the other hand, the inter  $\pi_F-\pi_F$  stacking showed the following values: C19-C24...C25-C30:  $[X, Y, Z, 3.334(16) \text{ \AA}; 3.185(13) \text{ \AA}; 0.981 \text{ \AA}; \text{ and } 8^\circ]$ . There is another inter  $\pi_F-\pi$  stacking, but according to the parameters, these are outside the cut-off to consider it a genuine interaction. This was established between a phosphine ring and another fluorinated thiolate ring: C1-C6-C25-C30:  $[-X, 1 - Y, 1 - Z, 4.325(14) \text{ \AA}; 3.586(11) \text{ \AA}; 2.897 \text{ \AA}; \text{ and } 9^\circ]$ .

In the case of the other polymorph HENXIH01, only the intra  $\pi_F-\pi_F$  stacking was observed, with the following parameters: C19-C24...C31-C36:  $[X, Y, Z, 3.363(6) \text{ \AA}; 3.172(4) \text{ \AA}; 0.663 \text{ \AA}; \text{ and } 11.3(5)^\circ]$ . Additionally, another  $\pi_F-\pi$  interaction was found, which is outside the cut-off parameters: C1-C6...C31-C36:  $[-X, 1 - Y, 1 - Z, 4.359(5) \text{ \AA}; 3.577(3) \text{ \AA}; 3.101 \text{ \AA}; \text{ and } 10.5(4)^\circ]$ . It is highlighted that instead of finding several stacking as was the case in HENXIH, the formation of T-shaped interactions (Fig. 4), C-H... $\pi$  were identified: C9-H7...C19-C24  $[X, 3/2 - Y, -1/2 + Z, 2.88 \text{ \AA} \text{ and } 140^\circ]$ , C11-H9...C1-C6 and  $[1 - X, 1 - Y, 1 - Z, 2.95 \text{ \AA} \text{ and } 147^\circ]$ . This indicates that the different conformations adopted by the polymorphs affect in such a way that the arrangement of the rings is parallel on the same axis so that stacking is established, but in the other polymorph, this array is lost, and the interaction T-shaped is favored.

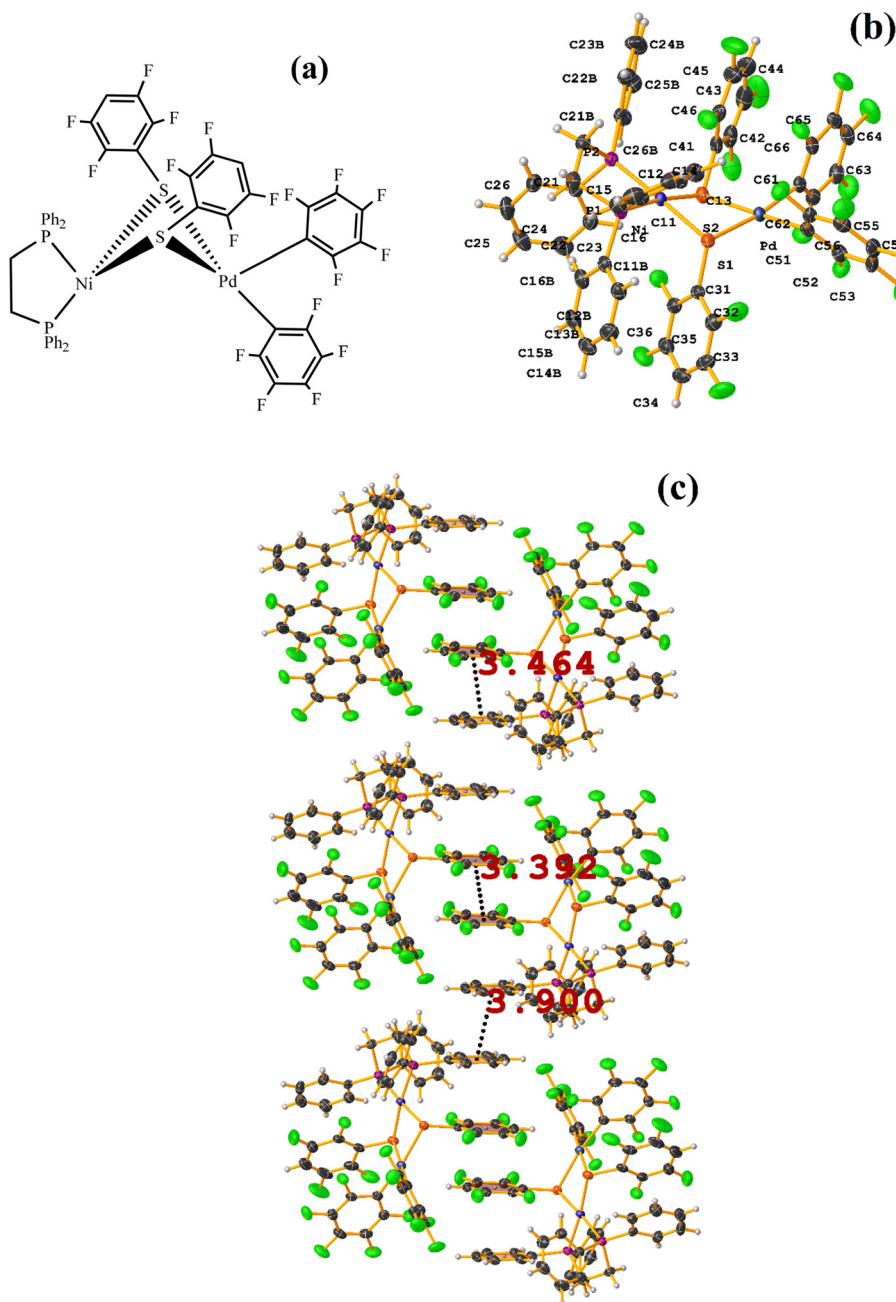


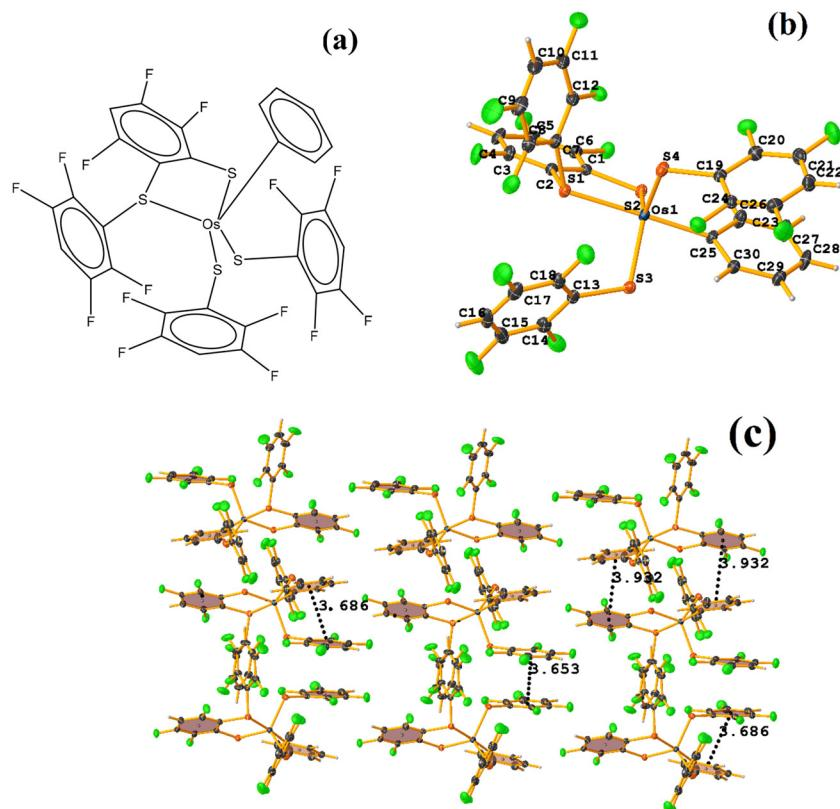
Fig. 23 (a) Schematization of the molecular structure WUNRAY. (b) Molecular structure of WUNRAY. (c) Supramolecular array of WUNRAY.

**QQEHO.** Cerón *et al.* described the preparation of the  $[\text{Os}(\text{iv})(2,3,5,6-\text{SC}_6\text{F}_4\text{-H-4})_4(\text{PPh}_2(\text{C}_6\text{F}_5))]$  complex, Fig. 29.<sup>74</sup>

When analyzing the structure supramolecularly, the stacking indicated by Conquest was observed: C13–C18...C19–C24:  $[X, Y, Z, 3.537(5) \text{ \AA}; 3.350(4) \text{ \AA}; 1.456 \text{ \AA}; \text{and } 13.4(4)^\circ]$ . This  $\pi_{\text{F}}-\pi_{\text{F}}$  interaction is established intramolecularly between two fluorinated benzene-thiolate rings. Additionally, two other  $\pi_{\text{F}}-\pi_{\text{F}}$  interactions were found that cannot be considered stackings since they are outside the established parameters. The first is established between the pentafluorinated ring of phosphine and a tetrafluorinated ring of a thiolate: C25–C30...C19–

C24:  $[X, 1/2 - Y, -1/2 + Z, 4.663(5); 3.607(3) \text{ \AA}; 3.570 \text{ \AA}; \text{and } 11.9(4)^\circ]$ . Interestingly, although it is not considered a true stacking, this interaction was formed between a pentafluorinated...tetrafluorinated ring. In the case of the other interaction, it occurred intermolecularly between two fluorinated rings of two thiolates: C1–C6...C13–C18:  $[2 - X, -1/2 + Y, 3/2 - Z, 4.250 (6) \text{ \AA}; 3.553(4) \text{ \AA}; 2.553 \text{ \AA}; \text{and } 5.0(4)^\circ]$ .

**QQEJAW.** Also, Cerón *et al.* reported obtaining the complex  $[\text{Os}(\text{iv})(2,3,5,6-\text{SC}_6\text{F}_4\text{-H-4})_4(\text{P}(\text{OPh})_3)]$ , Fig. 30.<sup>74</sup> At first glance, the stacking  $\pi_{\text{F}}-\pi$  indicated by Conquest was observed: C25–C30...C31–C36:  $[1 + X, Y, Z, 3.778(4) \text{ \AA}; 3.774(3) \text{ \AA}; 0.853 \text{ \AA}; \text{and } 11.9(4)^\circ]$ .



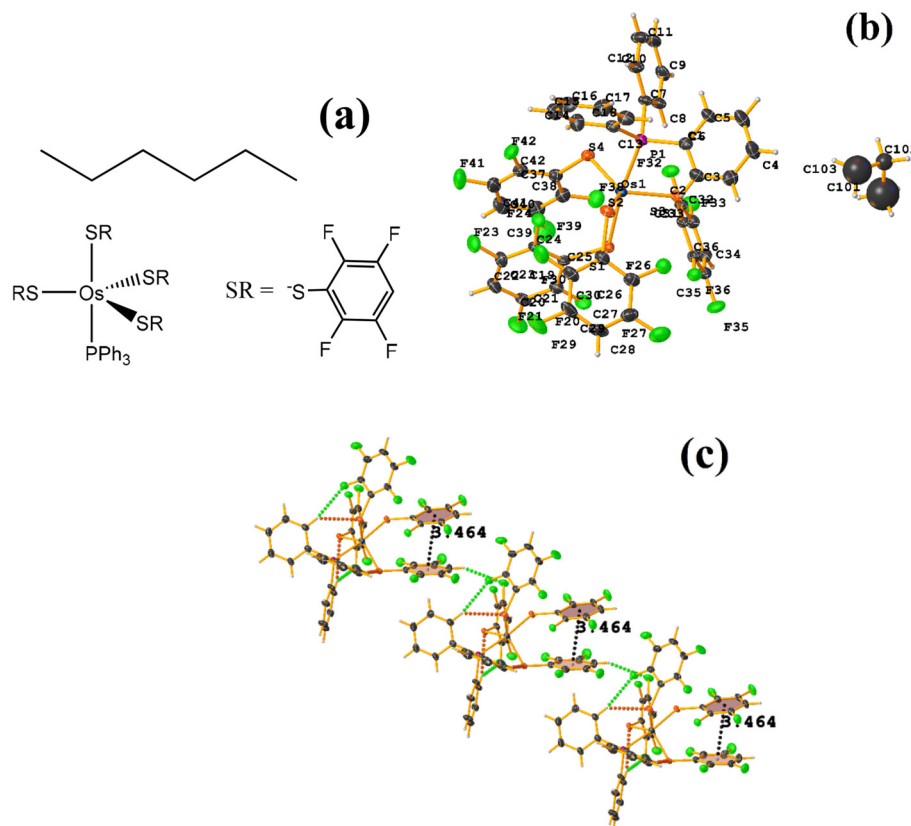


Fig. 26 (a) Schematization of the molecular structure GENWOM. (b) Molecular structure of GENWOM. (c) Supramolecular array of GENWOM.

12.1(3)°]. It must be mentioned that this interaction occurred between a tetrafluorinated ring of the thiolate and the ring of the O-Ph substituent of the phosphine. Additionally, another stack was observed that was found outside the parameters: C19-C24…C19-C24: [2 - X, 2 - Y, 1 - Z, 4.550(3) Å; 3.395(3) Å; 3.030 Å; and 0.0(3)°]. It is important to note that although this interaction is outside the geometric parameters, this serves as a bridge to establish the previously mentioned interaction between the aromatic ring of the phosphinite and the tetrafluorinated ring of the thiolate.

**ZAWWAV.** Moreno-Esparza *et al.* reported the synthesis of the compound [Os(III)(2,3,5,6-SC<sub>6</sub>F<sub>4</sub>H-4)<sub>2</sub>(SOC-CH<sub>3</sub>)(P(CH<sub>3</sub>)<sub>2</sub>Ph)<sub>2</sub>], Fig. 31.<sup>75</sup> The structure presented two crystallographically independent molecules. The results obtained by Conquest indicate the presence of different stackings, but when conducting the analysis, we found only two different types of  $\pi_F$ - $\pi_F$  interactions.

The first one found was: C3-C8…C3-C8: [1 - X, 1 - Y, 2 - Z, 3.647(4) Å; 3.323(2) Å; 1.502 Å; and 0.0(3)°]. However, Conquest does not indicate its presence within the analysis. The second exhibited the following parameters: C39-C44…C39-C44: [1 - X, 1 - Y, 1 - Z, 3.538(4) Å; 3.344(3) Å; 1.154 Å; and 0.0(3)°]. When comparing ERUHII [Os(III)(SR)<sub>2</sub>(S<sub>2</sub>CSR)(PMe<sub>2</sub>Ph)<sub>2</sub>] (R: 2,3,5,6-SC<sub>6</sub>F<sub>4</sub>H)<sup>67</sup> with ZAWWAV, it is observed that the two compounds are very similar structurally speaking, except by the thiocarboxylate and carboxylate

ligands. One has a terminal -CH<sub>3</sub> (ZAWWAV), and the other a fluorinated thiolate (2,3,5,6-SC<sub>6</sub>F<sub>4</sub>H) (ERUHII). This change may affect whether the  $\pi_F$ - $\pi_F$  interactions are established in this case. In the case of ERUHII, the  $\pi_F$ - $\pi_F$  interactions were not established; otherwise, these stackings were observed with ZAWWAV. We do not have a clear explanation as to why this situation occurred.

**Discussion  $\pi_F$ - $\pi_F$  interactions of Os complexes.** In this section, many structures met the parameters agreed with Conquest. The structures presented various geometries around the metallic center: octahedral and trigonal bipyramidal. This had no direct effect on establishing  $\pi_F$ - $\pi_F$  stackings since this interaction was observed interchangeably in both geometries. However, other properties were found that did influence the establishment of stacking. Firstly, we can talk about the case of polymorphism presented by structures HENXIH and HENXIH01. As seen in the molecular overlay between both structures, Fig. 28f, small differences, mainly conformational, in the spatial arrangement of the rings (primarily the tetrafluorinated ones of the thiolates) affect in such a way that in the *P*1 polymorph presented a large amount of intra and inter stacking  $\pi_F$ - $\pi_F$ , and in the case of the other these were more limited in number. It is highlighted that the  $\pi_F$ - $\pi_F$  interactions observed in the polymorph *P*1, were transformed into a T-shaped conformation on the other. In the case of ERUHII and ZAWWAV both complexes are structurally similar. But the



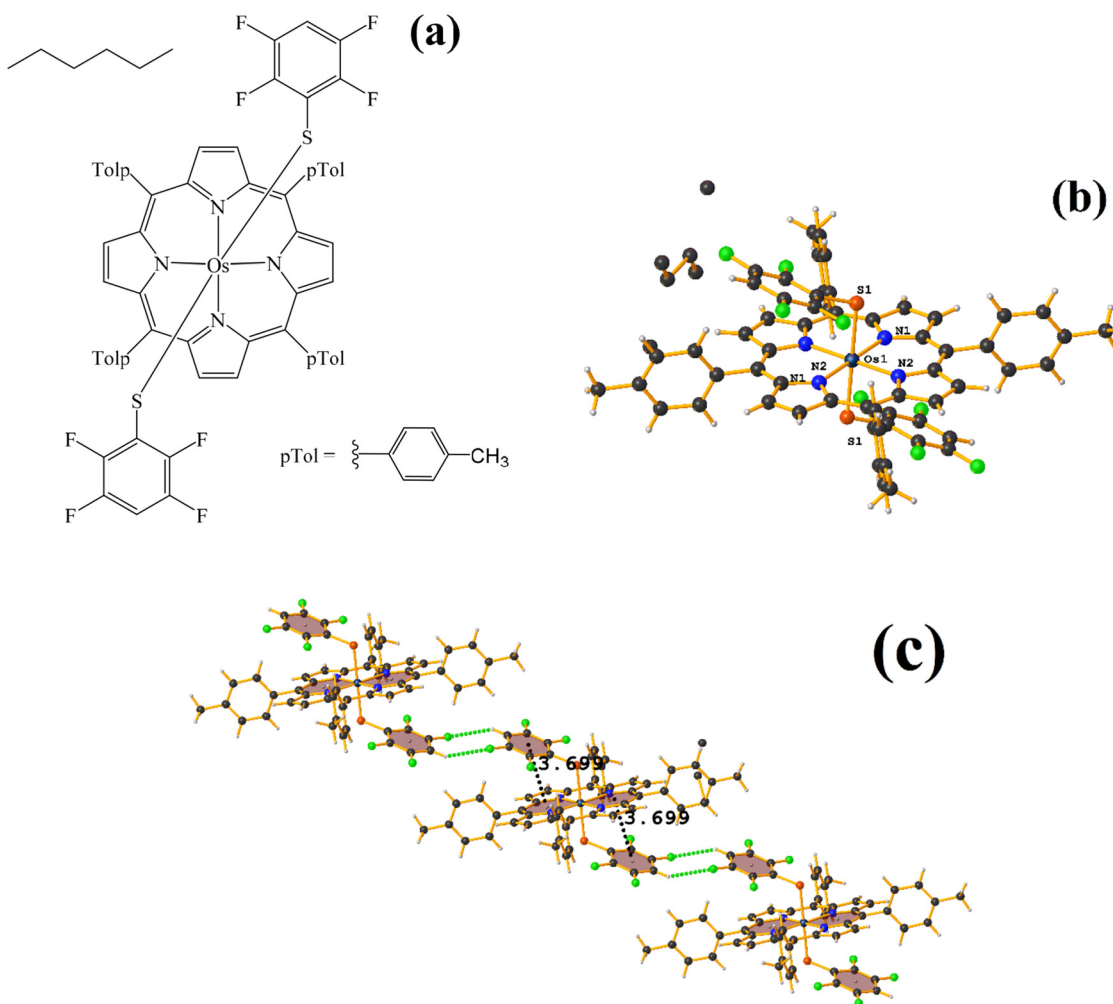


Fig. 27 (a) Schematization of the molecular structure HANGEI. (b) Molecular structure of HANGEI. (c) Supramolecular array of HANGEI.

changes mainly in the thiocarboxylate and carboxylate ligands (one has a  $-\text{CH}_3$  terminal (ZAWWAV), and the other a fluorinated thiolate (2,3,5,6- $\text{SC}_6\text{F}_4\text{H}$ )) influence such that the first presents stacking and in the other no. In the other cases, according to Conquest, the structures exhibited stacking. However, the  $\pi_{\text{F}}-\pi_{\text{F}}$  was not found when performing the analysis, and T-shape and C-F $\cdots$ H-C interactions, among others, were observed.

### Pb metal complexes

**CANWIA.** In a private communication, Burwood deposited the structure *catena*-[Pb( $\text{n}$ )-bis( $\mu$ -2,3,5,6- $\text{SC}_6\text{F}_4\text{H}$ )<sub>2</sub>(2,3,5,6- $\text{SC}_6\text{F}_4\text{H}$ )<sub>2</sub>] with the CCDC (<https://doi.org/10.5517/ccdc.csd.cc1385tc>), Fig. 32. When reviewing the structure supramolecularly, it is similar to what was observed in CANVUL *catena*-[Cd-bis( $\mu$ -2,3,5,6- $\text{SC}_6\text{F}_4\text{H}$ )<sub>2</sub>(DMSO)<sub>2</sub>] (<https://doi.org/10.5517/ccdc.csd.cc1385q8>).

Reviewing the structure, we found two types of  $\pi_{\text{F}}-\pi_{\text{F}}$  stackings. Notably, one was not detected through Conquest. The first presented the following parameters: C1-C6 $\cdots$ C7-C12: [-X,

2 - Y, 1 - Z, 3.589(3) Å; 3.341(2) Å; 1.374 Å; and 1.5(3)°]. And the other stacking presents values of: C1-C6 $\cdots$ C7-C12: [1 - X, 2 - Y, 1 - Z, 3.526(3) Å; 3.343(2) Å; 1.167 Å; and 1.5(3)°]. In this way,  $\pi_{\text{F}}-\pi_{\text{F}}$  stackings are established, but the Pb-S coordination bond imposes them. It should also be noted in CANVUL.

**Discussion  $\pi_{\text{F}}-\pi_{\text{F}}$  interactions of Pb complexes.** Only one structure containing Pb was found returned by Conquest. Establishing a 1D network imposed by the Pb-S coordinative bond, which requires observing the  $\pi_{\text{F}}-\pi_{\text{F}}$  stacking. It has already been mentioned that the geometry adopted by the coordination compound will help to orient the ligand, in this case, propagating towards the formation of a network. In this case, the coordination bond enforced these stackings.

### Pd metal complexes

**GUQBUQ.** Basauri-Molina *et al.* described the synthesis of the complex [Pd( $\text{n}$ )(2,3,4,6- $\text{SC}_6\text{F}_4\text{H}$ )<sub>2</sub>(TMEDA)], TMEDA: *N,N,N',N'*-tetramethylethylenediamine, Fig. 33.<sup>76</sup>

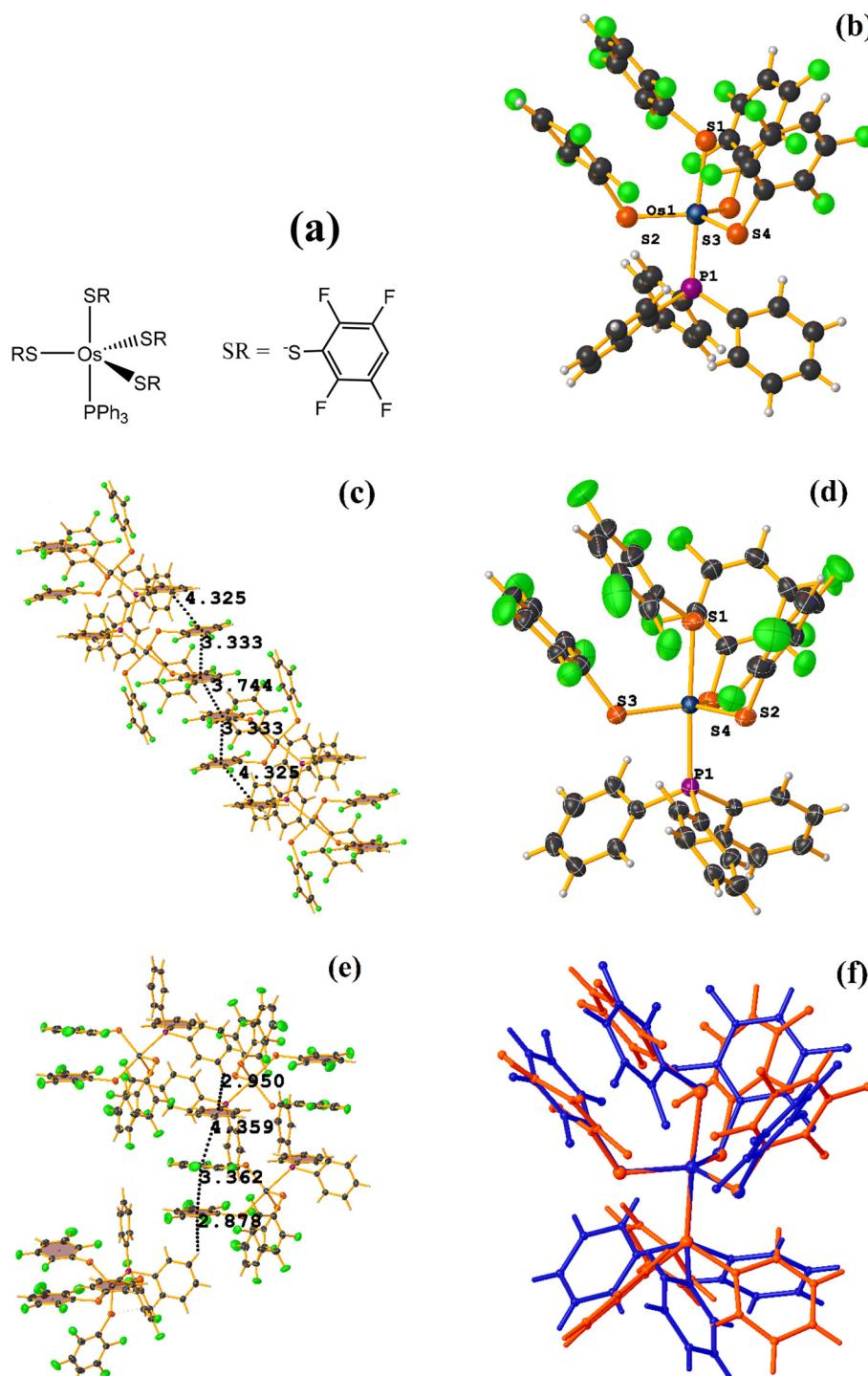


**Fig. 28** (a) Schematization of the molecular structure HENXIH and HENXIHO1. (b) Molecular structure of HENXIH. (c) Supramolecular array of HENXIH. (d) Molecular structure of HENXIHO1. (e) Supramolecular array of HENXIHO1. (f) Overlay of HENXIH (red) and HENXIHO1 (blue) structures.

The stacking pointed out by Conquest was found: C1–C6…C1–C6: [1/2 –  $X$ ,  $Y$ , 2 –  $Z$ , 5.5200(15) Å; 3.1945(9) Å; 4.502 Å; and 7.05(11)°]. It is highlighted that this interaction is established intermolecularly. On the other hand, the intramolecular interaction is outside the limits to be considered

stacking: C1–C6…C1–C6: [1/2 –  $X$ ,  $Y$ , 2 –  $Z$ , 5.5200(15) Å; 3.1945(9) Å; 4.502 Å; and 7.05(11)°].

Noteworthy is the fact that the complex's *cis* arrangement facilitates stacking. Still, it is interesting that the intermolecular and not the intramolecular  $\pi_F$ – $\pi_F$  interaction was formed.



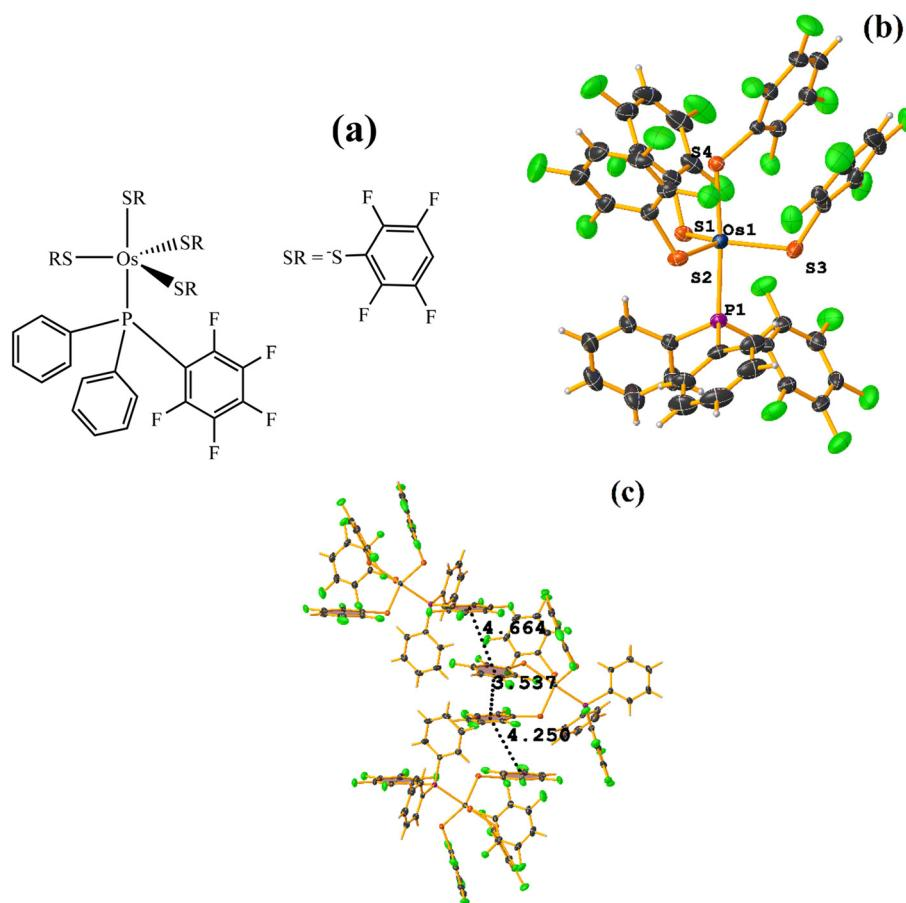


Fig. 29 (a) Schematization of the molecular structure OQEHO. (b) Molecular structure of OQEHO. (c) Supramolecular array of OQEHO.

**HIHREX and HIHREX01.** Lingen *et al.*<sup>77</sup> and our research group<sup>49</sup>  $[\text{Pd}(\text{II})(1,10\text{-phen})(2,3,4,6\text{-SC}_6\text{F}_4\text{-4-H})_2]$  reported HIHREX and HIHREX01. It is recommended that you consult our publication since the stackings indicated by Conquest are extensively described there.<sup>49</sup> The analysis of the observed stacking was also succinctly described in section 4 (previous work by our research group).

**HIHROH.** Lingen *et al.* additionally reported obtaining the crystalline structure  $[(\text{phen})_2\text{K}(\mu\text{-phen})_2\text{K}(\text{phen})_2]_2[(2,3,4,6\text{-SC}_6\text{F}_4\text{-4-H})_2\text{Pd}(\text{II})(\mu\text{-2,3,4,6-SC}_6\text{F}_4\text{-4-H})_2\text{Pd}(\text{II})(2,3,4,6\text{-SC}_6\text{F}_4\text{-4-H})_2]$ , Fig. 34.<sup>77</sup> Conquest identified many  $\pi\text{-}\pi$  stacking interactions that are involved with the dication and are established by the phen ligand. On the other hand, we found the  $\pi_F\text{-}\pi_F$  interactions established by the thiolate ligands. In this case, we identify two different types of stacking: C21–C26…C11–C16:  $[X, Y, Z, 3.606(9) \text{ \AA}; 3.462(5) \text{ \AA}; 0.422 \text{ \AA}; \text{ and } 9.6(7)^\circ]$  and C21–C26…C21–C26:  $[1 - X, -Y, 1 - Z, 3.813(8) \text{ \AA}; 3.230(5) \text{ \AA}; 2.025 \text{ \AA}; \text{ and } 0.0(6)^\circ]$ .

In addition, another  $\pi_F\text{-}\pi_F$  stacking was found that is outside the limits of the geometric parameters: C31–C36…C31–C36:  $[-X, 1 - Y, 1 - Z, 4.514(9) \text{ \AA}; 3.250(6) \text{ \AA}; 3.133 \text{ \AA}; \text{ and } 0.0(8)^\circ]$ . Interestingly, in this system, it can be observed that despite the presence of the phen ligands, these

do not affect the stacking of the thiolates even when the former has a larger  $\pi$  surface.<sup>53,54,78</sup>

**HIHRUN.** Again, Lingen *et al.* reported the preparation of the complex  $[\text{PdCl}(\text{n})(2,3,4,6\text{-SC}_6\text{F}_4\text{-4-H})(2,2'\text{-bipy})]$ , Fig. 35.<sup>77</sup> Of the stackings indicated by Conquest, when performing the analysis, we only found the intermolecular  $\pi_F\text{-}\pi_F$  interaction: C9/C11–C14/C16…C9/C11–C14/C16:  $[-X, 1 - Y, 1 - Z, 4.052(4) \text{ \AA}; 3.544(3) \text{ \AA}; 1.965 \text{ \AA}; \text{ and } 0.0(3)^\circ]$ . Although the parameter  $\text{Cg}\cdots\text{Cg}$  is out of limits, it cannot be denied that there is a tendency for the interaction to be established.

**HIHSAU.** Lingen *et al.* have described obtaining the complex  $[\text{Pd}(\text{II})(2,3,4,6\text{-SC}_6\text{F}_4\text{-4-H})_2(2,2'\text{-bipy})]$ , Fig. 36.<sup>77</sup> The  $\pi_F\text{-}\pi_F$  stackings indicated by Conquest were found: C2/C3/C8–C18/C20/C22…C4/C7–C12/C16:  $[X, Y, Z, 3.468(6) \text{ \AA}; 1.124 \text{ \AA}; \text{ and } 7.3(5)^\circ]$  and C2/C3/C8–C18/C20/C22…C2/C3/C8–C18/C20/C22:  $[-X, 1 - Y, 1 - Z, 3.909(5) \text{ \AA}; 3.396(4) \text{ \AA}; 1.313 \text{ \AA}; \text{ and } 0.0(5)^\circ]$ . Likewise, the presence of a T-shaped interaction ( $\text{C-H}\cdots\text{Cg}$ ) was detected: C102–H102…C11–C16 [ $3.589(3) \text{ \AA}$  and  $137.15^\circ$ ].

Comparing the supramolecular arrangement with MIXFAB ( $[(\text{Pt}(\text{II})(2,3,4,6\text{-SC}_6\text{F}_4\text{-4-H})_2(2,2'\text{-bipy})]$ ) that we have reported, it is observed that it is isomorphic, Fig. 6b.<sup>51</sup> It is important to highlight what Aakeröy *et al.* pointed out: “the probability that a certain motif will appear in a crystalline lattice is, in many

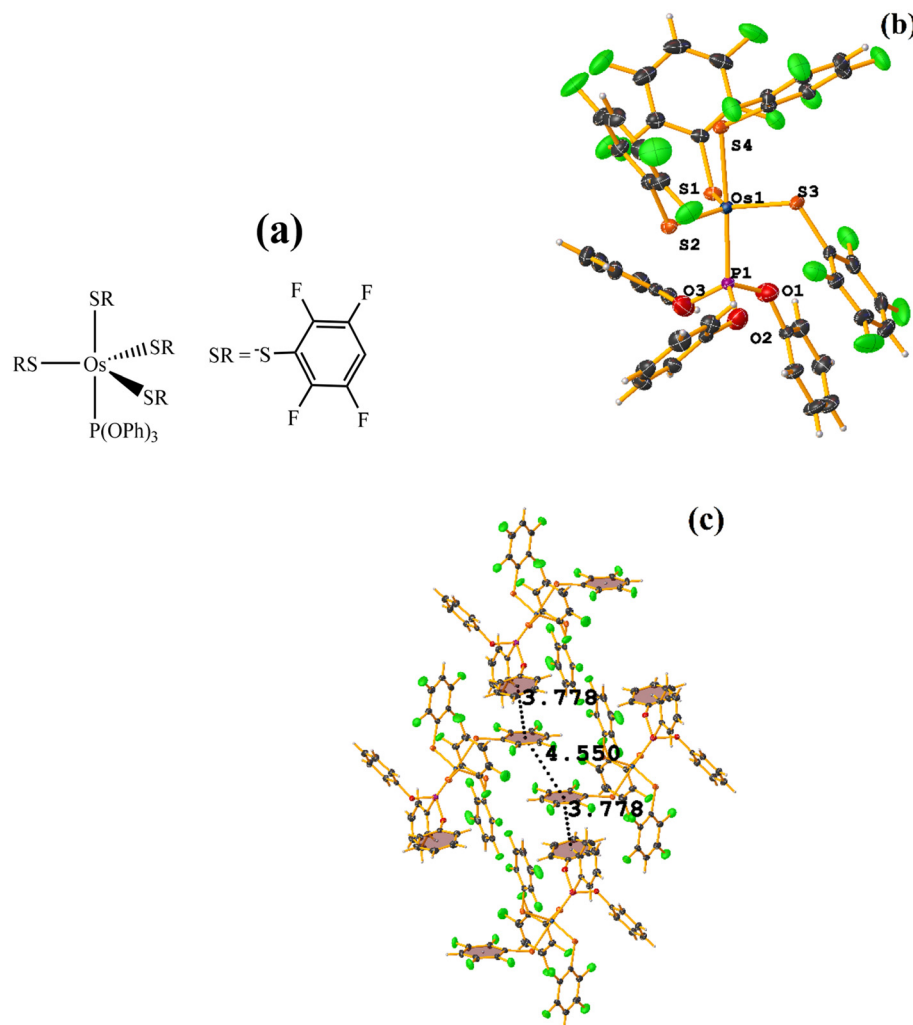


Fig. 30 (a) Schematization of the molecular structure OQEJAW. (b) Molecular structure of OQEJAW. (c) Supramolecular array of OQEJAW.

ways, a measure of the yield of a supramolecular reaction".<sup>79</sup> It can be noted that both tectons (HIHSAU and MIXFAB) present the same point group and are structurally similar, Fig. 36c; this implies that there is reproducibility in the expected motifs ( $\pi_F$ – $\pi_F$  stackings), and for this reason, the supramolecular arrangements are isomorphic. This connectivity indicates the robustness of this interaction in this type of tecton, showing efficient supramolecular yielding.

**Na.** Herrera-Álvarez *et al.* described the preparation of complex  $[\text{Pd}(\text{II})(\text{pdf})(2,3,4,6-\text{SC}_6\text{F}_4-4-\text{H})_2]$  (pdf: 1,10-bis (diphenylphosphine)ferrocene), Fig. 37.<sup>80</sup> When performing the analysis to find the stackings using Olex 2, the interaction returned by Conquest was not found. In fact, no stacking of any kind was found. The stacking suggested by Conquest, revised by Platon, indicates that it is between the five-membered rings of the dppf ligand: C37–C41…C42–C46: [X, Y, Z, 3.280(2) Å; 3.2793(17) Å; 0.022 Å; and 1.3(2)°]. However, we did not find it. Although various interactions were observed: C–F…H–C; S…H–C, as shown in Fig. 37.

**Discussion  $\pi_F$ – $\pi_F$  interactions of Pd complexes.** First observation is that establishing  $\pi_F$ – $\pi_F$  stacking with thiolate 2,3,4,6-SC<sub>6</sub>F<sub>4</sub>-4-H in this series of Pd-containing tectons has shown great versatility. Then, we have observed great effectiveness of the supramolecular yield shown by the HIHSAU (containing Pd) and MIXFAB (containing Pt) tectons, which presented supramolecular isomorphism because they have the same point group and are conformationally the same. It is also worth mentioning that the HIHROH tecton even with the presence of phen ligands, which are characterized by having a large  $\pi$  surface that preferentially form stacking; in this case, the desired  $\pi_F$ – $\pi_F$  interaction between the thiolates (2,3,4,6-SC<sub>6</sub>F<sub>4</sub>-4-H) is not disturbed. In other words, although stacking between phen is a dominant interaction, it does not affect the other. Concerning GUQBUQ and HIHRUN, the expected  $\pi_F$ – $\pi_F$  stackings were observed, but not with the desired control to exploit it from the point of view of crystal engineering. Finally, MADJAD, probably due to the geometry shown by the tecton, no  $\pi_F$ – $\pi_F$  stacking is observed.



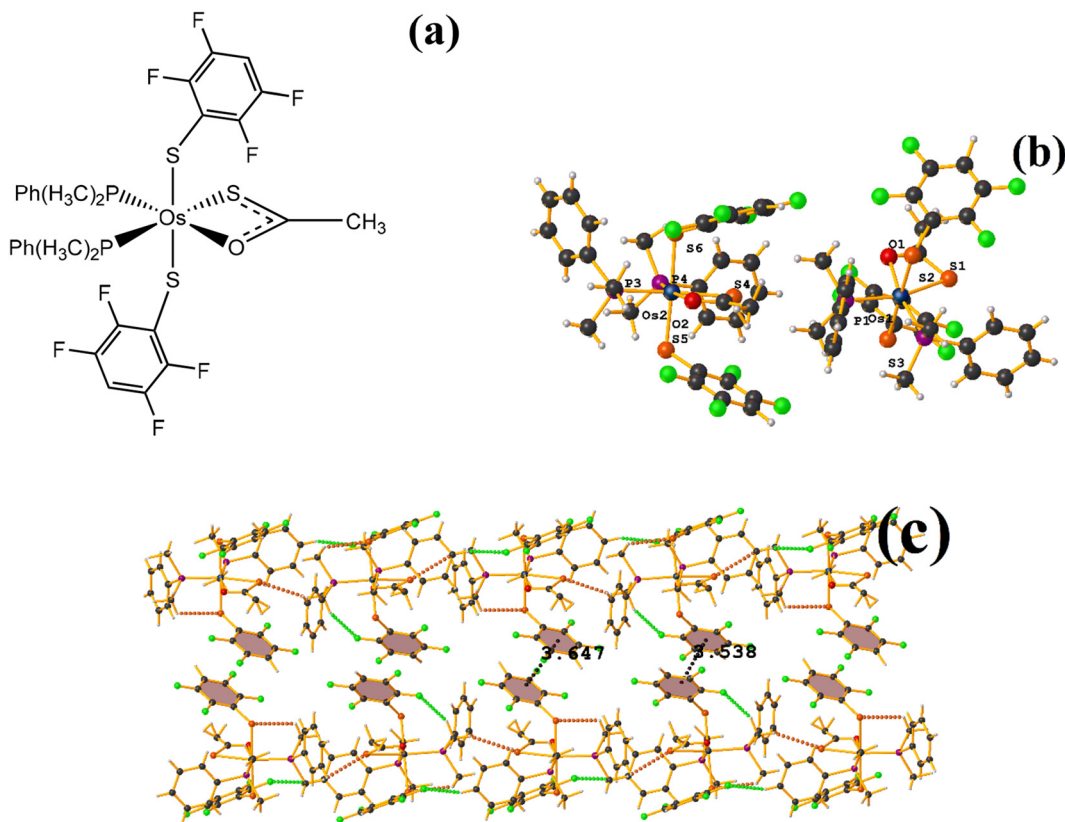


Fig. 31 (a) Schematization of the molecular structure ZAWWAV. (b) Molecular structure of ZAWWAV. (c) Supramolecular array of ZAWWAV.

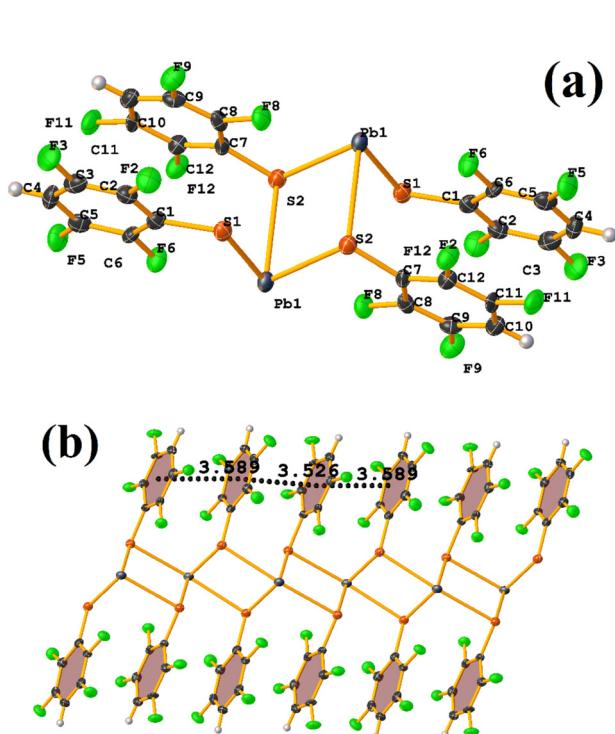


Fig. 32 (a) Molecular structure of CANWIA. (b) Supramolecular array of CANWIA.

### Pt metal complexes

**BIGXOF.** Villanueva *et al.* have described the synthesis of complex  $[\text{Pt}(\text{n})(2,3,4,6-\text{SC}_6\text{F}_4-4-\text{H})_2(1,2-\text{C}_6\text{F}_4(\text{SC}_6\text{HF}_4-4)(\text{PPh}_2))]$ , Fig. 38.<sup>81</sup> This compound is the result of the cleavage of an *ortho* C–F bond in a phosphine ligand.

The intermolecular  $\pi_{\text{F}}-\pi_{\text{F}}$  stacking indicated by Conquest was found: C31–C36…C31–C36:  $[-X, 1 - Y, -Z, 3.616(7) \text{ \AA}; 3.418(5) \text{ \AA}; 1.178 \text{ \AA}; \text{ and } 0.0(6)^\circ]$ . Another  $\pi_{\text{F}}-\pi_{\text{F}}$  stacking was found when analyzing the structure by Olex 2, but the parameters were out of limits: C25–C30…C25–C30:  $[-X, 1 - Y, 1 - Z, 5.176(5) \text{ \AA}; 3.431(4) \text{ \AA}; 3.877 \text{ \AA}; \text{ and } 0.0(4)^\circ]$ . The other intra  $\pi_{\text{F}}-\pi_{\text{F}}$  stacking shown in Fig. 38 is also outside the limits to be considered a genuine interaction: C25–C30…C31–C36:  $[X, Y, Z, 4.113(8) \text{ \AA}; 0.371(5) \text{ \AA}; 2.690 \text{ \AA}; \text{ and } 6.2(5)^\circ]$ .

**BIGXUL.** Villanueva *et al.* also described the obtaining of the coordination compound  $[\text{Pt}(\text{n})(2,3,4,6-\text{SC}_6\text{F}_4-4-\text{H})_2(1,2-\text{C}_6\text{F}_4(\text{SC}_6\text{HF}_4-4-\text{H})(\text{PPh}(\text{C}_6\text{F}_5)))]$ , Fig. 39.<sup>81</sup> It is the result of the cleavage of an *ortho* C–F bond in a phosphine ligand.

Two types of  $\pi_{\text{F}}-\pi_{\text{F}}$  stacking were found: C31–C36…C31–C36: (intermolecular stacking)  $[2 - X, 1 - Y, -Z, 3.441(4) \text{ \AA}; 3.349(3) \text{ \AA}; 0.778 \text{ \AA}; \text{ and } 0.0(4)^\circ]$  and, intramolecular stacking C25–C30…C31–C36:  $[X, Y, Z, 4.167(5) \text{ \AA}; 3.307(3) \text{ \AA}; 2.581 \text{ \AA}; \text{ and } 6.5 (4)^\circ]$ . Structurally, BIGXOF and BIGXUL are similar. However, the supramolecular arrangement presents differences. The first forms an infinite column of  $\pi_{\text{F}}-\pi_{\text{F}}$  stackings, although of all of these, only one can be consider a stacking interaction that meets the

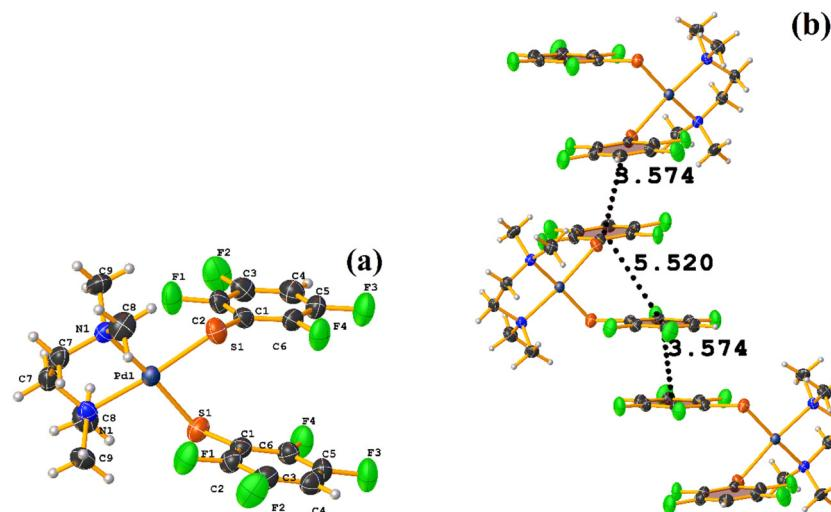


Fig. 33 (a) Molecular structure of GUQBUQ. (b) Supramolecular array of GUQBUQ.

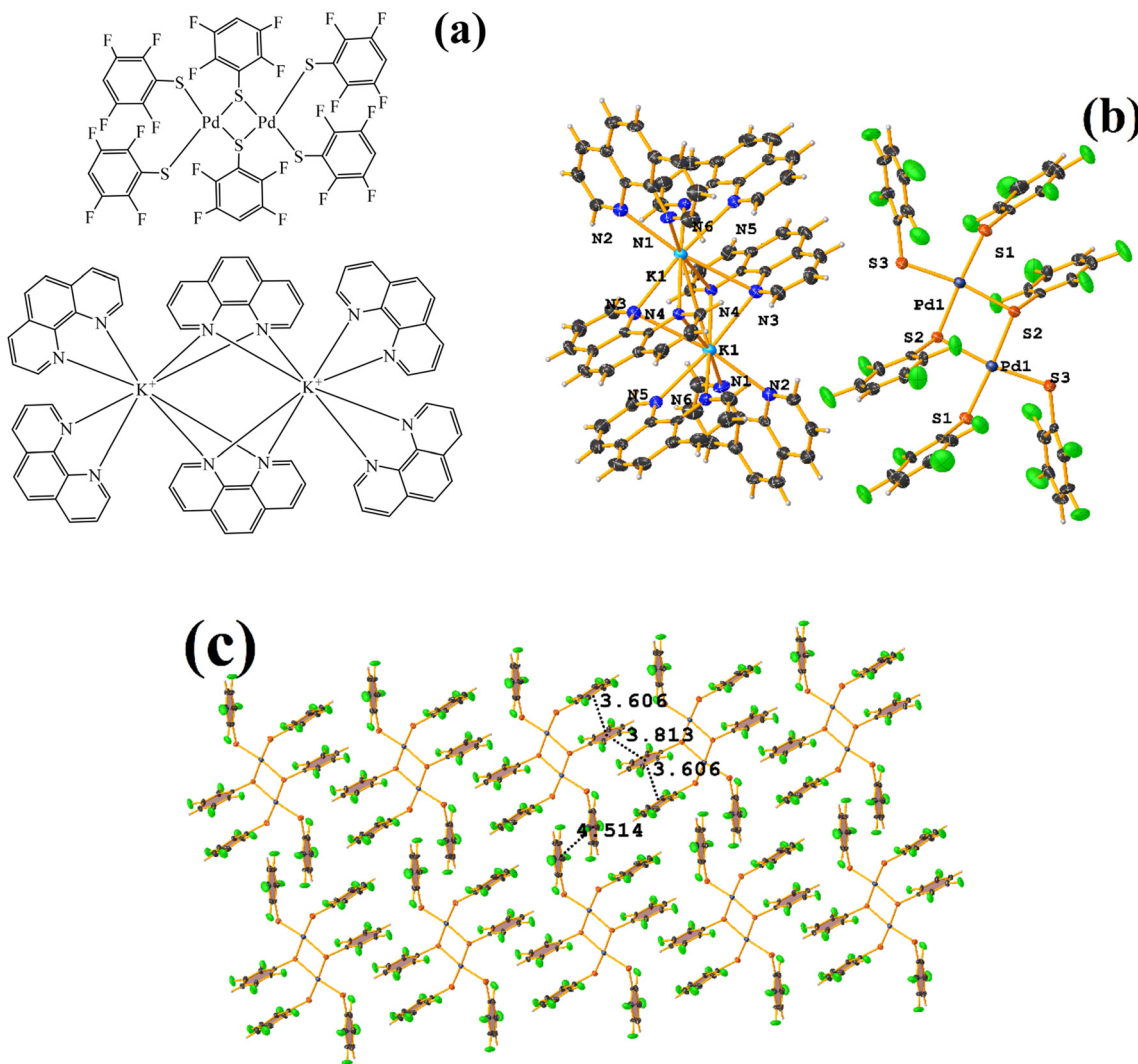


Fig. 34 (a) Schematization of the molecular structure of HIHROH. (b) Molecular structure of HIHROH. (c) Supramolecular array of HIHROH. The cation was removed for more clarity.

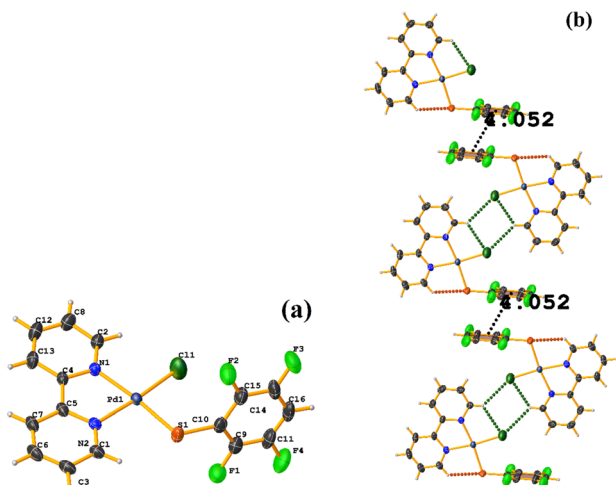


Fig. 35 (a) Molecular structure of HIHRUN. (b) Supramolecular array of HIHRUN.

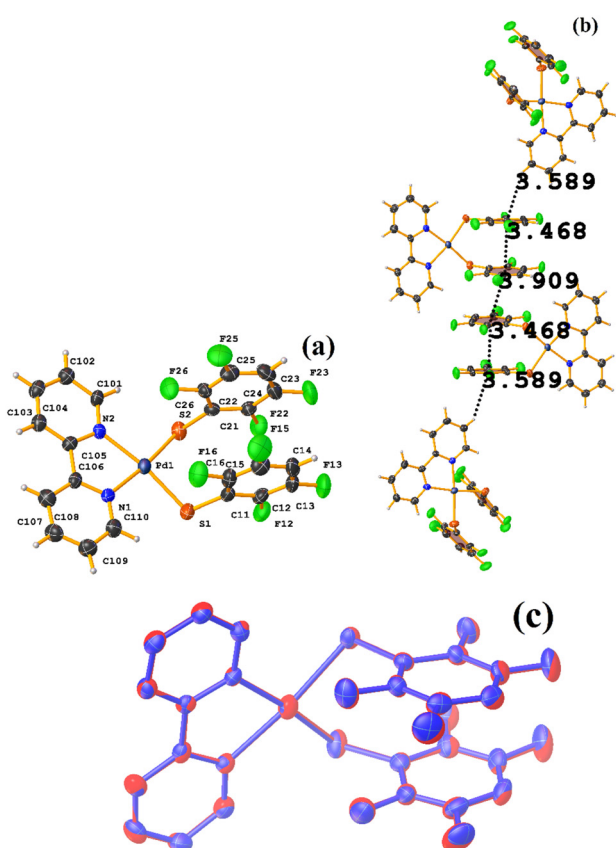


Fig. 36 (a) Molecular structure of HIHSAU. (b) Supramolecular array of HIHSAU. (c) Overlay of HIHSAU (blue) and MIXFAB (red) structures.

geometric parameters ( $Cg \cdots Cg$ : 3.616(7) Å). In the case of BIGXUL, this infinite  $\pi_F \cdots \pi_F$  stacking is not observed since the appearance of C–F $\cdots$ π interactions stops it. This being due to the presence of the phenyl ring (pentafluorinated) of phosphine, which is present in BIGXUL and not in BIGXOF.

**BOQHOG.** Lingen *et al.* have published the preparation of the complex  $K_2[\text{Pt}(\text{II})(2,3,4,6-\text{SC}_6\text{F}_4-4-\text{H})_4] \cdot \text{EtOH}$ , Fig. 40.<sup>82</sup>

The  $\pi_F \cdots \pi_F$  intramolecular stacking indicated by Conquest was found: C1–C6 $\cdots$ C7–C12: [2 – X, 2 – Y, 2 – Z, 3.586(3) Å; 3.539(2) Å; 1.344 Å; and 12.6(3)°]. In the supramolecular arrangement, a 2D array is observed; however, this is not due to the stacking. The arrangement is layered; in one, the potassium cations are accommodated with the EtOH solvates; and in the other, the anion  $[\text{Pt}(\text{II})(2,3,4,6-\text{SC}_6\text{F}_4-4-\text{H})_4]^{2-}$ . It should be noted that the ion–ion interaction (between  $\text{K}^+$  cation and complex anion) prevails and is more dominant than the  $\pi_F \cdots \pi_F$  stacking. This is mentioned because the latter could have persisted, but because the former is energetically stronger (ion–ion (100–350 kJ mol<sup>-1</sup>)<sup>83</sup> vs. stacking (0–10 kJ mol<sup>-1</sup>)<sup>34</sup>), this did not happen. Comparing LOKVUD ( $[\text{Et}_4\text{N}]^+[\text{Au}(2,3,4,6-\text{SC}_6\text{F}_4-4-\text{H})_4] \cdot \text{EtOH}$ , Fig. 11d) with this structure, it is observed that both exhibit a square plane geometry around the metal center. However, in the first structure, the  $\pi_F \cdots \pi_F$  stackings were fully established; in this case, the cation  $\text{Et}_4\text{N}^+$  does not interrupt these interactions as it happens in the case of the  $\text{K}^+$  cation that disrupts them.

**BOQJEY.** Lingen *et al.* have published the preparation of the complex  $[\text{Pt}(\text{II})(\text{C}_6\text{F}_5)(2,3,4,6-\text{SC}_6\text{F}_4-4-\text{H}) \cdot (\text{dppb})]$  ( $\text{dppb}$  = 1,4-bis (diphenylphosphino)butane), Fig. 41.<sup>82</sup> When performing the analysis with Olex 2, we found the  $\pi_F \cdots \pi$  stacking returned by Conquest ( $Cg \cdots Cg$ : 3.635(6) Å). Still, as established between the pentafluorinated ring and a phenyl ring of the dppb ligand, we will not review it in depth. On the other hand, we find two different types of intra  $\pi_F \cdots \pi_F$  stackings: C11–C16 $\cdots$ C21–C26: [X, Y, Z, 3.547(5) Å; 3.304(3) Å; 1.372 Å; and 16.5(4)°] and C11–C16 $\cdots$ C11–C16: [1 – X, –Y, 1 – Z, 3.614(4) Å; 3.332(3) Å; 1.399 Å; and 0.0(4)°]. In the case of the intra-stacking, it was established between the pentafluorinated ring and the tetra fluorinated thiolate 2,3,4,6-SC<sub>6</sub>F<sub>4</sub>-4-H, and the inter-stacking between the rings of the thiolate.

**FOKSUV.** Castillo-Blum *et al.* have published the synthesis of the complex *trans-anti*- $[\text{Pt}_2(\text{II})(\mu_2-2,3,4,6-\text{SC}_6\text{F}_4-4-\text{H})_2(2,3,4,6-\text{SC}_6\text{F}_4-4-\text{H})_2(\text{TBZ})_2] \cdot (\text{CH}_3)_2\text{C=O}$  ( $\text{TBZ}$  = 4-(1*H*-benzimidazol-2-yl)-1,3-thiazole), Fig. 42.<sup>84</sup> Reviewing the supramolecular arrangement, the stackings indicated by Conquest were found, and those of interest  $\pi_F \cdots \pi_F$  showed the following parameter values: both are intermolecular C20–C25 $\cdots$ C20–C25 [3 – X, 2 – Y, 1 – Z, 3.756(4) Å; 3.363(2) Å; 1.673 Å; and 0.0(3)°] and C14–C19 $\cdots$ C14–C19 [2 – X, 2 – Y, 2 – Z, 4.608(5) Å; 3.373(3) Å; 3.139 Å; and 0.0(4)°]. The second interaction is off-limits and should not be considered genuine stacking. A third intra-stacking of the type  $\pi_F \cdots \pi_F$  was established between the tetrafluorinated thiolate and the six-membered ring of the benzimidazole fragment having the following parameters: C4–C9 $\cdots$ C20–C25 [2 – X, 2 – Y, 1 – Z, 3.679(4) Å; 3.465(3) Å; 0.475 Å; and 12.5(3)°].

**FORMUW.** Cervantes *et al.* have published the preparation of the complex  $[\text{Pt}(\text{II})(2,3,4,6-\text{SC}_6\text{F}_4-4-\text{H})(\text{triphos})] \cdot (\text{CF}_3\text{SO}_3)$ , triphos:  $\text{PhP}(\text{CH}_2\text{CH}_2\text{PPh}_2)_2$ , Fig. 43.<sup>85</sup> The stacking indicated by Conquest was found; however, it is not established by the tetrafluorinated rings of the thiolates. The  $\pi_F \cdots \pi$  stacking



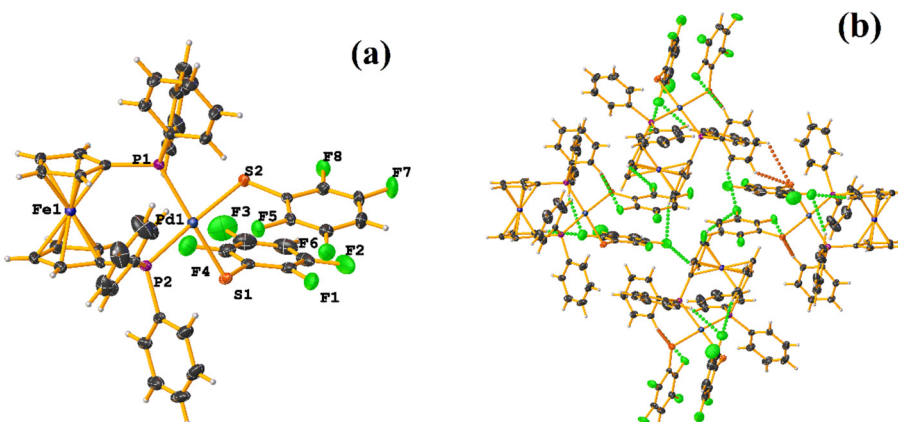


Fig. 37 (a) Molecular structure of MADJAD. (b) Supramolecular array of MADJAD.

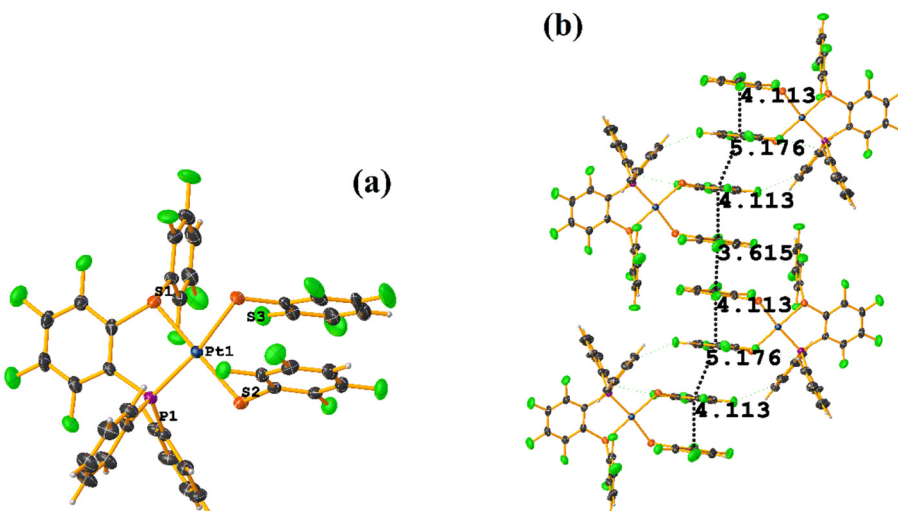


Fig. 38 (a) Molecular structure of BIGXOF. (b) Supramolecular array of BIGXOF.

showed the following values of the geometric parameters: C1–C6…C13–C18 [X, Y, Z, 3.679(12) Å; 3.325(8) Å; 1.161 Å; and 7.5 (9)°]. This involves a ring of the triphos ligand with a tetrafluorinated thiolate. In the case of  $\pi_F$ – $\pi_F$ , the parameters were: C1–C6…C1–C6 [4 – X, 3 – Y, 1 – Z, 3.609(12) Å; 3.319(7) Å; 1.419 Å; and 0.0(8)°].

**LUQMUI.** This structure was described supramolecularly in section 4 of this article (Fig. 7).<sup>52</sup>

**MIXFAB.** Section 4 of this article describes this structure supramolecularly. It is also recommended that you consult our article (Fig. 6).<sup>51</sup>

**OPOGOQ.** S. K. Lee *et al.* have described the obtaining of the compound  $[\text{Fe}(\text{II})(\eta^5\text{-C}_5\text{H}_4\text{PPh}_2)_2]\text{Pt}(\text{II})(2,3,4,6\text{-SC}_6\text{F}_4\text{-4-H})_2$ , Fig. 44.<sup>86</sup> By analyzing the structure supramolecularly, the stacking indicated by Conquest is due to an interaction between the five-membered rings of  $\text{FeCp}_2$  ( $\text{Cg} \cdots \text{Cg}$ : 3.293(5) Å). We find other  $\pi_F$ – $\pi_F$  ( $\text{Cg} \cdots \text{Cg}$ : 4.764(6) Å) and  $\pi_F$ – $\pi$  stackings ( $\text{Cg} \cdots \text{Cg}$ : 4.460(7) Å), but they are outside the limits to be considered genuine.

**TAGZUX.** Bautista *et al.* have described the synthesis of complex  $[\text{Pt}(\text{II})(2,3,4,6\text{-SC}_6\text{F}_4\text{-4-H})_2(\text{R}_F\text{S}-\text{CH}_2\text{CH}_2\text{-SR}_F)]$  ( $\text{R}_F$ :  $\text{C}_6\text{H}_4\text{F-4-F}$ ), Fig. 45.<sup>87</sup>

First, we find the  $\pi_F$ – $\pi_F$  stacking indicated by Conquest, which is intermolecular: C7–C12…C7–C12 [2 – X, 2 – Y, 2 – Z, 3.504(7) Å; 3.326(5) Å; 1.101 Å; and 0.0(6)°]. In addition, another  $\pi_F$ – $\pi_F$  stacking was found between the tetrafluorinated thiolate and the monofluorinated thiolate, which is intramolecular: C7–C12…C19–C24 [X, Y, Z, 3.704(7) Å; 3.332(5) Å; 1.489 Å; and 6.2(6)°]. Interestingly, it is not expected to observe monofluorinated thiolate rings participating in stacking interactions. We consider that this happened due to the order of stability indicated by Janiak ( $\pi_{\text{poor}}\text{-}\pi_{\text{poor}} > \pi_{\text{poor}}\text{-}\pi_{\text{rich}} > \pi_{\text{rich}}\text{-}\pi_{\text{rich}}$ ). This could be established since the molecule has only two types of aromatic rings. For example, the intermolecular  $\pi_F$ – $\pi_F$  stacking interaction was found between the two monofluorinated thiolate rings, and their geometric parameters were too far outside the limits to be considered genuine stacking: C19–C24…C19–C24 [1 – X, 3 – Y, 2 – Z,

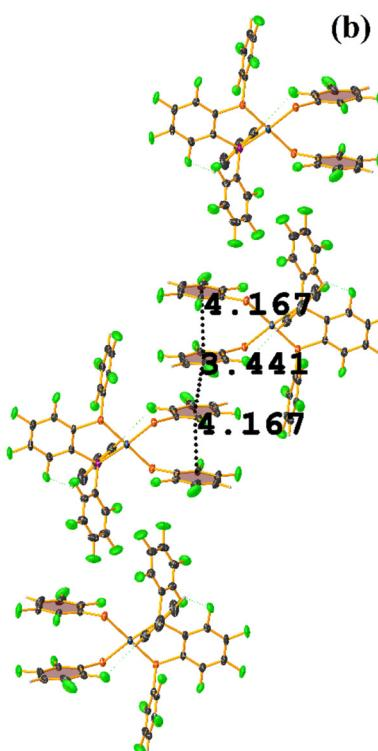


Fig. 39 (a) Molecular structure of BIGXUL. (b) Supramolecular array of BIGXUL.

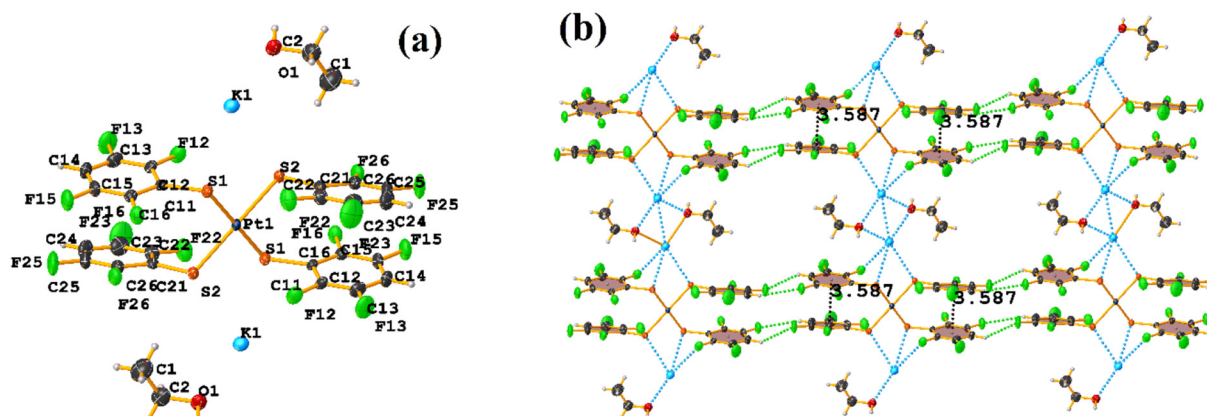


Fig. 40 (a) Molecular structure of BOQHOG. (b) Supramolecular array of BOQHOG.

4.119(7) Å; 2.379 Å; and 0.0(6)°]. These values indicate that there is some repulsion between the rings.

**VACTAX.** Bernès *et al.* have described attaining the complex  $[\text{Pt}(\text{II})(2,3,4,6-\text{SC}_6\text{F}_4-4-\text{H})_2(\text{P}(\text{Ph}_2\text{R}_\text{F})_2)]$  ( $\text{R}_\text{F}$ :  $\text{C}_6\text{F}_5$ ), Fig. 46.<sup>88</sup> The two stackings ( $\pi_\text{F}-\pi_\text{F}$  and  $\pi-\pi$ ) indicated by Conquest were found, both intramolecular: C7–C12…C13–C18 [ $X, Y, Z, 3.709(7)$  Å; 3.599(5) Å; 1.709 Å; and 17.2(6)°] and C25–C30…C43–C48 [ $X, Y, Z, 3.633(6)$  Å; 3.286(5) Å; 0.762 Å; and 15.8(5)°]. By checking for intermolecular stacking, no interaction was found.

**Discussion  $\pi_\text{F}-\pi_\text{F}$  interactions of Pt complexes.** In this section, numerous structures containing Pt adhere to the geometric values requested by Conquest. However, as was the case of OPOGOQ and MADJAD, there were cases in which we did not find the indicated stackings. It is emphasized that these two structures are decorated with ferrocenyl-type ligands. On the other hand, the different structures showed great persistence in establishing  $\pi_\text{F}-\pi_\text{F}$  stacking, mainly between the tetrafluorinated thiolate rings. Considering what was observed with tectons containing Pd, the square plane geometry greatly

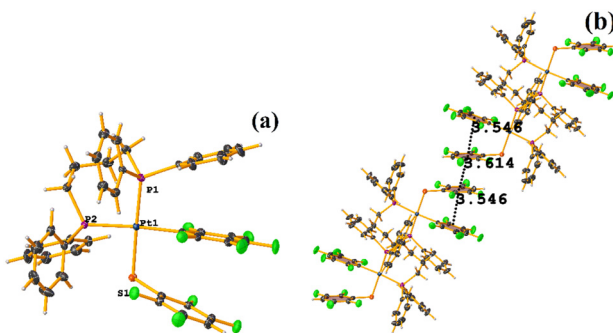


Fig. 41 (a) Molecular structure of BOQJEY. (b) Supramolecular array of BOQJEY.

benefits the propensity for  $\pi_F-\pi_F$  stackings to be established. However, it must be considered that this propensity is subject to the type of ligands coordinated to the metallic center and the nature of the complex, *i.e.*, whether is ionic or neutral. As mentioned previously with OPOGOQ and MADJAD, the presence of ferrocenyl-type ligands will affect the stacking since these were not observed. In the case of FORMUW or BOQHOG ionic tectons, stacking is affected by the nature of the ion. In the first case, the triflate anion did not affect it. However, in the case of the second, the  $K^+$  cation interfered. The positive charge on  $K^+$  (considering it a sphere) increases the ion–ion interaction because it is concentrated more effectively on it. The opposite is true with the triflate anion, where the charge is dispersed throughout the molecule due to electronegativity, inductive, and resonance effects.<sup>89</sup> The  $K^+$  with the anion complex causes the ion–ion interaction to be stronger than with triflate. This apparently can be demonstrated since with the LOKWE0 and LOKVUD tectons (see the section on Au complexes), both ionic compounds present a cation ( $Et_4N^+$ ), which does not interfere with the establishment of the  $\pi_F-\pi_F$  stackings. One way to demonstrate this hypothesis is to prepare the equivalent complex of  $[Et_4N][Pt(2,3,4,6-SC_6F_4-4-H)_4]$  to observe if that the cation does not alter the intermolecular stacking.

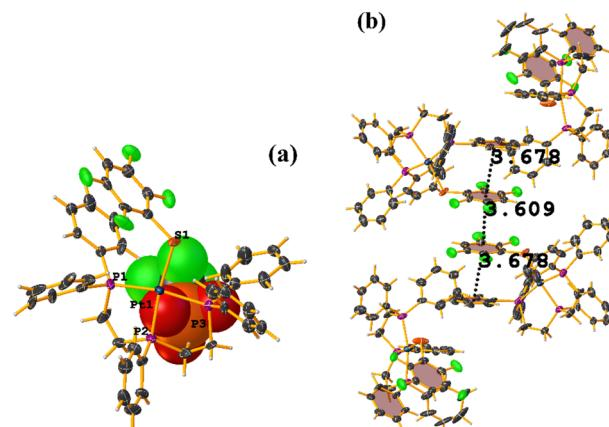


Fig. 43 (a) Molecular structure of FORMUW. The triflate anion is presented in a spacefill model. (b) Supramolecular array of FORMUW. The triflate anion was removed for clarity.

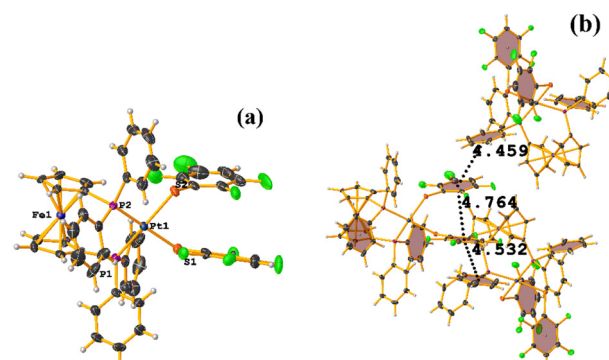


Fig. 44 (a) Molecular structure of OPOGOQ. (b) Supramolecular array of OPOGOQ.

## Rh metal complexes

**JISSOT.** Cruz-Garritz *et al.* have reported the preparation of complex  $[Rh(i)(\mu-2,3,4,6-SC_6F_4-4-H)(COD)]_2$ , COD: 1,5-cycloocta-

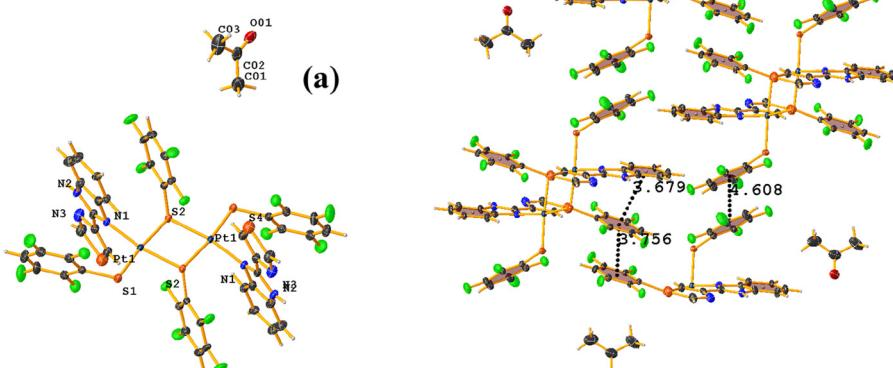


Fig. 42 (a) Molecular structure of FOKSUV. (b) Supramolecular array of FOKSUV.



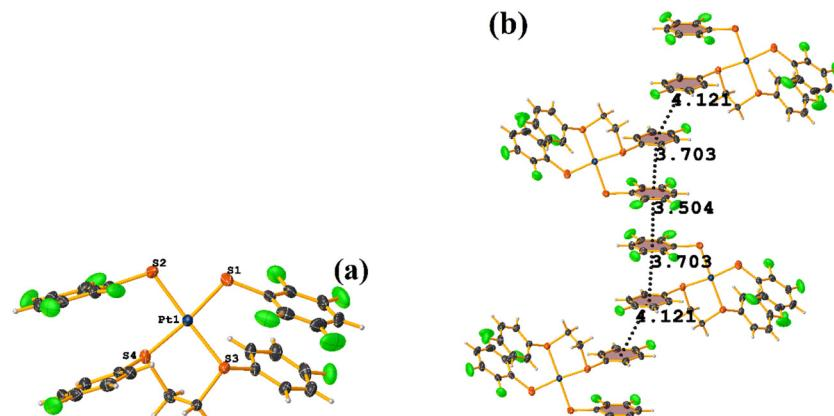


Fig. 45 (a) Molecular structure of TAGZUX. (b) Supramolecular array of TAGZUX.

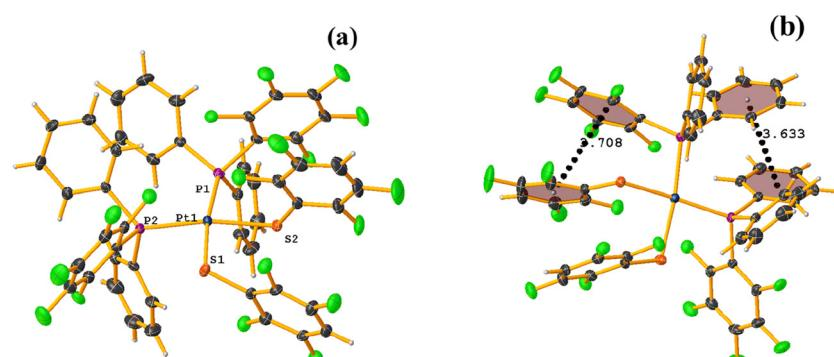


Fig. 46 (a) Molecular structure of VACTAX. (b) Supramolecular array of VACTAX.

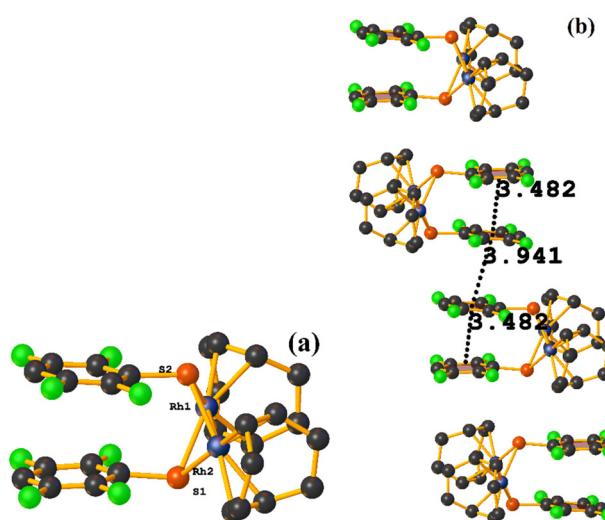


Fig. 47 (a) Molecular structure of JISSOT. (b) Supramolecular array of JISSOT.

diene, Fig. 47.<sup>90</sup> The  $\pi_F-\pi_F$  stacking indicated by Conquest was found, which is an intramolecular contact: C17-C22...C23-C28 [X, Y, Z, 3.482(3) Å; 3.3352(15) Å; 0.979 Å; and 7.52(18)°].

Additionally, an intermolecular  $\pi_F-\pi_F$  stacking not noted by Conquest was found: C23-C28...C23-C28 [1 - X, -Y, 1 - Z, 3.941(3) Å; 3.5254(15) Å; 1.762 Å; and 0.0(18)°].

**NADSUI.** Wiester *et al.* have described obtaining the complex  $[\text{Rh}(\text{i})\text{Cl}(\kappa^1\text{-Ph}_2\text{P-CH}_2\text{-CH}_2\text{-SR}_F)(\kappa^2\text{-Ph}_2\text{P-CH}_2\text{-CH}_2\text{-SR}_F)]$ , R<sub>F</sub>: 2,3,4,6-SC<sub>6</sub>F<sub>4</sub>-4-H, Fig. 48.<sup>91</sup> The stackings indicated by Conquest and others that were not marked were found.

The intermolecular  $\pi_F-\pi_F$  stacking was found where the fluorinated thiolate rings participated: C3-C8...C3-C8 [1 - X, -Y, 1 - Z, 3.8230(8) Å; 3.2912(6) Å; 1.945 Å; and 0.04(7)°]. In addition, other intra- and intermolecular stackings of the type  $\pi_F-\pi$  and  $\pi-\pi$  were found: C3-C8...C15-C20 [1 - X, 1 - Y, 1 - Z, 3.7912(9) Å; 3.7235(6) Å; 0.700 Å; and 18.70(7)°] and C15-C20...C29-C34 [X, Y, Z, 3.6461(9) Å; 3.6160(6) Å; 1.411 Å; and 15.84(7)°].

**Discussion  $\pi_F-\pi_F$  interactions of Rh complexes.** Only two structures that met the restrictions were found by Conquest. Both have a geometry close to a square plane around the Rh. However, as we mentioned in the Pt complexes section, this geometry benefits stacking, but for example, in the case of JISSOT, the presence of the COD ligand does not affect the formation of these interactions. But, in the case of NADSUI, the coordination modes of the Ph<sub>2</sub>P-CH<sub>2</sub>-CH<sub>2</sub>-SR<sub>F</sub> ligand decrease the global symmetry, and stacking is observed, but very much

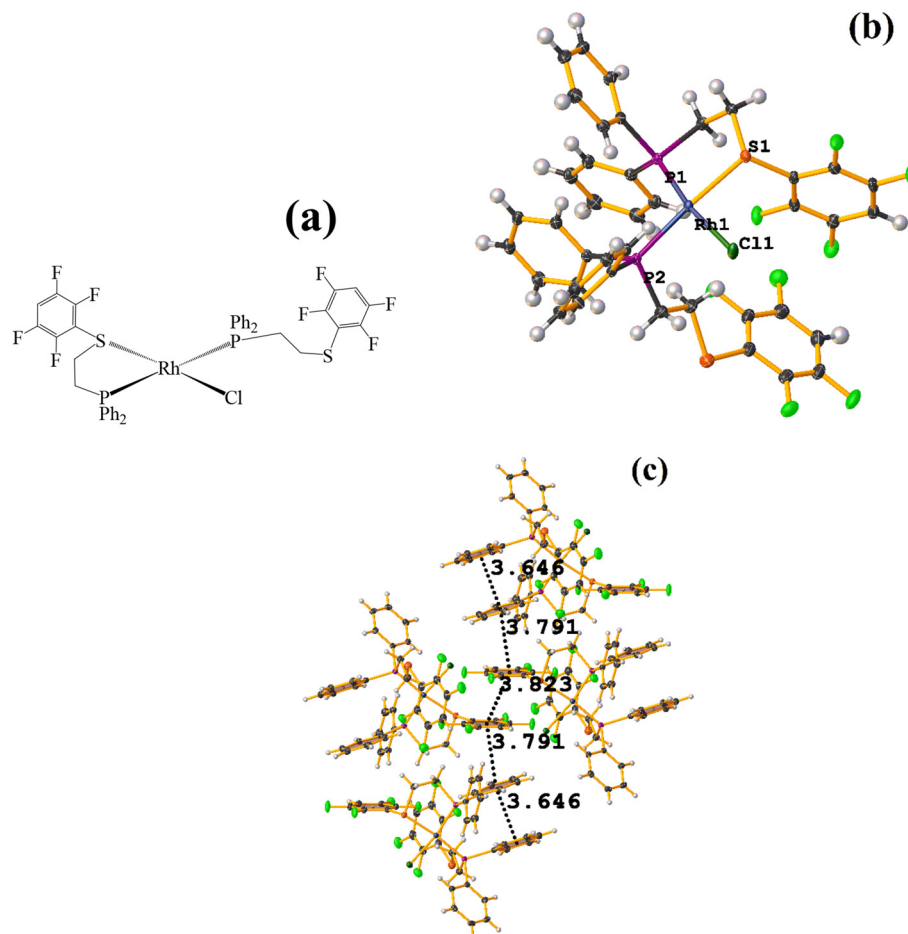


Fig. 48 (a) Schematization of the molecular structure of NADSUI. (b) Molecular structure of HIHROH. (c) Supramolecular array of NADSUI.

at the limit of the geometric parameters to be considered an interaction of this type. This corroborates that, in addition to considering the geometry of the complex, it must be taken into account that the ligands influence the global symmetry, which can affect the stacking.

### Ru metal complexes

**IQIDOD.** K. W. Chan *et al.* have reported the synthesis of the dinuclear complex, figure  $\text{Na}(\text{H}_2\text{O})_2[\text{Ru}(\text{IV})(\text{NO})_2(2,3,4,6-\text{SC}_6\text{F}_4-4-\text{H})_2]_2(\mu-2,3,4,6-\text{SC}_6\text{F}_4-4-\text{H})_2(\mu-\text{OH})\cdot(\text{CH}_2\text{Cl}_2)_2$  ( $\text{R}_\text{F}$ : 2,3,4,6-SC<sub>6</sub>F<sub>4</sub>-4-H), Fig. 49.<sup>92</sup> As the diagram shows (Fig. 49a), the  $\text{Na}^+$  is stabilized through dative bonds of the C-F  $\rightarrow$  Na type with the *ortho* fluorine atoms of the thiolates. The two stackings indicated by Conquest were found both are  $\pi_{\text{F}}-\pi_{\text{F}}$  intermolecular: C25-C30...C25-C30 [1 -  $X$ ,  $Y$ , 1/2 -  $Z$ , 3.796(2) Å; 3.5971(17) Å; 1.212 Å; and 6.7 (2)°] and C25-C30...C25-C30 [1 -  $X$ ,  $Y$ , 1/2 -  $Z$ , 3.722(2) Å; 3.2487(17) Å; 1.178 Å; and 13.83(19)°].

In addition, intramolecular  $\pi_{\text{F}}-\pi_{\text{F}}$  stacking was found: C1-C6...C1-C6 [ $X$ ,  $Y$ ,  $Z$ , 3.552(2) Å; 3.1422(15) Å; 1.275 Å; and 7.40 (17)°]. Another intermolecular  $\pi_{\text{F}}-\pi_{\text{F}}$  stacking ( $\text{Cg...Cg}$ : 4.682 Å) was also found, but the parameters are outside the limits to consider this interaction genuine.

**OFIBAG.** Q. Zhang *et al.* have reported the obtaining of the organometallic compound  $[\text{Cp}^*\text{Ru}(\text{IV})(\text{NO})(2,3,4,6-\text{SC}_6\text{F}_4-4-\text{H})_2](\text{Cp}^*:\eta^5-\text{C}_5\text{Me}_5)$ , Fig. 50.<sup>93</sup> The stacking found by Conquest was found, which was an intermolecular interaction, between the five-membered ring of  $\text{Cp}^*$  with a thiolate ring: C13-C1-C1-C6-C13 [3/2 -  $X$ , -1/2 +  $Y$ , -1/2 +  $Z$ , 3.6806(14) Å; 3.6699 (10) Å; 0.281 Å; and 8.48(12)°].

**Discussion  $\pi_{\text{F}}-\pi_{\text{F}}$  interactions of Ru complexes.** The two structures indicated by Conquest presented two different molecular arrangements, mainly in nuclearity, geometry around the metallic center, and type of ligands. In both cases, a geometry close to the octahedron is observed. However, in IQIDOD, the structure is dinuclear, and in OFIBAG, it is mononuclear. Concerning OFIBAG, it can be considered a molecule of lower molecular complexity compared to IQIDOD, which could initially lead us to think *a priori* that OFIBAG would present interactions involving the thiolate rings since there are no competitive interactions that will limit them. However, only the establishment between the  $\text{Cp}^*$  and thiolate rings was found. Furthermore, the methyl substituents around  $\text{Cp}^*$  were not an obstacle to limiting this interaction from the point of view of steric hindrance (Fig. 50).



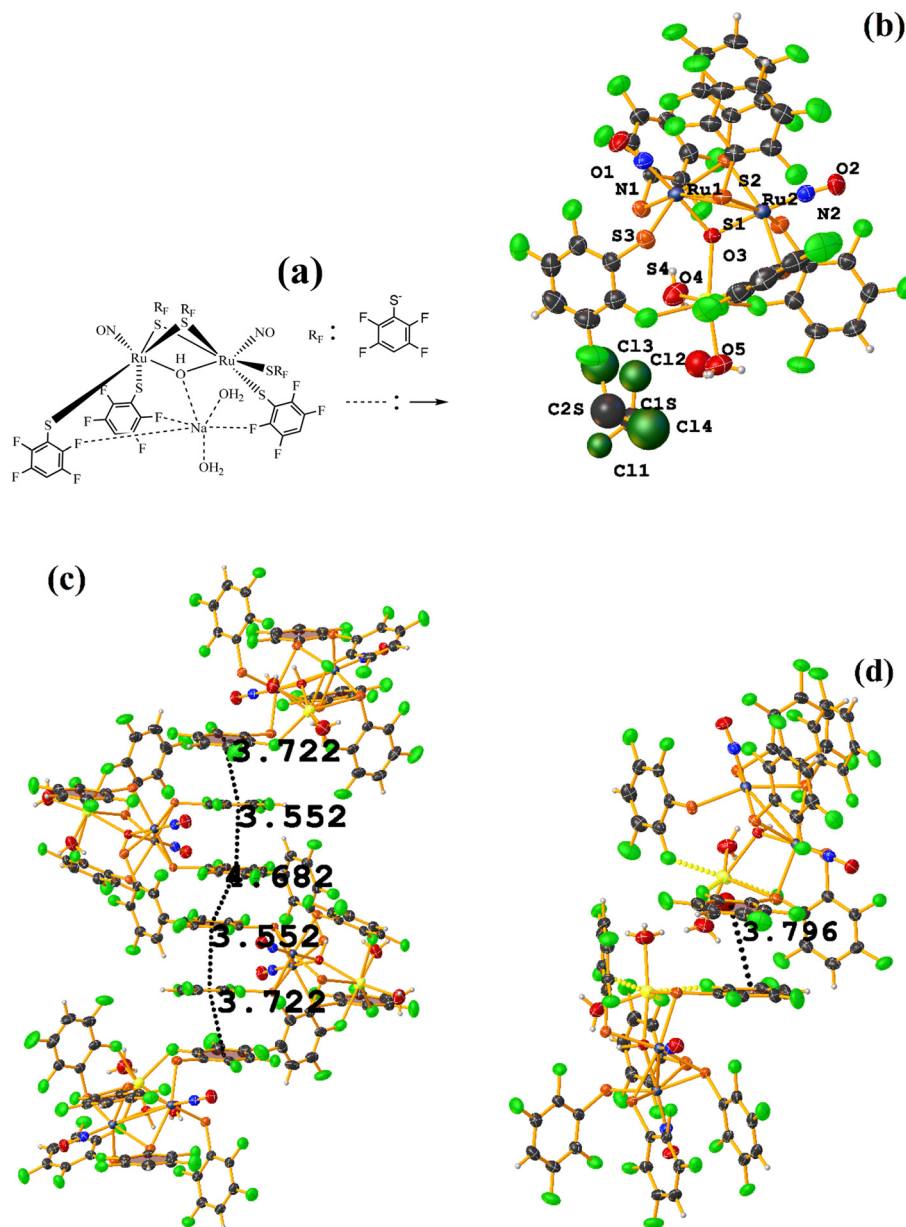


Fig. 49 (a) Schematization of the molecular structure of IQIDOD. (b) Molecular structure of IQIDOD. (c and d) Supramolecular arrays of IQIDOD.

On the other hand, the greater molecular complexity observed in IQIDOD in the first instance led us to think that stacking would not be established, and in this case, it was quite the opposite. In this situation, although in the first instance, the tecton is appropriately selected (geometry and ligands involved), and it is ensured that there are no competitive interactions that prevent stacking, other contributions affect this. For this reason, stacking is not a predictable interaction from the point of view of crystal engineering.

#### Sn metal complexes

**PIDMOF.** Estudante-Negrete *et al.* have described the preparation of the complex  $[\text{Sn}(\text{iv})\text{Ph}_2(2,3,4,6-\text{SC}_6\text{F}_4-4-\text{H})_2]$ , Fig. 51.

The two stackings ( $\pi_{\text{F}}-\pi_{\text{F}}$  and  $\pi_{\text{F}}-\pi$ ) indicated by Conquest were found, the first is intermolecular and the second is intramolecular: C13–C18…C13–C18 [1 – X, 1 – Y, –Z, 3.788(4) Å; 1.279 Å; and 18.3(3)°] and C19–C24…C1–C6 [X, Y, Z, 3.522(3) Å; 3.372(2) Å; 1.016 Å; and 0.0(3)°]. Another  $\pi_{\text{F}}-\pi_{\text{F}}$  intermolecular stacking was found (Cg…Cg; 4.560 Å), but the parameters are outside the limits to consider this genuine interaction.

**Discussion  $\pi_{\text{F}}-\pi_{\text{F}}$  interactions of Sn complexes.** PIDMOF presents a geometry around Sn close to the tetrahedron. Furthermore, it exhibits high symmetry. This favors the formation of  $\pi_{\text{F}}-\pi_{\text{F}}$  stackings that produce 1D arrays (infinite columns). However, an intermolecular interaction is outside

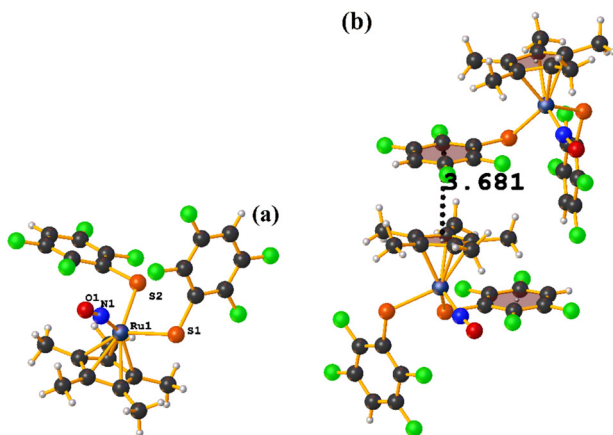


Fig. 50 (a) Molecular structure of OFIBAG. (b) Supramolecular arrays of OFIBAG.

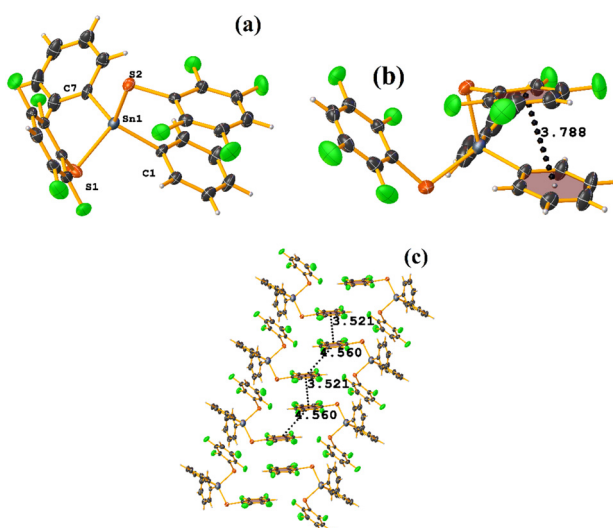


Fig. 51 (a) Molecular structure of PIDMOF. (b) Intramolecular stacking in PIDMOF. (c) Supramolecular arrays of PIDMOF.

the parameters' limits. It would be interesting to observe homoleptic tectons  $[C]_n[Sn^{II}(2,3,4,6-SC_6F_4-4-H)_4]$  or  $[Sn^{IV}(2,3,4,6-SC_6F_4-4-H)_4]$  ( $C$ : cation;  $n$ : 2 ( $C^+$ ) or  $n$ : 1 ( $C^{+2}$ )), to determine how efficiently they establish stacking. It would also be necessary to evaluate what effect the establishment of these interactions may have in the presence of the cation in the case of  $[C]_n[Sn^{II}(2,3,4,6-SC_6F_4-4-H)_4]$ .

## Miscellaneous

**EMEGAE.** In this section, we want to show the EMEGAE structure, which is the complex  $[Pt(n)(2,2'-bpy)(2,3,4,6-SC_6F_4-4-CN)_2]$ , Fig. 52.<sup>94</sup> It should be emphasized that Conquest did not throw this structure. Still, it appears to be a suitable tecton to form the desired  $\pi_F-\pi_F$  stackings preferentially. This allows the formation of infinite columns. Various intra- and intermolecular  $\pi_F-\pi_F$  stacking values were found: intra  $C1-C6\cdots C8-C13$  [3.336(3) Å; 3.175(2) Å; not found; and 2.9(3)°], intermolecular  $C8-C13\cdots C8-C13$  [− $X$ , 1 −  $Y$ , − $Z$ , 3.640(3) Å; −3.299(2) Å; 1.537 Å; and 0°], and intermolecular  $C1-C6\cdots C1-C6$  [1 −  $X$ , 2 −  $Y$ , − $Z$ , 3.753(3) Å; 3.352(2) Å; 1.689 Å; and 0°].

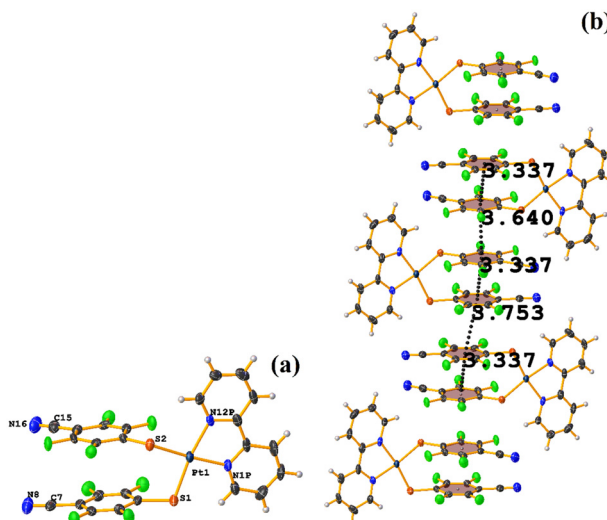


Fig. 52 (a) Molecular structure of EMEGAE. (b) Supramolecular arrays of EMEGAE.

$C13$  [ $X$ ,  $Y$ ,  $Z$ , 3.336(3) Å; 3.175(2) Å; not found; and 2.9(3)°], intermolecular  $C8-C13\cdots C8-C13$  [− $X$ , 1 −  $Y$ , − $Z$ , 3.640(3) Å; −3.299(2) Å; 1.537 Å; and 0°], and intermolecular  $C1-C6\cdots C1-C6$  [1 −  $X$ , 2 −  $Y$ , − $Z$ , 3.753(3) Å; 3.352(2) Å; 1.689 Å; and 0°].

Comparing this structure with the one we have published MIXFAB ( $[[Pt(n)(2,2'-bpy)(2,3,4,6-SC_6F_4-4-H)_2]]$ ), in our structure, we do not observe the formation of infinite columns dictated by the  $\pi_F-\pi_F$  stackings, see this in section 4.<sup>51</sup> This is due to the electron-attracting effect of the −CN group on the tetrafluorinated thiolate ring. This can decrease the repulsion between the rings, making them electron-deficient aromatic rings and promoting  $\pi_F-\pi_F$  stacking. In the case of the MIXFAB tecton, the H atom in position 4 within the ring does not promote this as efficiently, so we do not see the formation of infinite columns. In this way, we believe that the thiolate 2,3,4,6-SC<sub>6</sub>F<sub>4</sub>-4-CN should be exploited in other coordination and organometallic compounds to observe if  $\pi_F-\pi_F$  stacking can be favored more efficiently.

## 7. Conclusions

Throughout this analysis employing Conquest, specific points must be considered to answer the question initially asked: How reliable and predictable is the fluorinated thiolate 2,3,5,6-SC<sub>6</sub>F<sub>4</sub>-H-4 in establishing  $\pi_F-\pi_F$  stacking in metal complexes from crystal engineering's point of view?

1. First, the type of tecton used to form the supramolecular arrangements must be considered through this interaction. From this, we can point out that tectons with  $D_{h4}$  or  $T_h$  symmetry or within the subgroups of these point groups established the  $\pi_F-\pi_F$  stacking more efficiently.<sup>95</sup> This was corroborated with complexes with square planar or tetrahedral geometry. For instance,  $[Et_4N][Au(2,3,5,6-SC_6F_4-H-4)_4]\cdot EtOH$  (LOKVUD),  $[SnPh_2(2,3,4,6-SC_6F_4-4-H)_2]$  (PIDMOF), and  $[Pt(2,2'-$



bpy)(2,3,4,6-SC<sub>6</sub>F<sub>4</sub>-4-CN)<sub>2</sub>] (EMEGAE). Special mention should be made to complexes belonging to *C*<sub>2h</sub> point groups since in the case of [Et<sub>4</sub>N][Au(2,3,5,6-SC<sub>6</sub>F<sub>4</sub>-H-4)<sub>2</sub>] (LOKWEO), 1D arrangements were formed through  $\pi_F$ - $\pi_F$  stacking. Although it was the only structure detected by Conquest that presented this specific point group, the stacking was carried out efficiently. On the other hand, in the case of specific *O*<sub>h</sub> or *D*<sub>3h</sub> point groups or subgroups of these, there were a few cases in which  $\pi_F$ - $\pi_F$  stacking was established as a reliable synthon. For instance, in the case of complex [Os(IV)(2,3,5,6-SC<sub>6</sub>F<sub>4</sub>H-4)<sub>2</sub>(SC<sub>6</sub>F<sub>3</sub>H-4(2,3,5,6-SC<sub>6</sub>F<sub>4</sub>H)-2)(C<sub>6</sub>H<sub>5</sub>)]] (ECERIP, trigonal bipyramidal geometry) presented an arrangement of 2D packing. However, this was not precisely dictated by  $\pi_F$ - $\pi_F$  stacking but by various stacking ( $\pi_F$ - $\pi$ ) involving fluorinated and non-fluorinated rings. Also, in the case of complexes with octahedral geometry, a few examples presented a packing dictated by stacking, [Os(III)(2,3,5,6-SC<sub>6</sub>F<sub>4</sub>-H-4)<sub>2</sub>(SOC-CH<sub>3</sub>)(P(CH<sub>3</sub>)<sub>2</sub>Ph)<sub>2</sub>] (ZAWWAV), [NaC<sub>222</sub>][Co(III)(2,3,5,6-SC<sub>6</sub>F<sub>4</sub>-H-4)<sub>2</sub>(TPP)-C<sub>6</sub>H<sub>5</sub>Cl] (COSJOJ) and [NaC<sub>222</sub>][Co(III)(2,3,5,6-SC<sub>6</sub>F<sub>4</sub>-H-4)(TPP)] (COSJUP). From this, we can indicate that the selection of the point group of the tecton is crucial. In addition, the effect of coordinated ligands must be considered since this can modify the point group and decrease its symmetry, which affects stacking, because depending on the nature of the ligand, it can create molecular crowding or a hindering steric effect limiting the interaction.

2. Attention should be paid to ligands other than coordinated tetrafluorinated thiolates since, as observed in the structures, FOLWIM, FOLWOS, DIDCEY, GAHLIK, GAHLOQ, KUDWOD, the first two complexes of Co, and the last of Fe, not only the steric hindrance shown by the TPP<sup>-</sup> ligand avoid the formation of the stackings, but also the presence of heteroatoms (N, O) can cause the formation of hydrogen bonds and prevent this interaction.

3. It should be avoided the use of ligands with a large  $\pi$  surface area, *i.e.*, containing the 1,10-phen ligand (HIHROH, Pd complex, and LUQMOC Pt complex) or those coordinated to ferrocenyl-derived ligands (FORMUW or BOQHOG) since they prevent stacking. However, it should be emphasized that in the case of tectons with the 1,10-phen ligand, the  $\pi_F$ - $\pi_F$  stackings prevailed despite these ligands with a larger  $\pi$  surface area being present. Contrary to what was observed with ferrocenyl-derived ligands.

4. It is fundamental to observe the nature of the tecton, whether it is neutral or ionic. In the case of being ionic, select the nature of the participating cations or anions. This is mentioned for the specific case of K<sub>2</sub>[Pt(II)(2,3,5,6-SC<sub>6</sub>F<sub>4</sub>-H-4)<sub>4</sub>]-EtOH (BOQHOG), most likely the ion-ion interaction (between K<sup>+</sup> and the anion complex) limited the stacking. In this way, the establishment of stacking can be affected when it competes with an energetically stronger interaction.

5. It is important to emphasize what was observed in the structures of HIHSAU and MIXFAB (see the section on Pd complexes), which presented the term used by Aakeröy: supramolecular yielding.

Furthermore, it must be mentioned that other issues should be considered in addition to these recommendations regarding the type of tecton to use.

1. Stacking can be affected by polymorphism. This is observed for both Os complexes HENXIH and HENXIH01. Where small differences, mainly conformational, in the spatial arrangement of the rings (mainly the tetrafluorinated thiolates) affect the amount of intra- and intermolecular stacking.

These suggestions should be considered in the design of the tecton to ensure  $\pi_F$ - $\pi_F$  stacking. However, this interaction is susceptible to formation if it competes with energetically stronger interactions or from other factors discussed in this perspective. And hence unfortunately, no definitive answer can be given, at this point, as to how feasible and reliable this interaction can be exploited from a crystal engineering point of view. Nonetheless, considering the above points, researchers can largely guarantee that  $\pi_F$ - $\pi_F$  stacking would prevail in molecular packing and that it can be exploited as a crystal engineering tool.

Additionally, we encourage exploring the ability of the ligand 2,3,4,6-SC<sub>6</sub>F<sub>4</sub>-4-CN since, as indicated in the miscellaneous section, it may be a more suitable ligand to form the stacking instead of 2,3,5,6-SC<sub>6</sub>F<sub>4</sub>-H-4.

## Data availability

The data supporting this article has been included as part of the ESI.<sup>†</sup>

## Conflicts of interest

The authors declare that they have no known competing financial interests or personal relationships that could have appeared to influence the work reported in this paper.

## Acknowledgements

J. M. G.-A. would like to thank PAPIIT-DGAPA-UNAM for the financial support granted through project IT200523. J. M. G.-A. also thanks CONAHCYT for funding project CBF2023-2024-1325 through the Ciencia Básica y de Frontera 2023-2024 call. D. M.-M. gratefully thanks the generous financial support of DGAPA-UNAM PAPIIT IN223323 and CONAHCYT A1-S-033933.

## References

- 1 J. W. Steed and J. L. Atwood, *Supramolecular Chemistry*, Wiley, 2009.
- 2 D. Braga, *Chem. Commun.*, 2003, **3**, 2751-2754.
- 3 G. R. Desiraju, *Crystal Engineering: The Design of Organic Solids*, Elsevier, Amsterdam, 1989.

4 E. R. T. Tiekkink, J. Vittal and M. Zaworotko, *Organic Crystal Engineering: Frontiers in Crystal Engineering*, John Wiley & Sons, 2010.

5 K. Geng, T. He, R. Liu, S. Dalapati, K. T. Tan, Z. Li, S. Tao, Y. Gong, Q. Jiang and D. Jiang, *Chem. Rev.*, 2020, **120**, 8814–8933.

6 L. Brammer, *Chem. Soc. Rev.*, 2004, **33**, 476–489.

7 C. B. Aakeröy and A. M. Beatty, *Aust. J. Chem.*, 2001, **54**, 409–421.

8 D. Braga, *J. Chem. Soc., Dalton Trans.*, 2000, 3705–3713.

9 D. Braga and F. Grepioni, *Chem. Commun.*, 2005, 3635–3645.

10 T. R. Cook and P. J. Stang, *Chem. Rev.*, 2015, **115**, 7001–7045.

11 R. Chakrabarty, P. S. Mukherjee and P. J. Stang, *Chem. Rev.*, 2011, **111**, 6810–6918.

12 M. Fujita, M. Tominaga, A. Hori and B. Therrien, *Acc. Chem. Res.*, 2005, **38**, 369–378.

13 M. Kawano and M. Fujita, *Coord. Chem. Rev.*, 2007, **251**, 2592–2605.

14 M. J. Zaworotko, *Cryst. Growth Des.*, 2007, **7**, 4.

15 M. Safaei, M. M. Foroughi, N. Ebrahimpoor, S. Jahani, A. Omidi and M. Khatami, *TrAC, Trends Anal. Chem.*, 2019, **118**, 401–425.

16 L. Jiao, J. Y. R. Seow, W. S. Skinner, Z. U. Wang and H. L. Jiang, *Mater. Today*, 2019, **27**, 43–68.

17 L. Brammer, J. C. Mareque Rivas, J. Reinaldo Atencio, S. Fang and F. Christopher Pigge, *J. Chem. Soc., Dalton Trans.*, 2000, 3855–3867.

18 G. A. Jeffrey, *An introduction to hydrogen bonding*, Oxford University Press, New York, 1997.

19 G. Desiraju and T. Steiner, in *The Weak Hydrogen Bond: In Structural Chemistry and Biology*, ed. I. U. of C. M. on Crystallography, Oxford University Press, 2001.

20 T. Steiner, *Angew. Chem., Int. Ed.*, 2002, **41**, 48–76.

21 L. Brammer, in *Crystal Design: Structure and Function*, ed. G. R. Desiraju, John Wiley & Sons, Ltd., 2003, vol. 7, pp. 1–75.

22 L. J. Prins, D. N. Reinhoudt and P. Timmerman, *Angew. Chem., Int. Ed.*, 2001, **40**, 2382–2426.

23 M. Whitesides, E. E. Simanek, J. P. Mathias, C. T. Seto, D. Chin, M. Mammen and D. M. Gordon, *Acc. Chem. Res.*, 1995, **28**, 37–44.

24 *Self-Assembly in Supramolecular Systems*, ed. J. F. Stoddart, L. F. Lindoy and I. M. Atkinson, The Royal Society of Chemistry, 2000.

25 F. H. Allen, W. D. Samuel Motherwell, P. R. Raithby, G. P. Shields and R. Taylor, *New J. Chem.*, 1999, **23**, 25–34.

26 G. R. Desiraju, *Angew. Chem., Int. Ed. Engl.*, 1995, **34**, 2311–2327.

27 F. H. Allen, *Acta Crystallogr., Sect. B: Struct. Sci.*, 2002, **58**, 380–388.

28 C. B. Aakeröy and D. J. Salmon, *CrystEngComm*, 2005, **7**, 439–448.

29 S. K. Burley and G. A. Petsko, *Science*, 1985, **229**, 23–28.

30 J. Černý, M. Kabeláč and P. Hobza, *J. Am. Chem. Soc.*, 2008, **130**, 16055–16059.

31 E. A. Meyer, R. K. Castellano and F. Diederich, *Angew. Chem., Int. Ed.*, 2003, **42**, 1210–1250.

32 W. R. Zhuang, Y. Wang, P. F. Cui, L. Xing, J. Lee, D. Kim, H. L. Jiang and Y. K. Oh, *J. Controlled Release*, 2019, **294**, 311–326.

33 R. Thakuria, N. K. Nath and B. K. Saha, *Cryst. Growth Des.*, 2019, **19**, 523–528.

34 J. H. Deng, J. Luo, Y. L. Mao, S. Lai, Y. N. Gong, D. C. Zhong and T. B. Lu, *Sci. Adv.*, 2020, **6**, 1–9.

35 M. O. Sinnokrot and C. D. Sherrill, *J. Phys. Chem. A*, 2006, **110**, 10656–10668.

36 C. A. Hunter and J. K. M. Sanders, *J. Am. Chem. Soc.*, 1990, **112**, 5525–5534.

37 M. O. Sinnokrot and C. D. Sherrill, *J. Am. Chem. Soc.*, 2004, **126**, 7690–7697.

38 C. Janiak, *J. Chem. Soc., Dalton Trans.*, 2000, 3885–3896.

39 Y. C. Chang, Y. Da Chen, C. H. Chen, Y. S. Wen, J. T. Lin, H. Y. Chen, M. Y. Kuo and I. Chao, *J. Org. Chem.*, 2008, **73**, 4608–4614.

40 O. V. Dolomanov, L. J. Bourhis, R. J. Gildea, J. A. K. Howard and H. Puschmann, *J. Appl. Crystallogr.*, 2009, **42**, 339–341.

41 A. L. Spek, *Acta Crystallogr., Sect. D: Biol. Crystallogr.*, 2009, **65**, 148–155.

42 J. C. Páez-Franco, M. R. Zermeño-Ortega, C. M. De O-Contreras, D. Canseco-González, J. R. Parra-Unda, A. Avila-Sorrosa, R. G. Enríquez, J. M. Germán-Acacio and D. Morales-Morales, *Pharmaceutics*, 2022, **14**, 402.

43 S. Mishra and S. Daniele, *Chem. Rev.*, 2015, **115**, 8379–8448.

44 R. Berger, G. Resnati, P. Metrangolo, E. Weber and J. Hulliger, *Chem. Soc. Rev.*, 2011, **40**, 3496–3508.

45 P. Panini and D. Chopra, in *Hydrogen Bonded Supramolecular Structures*, 2015, vol. 87, pp. 37–67, *lecture notes in chemistry*.

46 K. Reichenbächer, H. I. Süss and J. Hulliger, *Chem. Soc. Rev.*, 2005, **34**, 22–30.

47 S. Bacchi, M. Benaglia, F. Cozzi, F. Demartin, G. Filippini and A. Gavezzotti, *Chem. – Eur. J.*, 2006, **12**, 3538–3546.

48 F. Cozzi, S. Bacchi, G. Filippini, T. Pilati and A. Gavezzotti, *CrystEngComm*, 2009, **11**, 1122–1127.

49 H. Juarez-Garrido, J. M. Germán-Acacio, E. Jaime-Adán, J. Barroso-Flores, V. Lara, R. Reyes-Martínez, R. A. Toscano, S. Hernández-Ortega and D. Morales-Morales, *CrystEngComm*, 2022, **24**, 7932–7943.

50 H. Torrens, *Coord. Chem. Rev.*, 2000, **196**, 331–352.

51 M. Corona-Rodríguez, S. Hernández-Ortega, J. Valdés-Martínez and D. Morales-Morales, *Supramol. Chem.*, 2007, **19**, 579–585.

52 G. Backman-Blanco, H. Valdés, M. T. Ramírez-Apan, P. Cano-Sánchez, S. Hernandez-Ortega, A. L. Orjuela, J. Alí-Torres, A. Flores-Gaspar, R. Reyes-Martínez and D. Morales-Morales, *J. Inorg. Biochem.*, 2020, **211**, 111206.

53 Y.-M. Sun, F.-Y. Dong, D.-Q. Wang, Y.-L. Wang, Y.-T. Li and J.-M. Dou, *J. Inorg. Organomet. Polym. Mater.*, 2010, **20**, 168–176.

54 G. V. Janjić, P. V. Petrović, D. B. Ninković and S. D. Zarić, *J. Mol. Model.*, 2011, **17**, 2083–2092.



55 S. Watase, T. Kitamura, N. Kanehisa, M. Nakamoto, Y. Kai and S. Yanagida, *Acta Crystallogr., Sect. C: Cryst. Struct. Commun.*, 2004, **60**, 104–106.

56 G. Moreno-Alcántar, L. Turcio-García, J. M. Guevara-Vela, E. Romero-Montalvo, T. Rocha-Rinza, Á. M. Pendás, M. Flores-Álamo and H. Torrens, *Inorg. Chem.*, 2020, **59**, 8667–8677.

57 G. Romo-Islas, G. Moreno-Alcántar, M. Flores-Álamo and H. Torrens, *J. Fluor. Chem.*, 2020, **236**, 109578.

58 G. Moreno-Alcántar, C. Díaz-Rosas, A. Fernández-Alarcón, L. Turcio-García, M. Flores-Álamo, T. Rocha-Rinza and H. Torrens, *Inorganics*, 2021, **9**, 1–15.

59 P. Doppelt, J. Fischer and R. Weiss, *J. Am. Chem. Soc.*, 1984, **106**, 5188–5193.

60 P. Doppelt, J. Fischer, L. Ricard and R. Weiss, *New J. Chem.*, 1987, **11**, 357–364.

61 P. Doppelt, J. Fischer and R. Weiss, *Croat. Chem. Acta*, 1984, **57**, 507–518.

62 M. Schappacher, L. Ricard, J. Fischer, R. Weiss, E. Bill, R. Montiel-Montoya, H. Winkler and A. X. Trautwein, *Eur. J. Biochem.*, 1987, **168**, 419–429.

63 H. Nasri, K. J. Halier, Y. Wang, B. H. Huynh and W. R. Scheidt, *Inorg. Chem.*, 1992, **31**, 3459–3467.

64 I. Eslava-Gonzalez, H. Valdés, M. Teresa Ramírez-Apan, S. Hernandez-Ortega, M. Rosario Zermeño-Ortega, A. Avila-Sorrosa and D. Morales-Morales, *Inorg. Chim. Acta*, 2020, **507**, 119588.

65 M. A. Usón and J. M. Llanos, *J. Organomet. Chem.*, 2002, **663**, 98–107.

66 M. Cerón, L. Meléndez, S. Bernès, M. Arroyo and A. Ramírez-Monroy, *J. Chem. Crystallogr.*, 2012, **42**, 1119–1123.

67 M. Arroyo, S. Bernes, J. Cerón, J. Rius and H. Torrens, *Inorg. Chem.*, 2004, **43**, 986–992.

68 M. Cerón, M. Arroyo and S. Bernès, *Acta Crystallogr., Sect. E: Struct. Rep. Online*, 2006, **62**, 2167–2169.

69 J. P. Collman, D. S. Bohle and A. K. Powell, *Inorg. Chem.*, 1993, **32**, 4004–4011.

70 M. C. Etter, J. C. MacDonald and J. Bernstein, *Acta Crystallogr., Sect. B: Struct. Sci.*, 1990, **46**, 256–262.

71 J. Bernstein, R. E. Davis, L. Shimoni and N.-L. Chang, *Angew. Chem., Int. Ed. Engl.*, 1995, **34**, 1555–1573.

72 M. Arroyo, J. A. Chamizo, D. L. Hughes, R. L. Richards, P. Roman, P. Sosa and H. Torrens, *J. Chem. Soc., Dalton Trans.*, 1994, 1819–1824.

73 P. Zeleny, M. Arroyo, L. Meléndez and S. Bernès, *IUCrData*, 2019, **4**, 2–13.

74 M. Cerón, V. Cortina, A. Ramírez-Monroy, S. Bernès, H. Torrens and M. Arroyo, *Polyhedron*, 2011, **30**, 1250–1257.

75 R. Moreno-Esparza, H. Torrens, M. Arroyo, J. Briansó, C. Miravitles and J. Rius, *Polyhedron*, 1995, **14**, 1601–1606.

76 M. Basauri-Molina, S. Hernández-Ortega, R. A. Toscano, J. Valdés-Martínez and D. Morales-Morales, *Inorg. Chim. Acta*, 2010, **363**, 1222–1229.

77 V. Lingen, A. Lüning, C. Strauß, I. Pantenburg, G. B. Deacon, A. Klein and G. Meyer, *Eur. J. Inorg. Chem.*, 2013, 4450–4458.

78 S. Grimme, *Angew. Chem., Int. Ed.*, 2008, **47**, 3430–3434.

79 C. B. Aakeröy, A. M. Beatty and B. A. Helfrich, *J. Am. Chem. Soc.*, 2002, **124**, 14425–14432.

80 C. Herrera-Álvarez, V. Gómez-Benítez, R. Redón, J. J. García, S. Hernández-Ortega, R. A. Toscano and D. Morales-Morales, *J. Organomet. Chem.*, 2004, **689**, 2464–2472.

81 L. Villanueva, M. Arroyo, S. Bernès and H. Torrens, *Chem. Commun.*, 2004, **2**, 1942–1943.

82 V. Lingen, A. Lüning, C. Strauß, I. Pantenburg, G. B. Deacon, G. Meyer and A. Klein, *Inorg. Chim. Acta*, 2014, **423**, 152–162.

83 J. W. Steed and J. L. Atwood, in *Supramolecular Chemistry*, John Wiley & Sons, Ltd, 2009, pp. 1–48.

84 S. E. Castillo-Blum, M. Flores-Alamo, D. Franco-Bodek, G. Hernandez and H. Torrens, *Inorg. Chem. Commun.*, 2014, **45**, 44–47.

85 R. Cervantes, J. Tiburcio and H. Torrens, *New J. Chem.*, 2015, **39**, 631–638.

86 S. K. Lee and D. Y. Noh, *Inorg. Chem. Commun.*, 2010, **13**, 183–186.

87 J. Bautista, A. Bertran, S. Bernés, U. Duran and H. Torrens, *Rev. Soc. Quim. Mex.*, 2003, **47**, 44–52.

88 S. Bernès, F. J. Meléndez and H. Torrens, *Acta Crystallogr., Sect. C: Struct. Chem.*, 2016, **72**, 268–273.

89 L. G. Wade, *Química Orgánica*, Pearson, México, Séptima edn, 2011.

90 D. Cruz-Garritz, J. Garcia-Alejandre, H. Torrens, C. Alvarez, R. A. Toscano, R. Poilblanc and A. Thorez, *Transition Met. Chem.*, 1991, **16**, 130–135.

91 M. J. Wiester, A. B. Braunschweig, H. Yoo and C. A. Mirkin, *Inorg. Chem.*, 2010, **49**, 7188–7196.

92 K. W. Chan, W. M. Ng, W. M. Cheung, C. S. Lai, H. H. Y. Sung, I. D. Williams and W. H. Leung, *J. Organomet. Chem.*, 2016, **812**, 151–157.

93 Q. Zhang, F. K. M. Cheung, W.-Y. Wong, I. D. Williams and W.-H. Leung, *Organometallics*, 2001, **20**, 3777–3781.

94 J. A. Weinstein, A. J. Blake, E. S. Davies, A. L. Davis, M. W. George, D. C. Grills, I. V. Lileev, A. M. Maksimov, P. Matousek, M. Y. Mel'nikov, A. W. Parker, V. E. Platonov, M. Towrie, C. Wilson and N. N. Zheligovskaya, *Inorg. Chem.*, 2003, **42**, 7077–7085.

95 G. L. Miessler, P. J. Fischer and D. A. Tarr, *Inorganic Chemistry*, Pearson, Boston, 5th edn, 2014.

